1977

Subsynchronous resonance in power systems: damping of torsional oscillations

Kim Touy Khu
Iowa State University

INFORMATION TO USERS

This material was produced from a microfilm copy of the original document. While the most advanced technological means to photograph and reproduce this document have been used, the quality is heavily dependent upon the quality of the original submitted.

The following explanation of techniques is provided to help you understand markings or patterns which may appear on this reproduction.

1. The sign or "target" for pages apparently lacking from the document photographed is "Missing Page(s)". If it was possible to obtain the missing page(s) or section, they are spliced into the film along with adjacent pages. This may have necessitated cutting thru an image and duplicating adjacent pages to insure you complete continuity.

2. When an image on the film is obliterated with a large round black mark, it is an indication that the photographer suspected that the copy may have moved during exposure and thus cause a blurred image. You will find a good image of the page in the adjacent frame.

3. When a map, drawing or chart, etc., was part of the material being photographed the photographer followed a definite method in "sectioning" the material. It is customary to begin photoing at the upper left hand corner of a large sheet and to continue photoing from left to right in equal sections with a small overlap. If necessary, sectioning is continued again — beginning below the first row and continuing on until complete.

4. The majority of users indicate that the textual content is of greatest value, however, a somewhat higher quality reproduction could be made from "photographs" if essential to the understanding of the dissertation. Silver prints of "photographs" may be ordered at additional charge by writing the Order Department, giving the catalog number, title, author and specific pages you wish reproduced.

5. PLEASE NOTE: Some pages may have indistinct print. Filmed as received.

University Microfilms International
300 North Zeeb Road
Ann Arbor, Michigan 48106 USA
St. John's Road, Tyler's Green
High Wycombe, Bucks, England HP10 8HR

Subsynchronous resonance in power systems: Damping of torsional oscillations

by

Kim Touy Khu

A Dissertation Submitted to the
Graduate Faculty in Partial Fulfillment of
The Requirements for the Degree of
DOCTOR OF PHILOSOPHY

Major: Electrical Engineering

Approved:

Signature was redacted for privacy.

In Charge of Major Work

Signature was redacted for privacy.

For the Major Department

Signature was redacted for privacy.

For the Graduate College

Iowa State University
Ames, Iowa
1977

TABLE OF CONTENTS

LIST OF FIGURES

LIST OF TABLES

LIST OF SYMBOLS AND DEFINITIONS

abc Subscripts, denoting variable in abc-components.

C_e Series capacitance of the transmission line.

D_i Mechanical damping coefficient of mass i.

$\cdot$ Dot, denoting time-derivative operator, d/dt.

d Subscript, denoting variable on d-axis.

$d_i = D_i\omega_B$ Mechanical damping coefficient of mass i.

δ_{Ei} Modal angular deviation corresponding to mode i.

δ_i Angular deviation of rotor i with respect to synchronous reference frame.

Δ Prefix, denoting incremental value of a variable.

E_{FD} Field voltage referred to armature side.

EXC Exciter rotor mass.

f_{60} Synchronous frequency (60 Hz).

f_e Electrical network frequency as seen by generator rotor.

f_{en} Electrical network natural frequency.

f_m Mechanical system's natural frequency.

Gen Generator rotor mass, or electric power source.

H_{Ei} Modal moment of inertia corresponding to mode i.

H_i Moment of inertia of mass i.

HP High-pressure turbine rotor mass.

IP Intermediate-pressure turbine rotor mass.

K_{Ei} Modal spring constant corresponding to mode i.

K_{ij} Spring constant of shaft between mass i and mass j.

kM_D Mutual coupling inductance between d-axis circuit and d-axis damper winding.

kM_F Mutual coupling inductance between d-axis circuit and field circuit.

kM_{Qi} Mutual coupling inductance between q-axis circuit and damper circuit i.

L_{AD} Magnetizing inductance on d-axis.

L_{AQ} Magnetizing inductance on q-axis.

ℓ_D d-axis damper winding leakage reactance.

ℓ_d d-axis circuit leakage reactance.

$L_D = L_{AD} + \ell_D$ d-axis damper winding self-inductance.

$L_d = L_{AD} + \ell_d$ d-axis circuit self-inductance.

L_e Line inductive reactance.

ℓ_F Field circuit leakage reactance.

$L_F = L_{AD} + \ell_F$ Field circuit self-inductance.

LPA Low-pressure turbine rotor mass A.

LPB Low-pressure turbine rotor mass B.

ℓ_{Qi} q-axis damper winding i leakage inductance.

$L_{Qi} = L_{AQ} + \ell_{Qi}$ q-axis damper winding i self-inductance.

ℓ_q q-axis circuit leakage reactance.

$L_q = L_{AQ} + \ell_q$ q-axis circuit self-inductance.

λ_i Flux-linkage of circuit i.

M_Q Mutual coupling inductance between q-axis damper circuits.

M_R Mutual coupling inductance between field circuit and d-axis damper circuit.

ω_B Synchronous speed (377 rad/sec)

ω_{Ei} Modal velocity corresponding to mode i.

ω_i Velocity of mass i.

$\underline{P}$ Modified Park's transformation matrix.

P_0 Generator power output.

PF Power factor.

$\underline{Q}$ Orthogonal transformation matrix.

q Subscript, denoting variable on q-axis.

r Armature resistance.

R_e Line resistance.

r_D D-damper winding resistance.

r_F Field circuit resistance.

r_{Qi} q-axis damper winding i resistance.

$S = \frac{f_e - f_{60}}{f_e}$ Slip

$\underline{T}$ Input torque vector.

$\underline{T_a}$ Accelerating torque vector.

T_e Electrical developed torque.

τ_d' Effective field circuit time constant.

T_{mi} Mechanical torque applied on mass i.

$\underline{U}$ Forcing function matrix.

v_c Voltage across series capacitor.

v_F Field voltage applied to field winding.

v_∞ Infinite bus voltage.

V_t Generator terminal (rms phase) voltage.

V_∞ rms phase voltage of infinite bus.

x_d'' Subtransient reactance of generator.

X_c Series capacitor reactance.

X_F Fault reactance.

X_t Transformer reactance.

X_ℓ Transmission line reactance.

X_S Reactance before infinite bus voltage source.

Z Impedance.

Z_D d-axis damper circuit impedance.

Z_r Field circuit impedance.

I. INTRODUCTION

The demand for electric energy has continued to increase in the last few decades. Economic considerations have dictated the trend toward increased size of generating plants. The location of hydro sites and the location of mines for good quality coal, as well as environmental considerations, have made it desirable to locate the power plants at considerable distances from the load centers. This is particularly true in the Western United States, where bulk power is being transmitted over distances of several hundred miles.

When electric power is transmitted over long distances, there are problems that are introduced by the transmission lines' excessive inductive reactance. The amount of power that can be transmitted is significantly reduced because of the lower stability limits. To increase the power limits, the series reactance of the transmission lines must be reduced.

There are simple means to reduce the series reactance of a given transmission network. For example, adding more transmission lines in parallel, and/or using bundled conductors would result in a reduced effective series inductance. These solutions, however, are too costly on account of the right-of-way problems and the increased costs of tower structures and conductors.

A more economical alternative has been adopted in recent years, namely inserting capacitors in series with the transmission lines to reduce the overall inductive reactance of the lines. Inasmuch as it is simple and direct, this solution has, however, introduced the phenomena of Subsynchronous Resonance (SSR) which brought about some serious problems.

A. Problems Related to Series Compensated Transmission Lines

In the 1920's and 1930's, it was discovered that the use of series capacitors in a power system, composed of synchronous and induction machines, may give rise to the following phenomena (1): self-excitation, which is primarily of electrical nature; hunting, which is an abnormal electromechanical condition; and a phenomenon known as ferro-resonance, which is caused by the excessively large transformer exciting current at no-load or at light load when the transformer is charged through a series capacitor. While the phenomenon of hunting may occur without the presence of series capacitors, their presence in the system is likely to cause the synchronous generators to hunt. The above phenomena were studied either through conducting tests on real systems (using oscilloscopes), or by analyzing a mathematical model of the system using circuit differential analyzers. It is interesting to note that these studies have revealed the existence of subharmonic currents or voltages in the system subjected to any one of the above mentioned phenomena.

Another phenomenon, which is also related to the use of series capacitors in transmission lines, was not detected until the 1970's when two turbo-generator shafts were destroyed on two separate occasions at the same generating station in the southwestern part of the United States. This phenomenon, which is now known as Torsional Interaction, is one of the most damaging effects caused by subsynchronous resonance. For this reason, subsynchronous resonance has become the subject of considerable research by the power industry and the machine manufacturers.

B. Scope of the Work

This dissertation is devoted to the study of the phenomena of subsynchronous resonance in a power system with series-compensated transmission lines. The work consists of two main parts:

1) To model and analyze a complete electromechanical system subjected to subsynchronous resonance; and to study the effects of the various system parameters.
2) To explore some methods to damp out torsional oscillations through the use of Stabilizing Control Signals.

II. LITERATURE REVIEW

Surveying the papers dealing with the use of series capacitors and published before 1971 (1-6), we find that none had mentioned the effect of torsional interaction.

In Reference 1, Butler and Concordia, using a circuit differential analyzer, have made an excellent analysis of self-excitation and hunting of synchronous and induction machines. In later works, Rustebakke and Concordia (4) went on to establish an analytical method to define the stability borderline of a system as a function of the amount of the series capacitances used and the line resistance. No mention of the field circuit resistance appears in their studies.

In 1970, the phenomenon of self-excitation was studied by Kilgore et al. (5). They showed that it is caused by excessive negative rotor resistance, i.e., it is an induction generator effect.

In all these studies, the mechanical system was not included in the system model. This may have been due to the relatively large size of the system of simultaneous differential equations governing the dynamic behavior of machines and networks, which has to be solved analytically.

On December 9, 1970, a line switching was followed by the breakdown of a generator shaft at Mohave Generating Station in Northwestern Arizona. Originally, the damage was thought to be caused by a mere incident of a severe case of short-circuit at the collector rings (7). It was only after a second incident (similar to the first) at this same station, which occurred on October 26, 1971, that it was hypothesized that the damage of

both shafts is attributed to self-excitation or torsional interaction or both (7,8).

Following the report of Reference 7, many researchers pooled their efforts to analyze the problem, and to determine appropriate solutions to these abnormal conditions.

Interest in this phenomenon is manifested by a large number of papers presented at various technical meetings in the last five years. Two particularly comprehensive papers were presented by Bowler et al. (9) and by Kilgore et al. (10). They deal specifically with self-excitation and torsional interaction, both later known as Subsynchronous Resonance Effects (SSR). Bowler used the Root Locus method to analyze the phenomenon of resonance between two coupled systems composed of resistance, inductance, and capacitance in series. Kilgore undertook the task of representing the entire power system, with the mechanical system included, in a simplified form. In his analysis, Kilgore stressed the potential presence of the induction generator effect and torsional oscillations. Their work set the stage for improved techniques to study the phenomenon and, ultimately, to devise measures to prevent and to eliminate subsynchronous resonance effects.

A special Task Force was formed by the Working Group in Dynamic System Performance, Power System Engineering Committee of the Power Engineering Society (IEEE), to study the SSR phenomenon. Among the Task Force's contributions are: a special IEEE publication on the subject of SSR (11), which includes a paper on proposed terms and definitions (12), and the development of a bench-mark power system model for studying the

phenomenon (13). The model will offer a common basis for comparison of results obtained independently by research workers. This model is used in the investigations reported upon in this dissertation.

As techniques of controlling and preventing subsynchronous resonance are being developed, SSR-prone interconnected power systems, like those of the southwestern part of the United States, are being operated at a far-from-optimum level of line compensation (14).

III. THE PHENOMENA OF SUBSYNCHRONOUS RESONANCE

A. Existence of Subsynchronous Resonance

A power system is essentially an electromechanical system having two dynamical systems: a mechanical system and an electrical system. The coupling between these two systems takes place at the synchronous generator.

The mechanical system consists of one or more turbines connected in tandem or in cross compound (15). The generator rotor is on the main turbine shaft, while the exciter may either be driven by the same shaft or independently driven.

The electrical system consists of the synchronous generator's rotor and stator windings and the external network including transformers and transmission lines.

These two systems are mutually coupled such that mechanical energy can be converted to electrical energy and vice-versa. An important feature of any dynamical system is that when disturbed, its equilibrium state is lost temporarily or indefinitely depending upon whether it can reach a new state of equilibrium. During this transient state, energy is being transferred from one energy-storing element of the system to another with a frequency equal to the system's natural frequency. When two such dynamical systems are bilaterally coupled, energy transfer of one system affects that of the other. Thus, two basically stable systems, when coupled, may result in a system which can be unstable (9).

Appendix A shows the existence of supersynchronous and subsynchronous components of current or voltage in the electric network when the

generator rotor is subjected to a sinusoidal disturbance of amplitude A and frequency μ (see equation A-15). The effect of the disturbance on the rotor is to give rise to two voltages: one of frequency $(\omega_0 + \mu)$, and the other of frequency $(\omega_0 - \mu)$. The two voltages are of opposite sign.

Furthermore, Appendix A shows that to the supersynchronous frequency $(\omega_0 + \mu)$, the generator appears to be an induction motor, since the slip is positive $(\omega_r < \omega_0)$. On the other hand, to the subsynchronous frequency $(\omega_0 - \mu)$, the generator appears to be an induction generator, since the slip is negative $(\omega_r > \omega_0)$.

The supersynchronous frequency poses no threat to the system stability, since an induction motor effect absorbs energy from the disturbance. Thus, its effect is similar to the action of a braking resistor. The subsynchronous frequency poses, however, a potential danger to the system stability, because a disturbance seems to inject more energy into the system by its generator action. If the system net resistance is negative, this induction generator action will be greatly amplified with time, causing system instability. This type of instability, which is purely electrical in nature, is termed Self-Excitation.

In the next chapter it will be shown that the natural frequencies of the mechanical and electrical systems normally lie below operating frequency (60 Hz in the United States).

We have outlined above the effect of a disturbance upon the generator rotor's movement. If, however, the disturbance is applied to the electrical network, the same analysis would give the similar results. A disturbance of amplitude A and frequency μ applied to the electrical network will

also result in supersynchronous and subsynchronous currents or voltages. The generator rotor will be forced to oscillate with these same frequencies.

If the frequency of the disturbing force whose resulting subsynchronous frequency ($\omega_0 - \mu$) is near or equal to one of the natural frequencies of the mechanical system, resonance will occur. This phenomenon can be easily understood from the classical theory of forced vibration impressed upon an oscillatory system described by the following equation

$$A\ddot{\theta}_S + D\dot{\theta}_S + K\theta_S = F\sin\omega_f t \qquad (1)$$

where A, D, K, and F are constant coefficients. The solution of Eq. 1 shows that if $\sqrt{\frac{K}{A}}$ and ω_f are near or equal to each other, the resulting amplitude of oscillation will be greatly amplified, limited only by the system's damping coefficient D. The phenomenon is termed Torsional Interaction. It is electromechanical in nature.

B. Effects of Subsynchronous Resonance on Power Systems

Reference 8 gives an extensive report on the actual effects of subsynchronous resonance as experienced at Mohave Generating Station. Due to the relatively low resulting frequency, fluctuation of voltage and flickering of light were observed. The most damaging effect of subsynchronous resonance, however, was the torsional stress impressed upon the shaft. During the incident, an abnormal vibration of the control room floor was noticed.

Since turbo-generator shafts are known to have cyclic fatigue, manufacturers usually give a relationship between the percent loss of shaft life versus the number of stress cycles experienced (16). Torsional

interaction increases the stress cycles, and thus reduces the life of the shaft. The effect of torsional interaction is therefore most critical, since the effect of cyclic fatigue is cumulative.

IV. MATHEMATICAL MODELS

A. The Mechanical System

Figure 1 shows a schematic illustration of a typical tandem compound steam turbo-generator set consisting of a high pressure turbine (HP), an intermediate pressure turbine (IP), and two low pressure turbines, A and B (LPA and LPB). Attached to the common shaft are the generator and exciter rotors.

The following assumptions are made:

a) All rotor masses are lumped and located at discrete mass-points;

b) The shaft mass, which can be distributed and imbedded in rotor masses, is neglected;

c) The shaft damping coefficient is neglected;

d) Mechanical torque inputs are constant, i.e., governor action is not considered.

1. The full model

This mechanical system is an oscillatory system. For each mass, the dynamical behavior is governed by Eq. 1. The complete set of second order differential equations for the system shown in Fig. 1 is given by:

$$\left(\frac{1}{\omega_B}\right)2H_1\ddot{\delta}_1 + D_1\dot{\delta}_1 + K_{12}(\delta_1 - \delta_2) = T_{m1} \qquad (a)$$

$$\left(\frac{1}{\omega_B}\right)2H_2\ddot{\delta}_2 + D_2\dot{\delta}_2 + K_{12}(\delta_2 - \delta_1) + K_{23}(\delta_2 - \delta_3) = T_{m2} \qquad (b)$$

$$\left(\frac{1}{\omega_B}\right)2H_3\ddot{\delta}_3 + D_3\dot{\delta}_3 + K_{23}(\delta_3 - \delta_2) + K_{34}(\delta_3 - \delta_4) = T_{m3} \qquad (c)$$

$$\left(\frac{1}{\omega_B}\right)2H_4\ddot{\delta}_4 + D_4\dot{\delta}_4 + K_{34}(\delta_4 - \delta_3) + K_{45}(\delta_4 - \delta_5) = T_{m4} \qquad (d)$$

$$\left(\frac{1}{\omega_B}\right)2H_5\ddot{\delta}_5 + D_5\dot{\delta}_5 + K_{45}(\delta_5 - \delta_4) + K_{56}(\delta_5 - \delta_6) = -T_e \qquad (e)$$

$$\left(\frac{1}{\omega_B}\right)2H_6\ddot{\delta}_6 + D_6\dot{\delta}_6 + K_{56}(\delta_6 - \delta_5) = 0 \qquad (f)(2)$$

where H is in seconds, δ in radians, D in per unit torque per rad/sec, K in per unit torque per radian, and time in seconds.

The system of Eq. 2 can be written in the matrix form:

$$\left(\frac{1}{\omega_B}\right)2\,\underline{H}\,\ddot{\underline{\delta}} + \underline{D}\,\dot{\underline{\delta}} + \underline{K}\,\underline{\delta} = \underline{T} \qquad (3)$$

where

$\underline{H}$: a diagonal matrix of inertia constants,

$\underline{D}$: a diagonal matrix of mechanical damping constants,

$\underline{K}$: A tridiagonal matrix of shaft stiffness constants, and

$\underline{T}$: a column matrix of forcing torques.

a. Natural frequencies and mode shapes Appendix B shows how the natural frequencies of this mechanical system are determined. It is noted that, for a system of N masses, there are (N-1) natural frequencies. These frequencies are caused by the oscillation of the masses with respect to one another during a disturbance.

For each natural frequency there is a corresponding mode shape as illustrated in Fig. 2. The mode shape is constructed to show the relative angular displacement of each rotor mass-point for a given frequency of oscillation. These modes are identified as mode 1, mode 2, etc., up to mode (N-1).

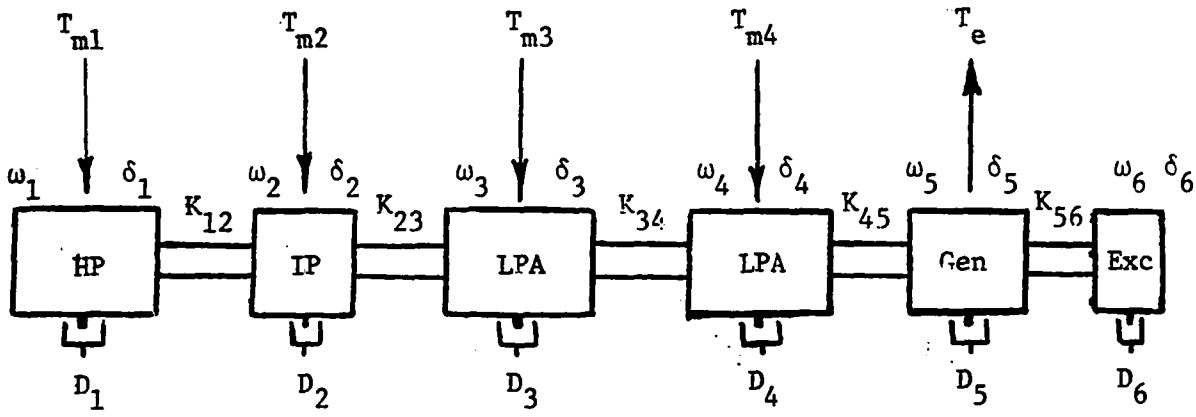

Figure 1. A typical tandem compound steam turbo-generator set.

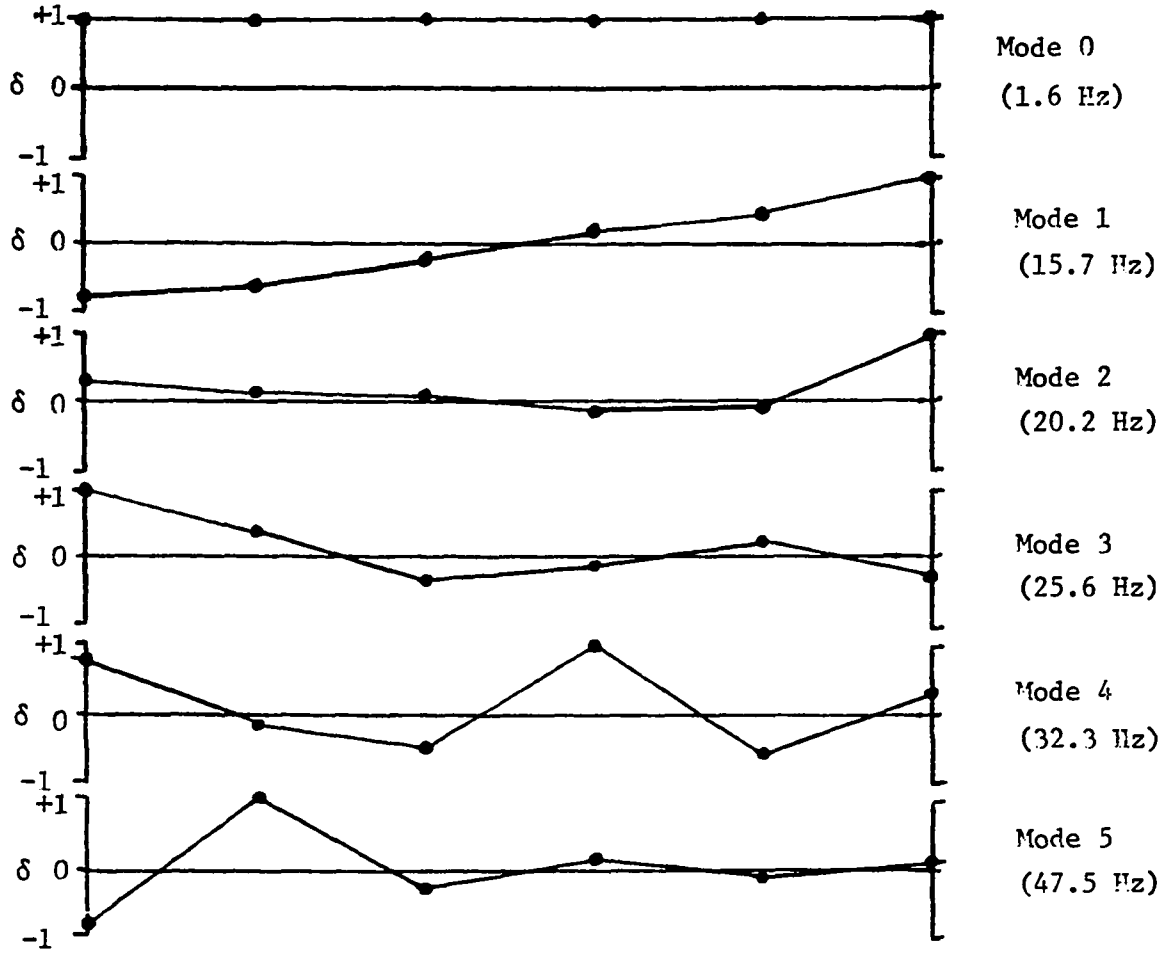

Figure 2. Mode shapes of the mechanical system illustrated in Figure 1.

b. Mode 0 (inertial oscillation) For completeness, it is convenient to denote mode 0 as the mode which corresponds to the frequency by which the mechanical system as a whole oscillates with respect to a given synchronous reference frame. In other words, for mode 0, all masses are rotating in unison. The frequency of oscillation of mode 0 has in fact been known as that of inertial oscillation in power system stability studies. It depends on the system moment of inertia and operating conditions (17). The (N-1) system natural frequencies range normally from 15 Hz to 45 Hz, while the inertial oscillation has a very low range, about 0.50 Hz to 2.5 Hz.

2. The reduced model for modal analysis

If the damping matrix $\underline{D}$ is neglected in Eq. 3, we get

$$\left(\frac{1}{\omega_B}\right) 2\underline{H}\ \ddot{\underline{\delta}} + \underline{K}\ \underline{\delta} = \underline{T} \tag{4}$$

This equation can be transformed into canonical form (18) through a transformation matrix $\underline{Q}$, defined by

$$\underline{\delta}\ \underline{\Delta}\ \underline{Q}\ \underline{\delta}_E \tag{5}$$

We can show that $\underline{Q}$ is a matrix made up of vectors representing the mode shapes discussed previously (see Appendix B).

Equation 4 can be written as

$$\left(\frac{1}{\omega_B}\right) 2\underline{Q}^t\underline{H}\ \underline{Q}\ \ddot{\underline{\delta}}_E + \underline{Q}^t\underline{K}\ \underline{Q}\ \underline{\delta}_E = \underline{Q}^t\underline{T}$$

or

$$\left(\frac{1}{\omega_B}\right) 2\underline{H}_E\ \ddot{\underline{\delta}}_E + \underline{K}_E\ \underline{\delta}_E = \underline{T}_a \tag{6}$$

where

$\underline{H}_E = \underline{Q}^t \underline{H}\ \underline{Q}$, a diagonal matrix,

$\underline{K}_E = \underline{Q}^t \underline{K}\ \underline{Q}$, a diagonal matrix, and

$\underline{T}_a = \underline{Q}^t \underline{T}$, a column matrix.

In this case, it is said that the modes are uncoupled.

If the damping matrix $\underline{D}$ is considered, Eq. 6 becomes:

$$\left(\frac{1}{\omega_B}\right) 2\underline{H}_E\ \ddot{\underline{\delta}}_E + \underline{Q}^t \underline{D}\ \underline{Q}\ \dot{\underline{\delta}}_E + \underline{K}_E\ \underline{\delta}_E = \underline{T}_a \tag{7a}$$

where $\underline{Q}^t \underline{D}\ \underline{Q}$ is generally a non-diagonal but a symmetric matrix.

The solution of Eq. 7a is given in Appendix C. It confirms that the modes which are uncoupled, damping-wise, are coupled amplitude-wise in the presence of mechanical damping.

There is no known method of determining mechanical damping coefficients D's, but the damping coefficients of the individual modes can be measured by tests (19). For this reason, many investigators (12,13,20) use the following modified version of Eq. 7a:

$$\left(\frac{1}{\omega_B}\right) 2\underline{H}_E\ \ddot{\underline{\delta}}_E + \underline{\varepsilon}_M\ \dot{\underline{\delta}}_E + \underline{K}_E\ \underline{\delta}_E = \underline{T}_a \tag{7b}$$

where $\underline{\varepsilon}_M$ is a diagonal matrix whose elements are termed modal damping coefficients, and $\underline{T}_a$ is a column matrix of accelerating torques.

No relation between mechanical damping and modal damping coefficients has yet been established (21). Values of H_E's and K_E's for each mode and for various reference masses are tabulated in Appendix B.

B. The Electrical System

Figure 3 illustrates a bench-mark mmodel of an electrical network as suggested by Reference 13 and used in SSR studies by the IEEE SSR Task Force. Figure 3a shows a one-line diagram of a generator connected to an infinite bus via a series compensated transmission line. Figure 3b shows the d- and q-axes circuits of the generator model, and Fig. 3c shows the relative position of the d- and q-axes with respect to a synchronous reference frame.

The following assumptions are made:

1) Effect of saliency is neglected;
2) Effect of saturation of generator core is omitted;
3) The generator has: one field winding and one damper winding on the d-axis, and two damper windings on the q-axis;
4) Resistance coupling bewteen damper windings is neglected;
5) The impedance of the transmission line is lumped, and its conductance and susceptance are neglected;
6) No local load.

The system of Fig. 3b is described by a set of first order differential equations as follows (see References 17, 22, and 23), where all parameters are in per unit, including time:

Generator:

$$v_d = -ri_d - \dot{\lambda}_d - \omega\lambda_q \qquad (a)$$

$$v_F = r_F i_F + \dot{\lambda}_F \qquad (b)$$

$$0 = r_D i_D + \dot{\lambda}_D \qquad (c)$$

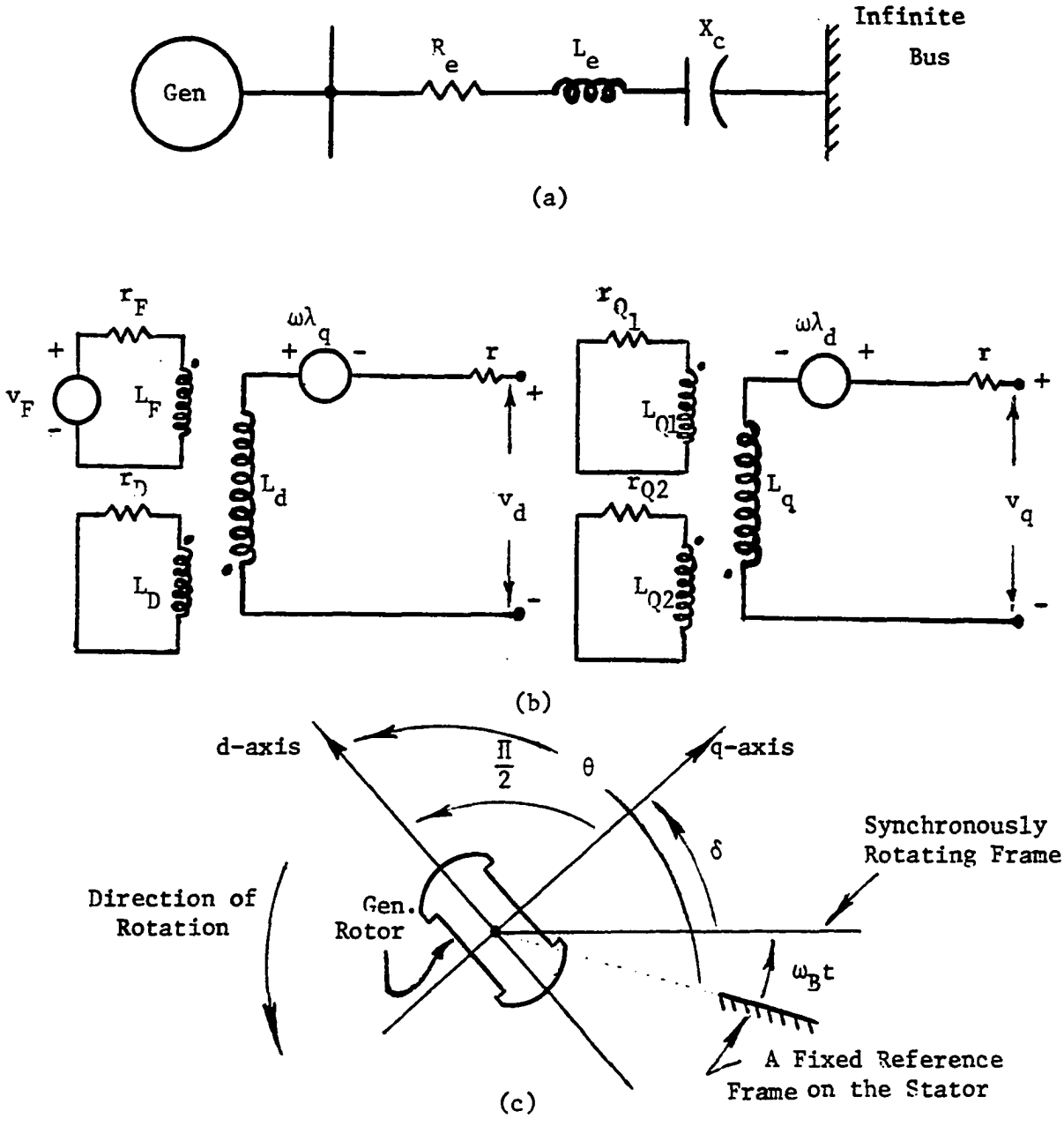

Figure 3. IEEE Task Force's bench-mark model of the electrical system.
(a) One-line diagram.
(b) d- and q-axes of the generator model.
(c) Relative position of the d- and q-axes.

$$v_q = -ri_q - \dot{\lambda}_q + \omega\lambda_d \quad (d)$$

$$0 = r_{Q1}i_{Q1} + \dot{\lambda}_{Q1} \quad (e)$$

$$0 = r_{Q2}i_{Q2} + \dot{\lambda}_{Q2} \quad (f) \quad (8)$$

where

$$\lambda_d = L_d i_d + kM_F i_F + kM_D i_D \quad (a)$$

$$\lambda_F = L_F i_F + kM_F i_d + M_R i_D \quad (b)$$

$$\lambda_D = L_D i_D + kM_D i_d + M_R i_F \quad (c)$$

$$\lambda_q = L_q i_q + kM_{Q1} i_{Q1} + kM_{Q2} i_{Q2} \quad (d)$$

$$\lambda_{Q1} = L_{Q1} i_{Q1} + kM_{Q1} i_q + M_Q i_{Q2} \quad (e)$$

$$\lambda_{Q2} = L_{Q2} i_{Q2} + kM_{Q2} i_q + M_Q i_{Q1} \quad (f) \quad (9)$$

Line:

Starting from abc-frame, we can write:

$$\underline{v}_{abc} = \underline{R}_e \underline{i}_{abc} + \underline{L}_e \dot{\underline{i}}_{abc} + \underline{v}_{cabc} + \underline{v}_{\infty abc} \quad (10)$$

Using a modified Park's transformation matrix (17) defined as:

$$\underline{v}_{0dq} \triangleq \underline{P}\, \underline{v}_{abc} \quad (11)$$

$$\underline{P} = \sqrt{\frac{2}{3}} \begin{bmatrix} 1/\sqrt{2} & 1/\sqrt{2} & 1/\sqrt{2} \\ \cos\theta & \cos(\theta - 2\Pi/3) & \cos(\theta + 2\Pi/3) \\ \sin\theta & \sin(\theta - 2\Pi/3) & \sin(\theta + 2\Pi/3) \end{bmatrix} \quad (12a)$$

where (see Fig. 3c):

$$\theta \triangleq \omega t = \omega_B t + \delta + \Pi/2 \quad (12b)$$

$\underline{P}$ is a non-singular matrix, and the transformation is orthogonal, i.e.,

$$\underline{P}^t = \underline{P}^{-1} \quad (13)$$

Premultiplying Eq. 10 by $\underline{P}$, we get:

$$\underline{v}_{0dq} = \underline{R}_e \underline{i}_{0dq} + \underline{L}_e (\underline{P}\ \dot{\underline{i}}_{abc}) + \underline{v}_{c0dq} + \underline{v}_{\infty 0dq} \tag{14}$$

The term $(\underline{P}\ \dot{\underline{i}}_{abc})$ can be computed in terms of 0dq-components (see Reference 17) to give:

$$(\underline{P}\ \dot{\underline{i}}_{abc}) = \dot{\underline{i}}_{0dq} - \begin{bmatrix} 0 \\ -\omega i_q \\ \omega i_d \end{bmatrix} \tag{15}$$

Equation 14 then becomes:

$$\underline{v}_{0dq} = \underline{R}_e \underline{i}_{0dq} + \underline{L}_e \dot{\underline{i}}_{0dq} - \underline{L}_e \begin{bmatrix} 0 \\ -\omega i_q \\ \omega i_d \end{bmatrix} + \underline{v}_{c0dq} + \underline{v}_{\infty 0dq} \tag{16}$$

Since $\underline{v}_{c0dq}$ are function of $\underline{i}_{0dq}$ and x_c, the series capacitive reactance, we must also express $\underline{v}_{c0dq}$ as state-variables as follows:

$$\dot{\underline{v}}_{cabc} = \left(\frac{1}{C_e}\right) \underline{i}_{abc} \tag{17}$$

Premultiplying Eq. 17 by $\underline{P}$, we get:

$$(\underline{P}\ \dot{\underline{v}}_{cabc}) = \left(\frac{1}{C_e}\right) \underline{P}\ \underline{i}_{abc} = \left(\frac{1}{C_e}\right) \underline{i}_{0dq}$$

From the result obtained in Eq. 15, we have:

$$\dot{\underline{v}}_{c0dq} = \left(\frac{1}{C_e}\right) \underline{i}_{0dq} + \begin{bmatrix} 0 \\ -\omega v_{cq} \\ \omega v_{cd} \end{bmatrix} \tag{18}$$

In per unit system, $\left(\frac{1}{C_e}\right) = (X_c)$. So:

$$\dot{\underline{v}}_{c0dq} = \underline{X}_c \underline{i}_{0dq} + \begin{bmatrix} 0 \\ -\omega v_{cq} \\ \omega v_{cd} \end{bmatrix} \tag{19}$$

Infinite bus voltage:

Let

$$\underline{v}_{\infty abc} = \sqrt{2}\, V_\infty \begin{bmatrix} \cos(\omega_B t) \\ \cos(\omega_B t - 2\Pi/3) \\ \cos(\omega_B t + 2\Pi/3) \end{bmatrix} \tag{20}$$

We can show that (see Reference 17):

$$v_{\infty 0dq} = \underline{P}\, \underline{v}_{\infty abc} = \sqrt{3}\, V_\infty \begin{bmatrix} 0 \\ -\sin\delta \\ \cos\delta \end{bmatrix} \tag{21}$$

where V_∞ is the magnitude of the rms phase voltage of the infinite bus, and δ is defined in Eq. 12b and shown in Fig. 3c. Assuming balanced three-phase operation, we can neglect the zero-sequence component. From Eqs. 14, 19, and 21, we obtain:

$$v_d = R_e i_d + L_e \dot{i}_d + \omega L_e i_q + v_{cd} - \sqrt{3} V_\infty \sin\delta \tag{22a}$$

$$v_q = R_e i_q + L_e \dot{i}_q - \omega L_e i_d + v_{cq} + \sqrt{3} V_\infty \cos\delta \tag{22b}$$

$$\dot{v}_{cd} = X_c i_d - \omega v_{cq} \tag{22c}$$

$$\dot{v}_{cq} = X_c i_q + \omega v_{cd} \tag{22d}$$

Natural frequency of electric system:

The natural frequency of the electrical system (see Fig. 3a) is determined by the ratio of its capacitive reactance to its inductive reactance, i.e.,

$$f_e = \omega_B \sqrt{\frac{X_c}{X_{syst.}}} \qquad \text{(rad/sec)} \tag{23}$$

where $X_{syst.}$ is the net system inductive reactance including the generator inductance which is taken roughly equal to (24):

$$X_{gen} = \left(\frac{f_m}{f_{60}}\right) x''_d \tag{24}$$

The optimum value of X_c used in a given system (2) usually gives a natural frequency that is normally below the synchronous frequency.

Note that there are as many natural frequencies as there are number of circuit configurations that can be made through switching.

C. The Complete Electromechanical System

To tie, mathematically, the mechanical system to the over-all electromechanical system, the system of equations (2) must be in the form of a set of first order differential equations. The procedure is as follows:

Differentiating Eq. 12b with respect to time, we get:

$$\omega = \omega_B + \dot{\delta}$$

or, in per unit,

$$\left(\frac{1}{\omega_B}\right) \dot{\delta} = \omega - 1 \tag{25a}$$

and

$$\left(\frac{1}{\omega_B}\right) \ddot{\delta} = \dot{\omega} \tag{25b}$$

Using Eqs. 25a and 25b, and letting $d = D\omega_B$, the system of equations (2) becomes:

$$2H_1\dot{\omega}_1 + d_1\omega_1 + K_{12}(\delta_1 - \delta_2) = T_{m1} + d_1 \quad \text{(a)}$$

$$2H_2\dot{\omega}_2 + d_2\omega_2 + K_{12}(\delta_2 - \delta_1) + K_{23}(\delta_2 - \delta_3) = T_{m2} + d_2 \quad \text{(b)}$$

$$2H_3\dot{\omega}_3 + d_3\omega_3 + K_{23}(\delta_3 - \delta_2) + K_{34}(\delta_3 - \delta_4) = T_{m3} + d_3 \quad \text{(c)}$$

$$2H_4\dot{\omega}_4 + d_4\omega_4 + K_{34}(\delta_4 - \delta_3) + K_{45}(\delta_4 - \delta_5) = T_{m4} + d_4 \quad \text{(d)}$$

$$2H_5\dot{\omega}_5 + d_5\omega_5 + K_{45}(\delta_5 - \delta_4) + K_{56}(\delta_5 - \delta_6) = -T_e + d_5 \quad \text{(e)}$$

$$2H_6\dot{\omega}_6 + d_6\omega_6 + K_{56}(\delta_6 - \delta_5) = d_6 \quad \text{(f)} \quad (26)$$

From Eq. 25a, we have:

$$\left(\frac{1}{\omega_B}\right)\dot{\delta}_i = \omega_i - 1, \; i = 1, 2, \ldots, 6 \quad (27)$$

There are 21 unknowns, namely: i_d, i_F, i_D, i_q, i_{Q1}, i_{Q2}; v_{cd}, v_{cq}; ω_1, ω_2, ω_3, ω_4, ω_5, ω_6; δ_1, δ_2, δ_3, δ_4, δ_5, δ_6; and T_e.

And there are 20 equations (from Eqs. 8, 22, 26, and 27). However, in Eq. 26e, the electrical developed torque T_e can be expressed as a function of the first 6 variables, using the relation

$$T_e = \lambda_d i_q - \lambda_q i_d \quad (28)$$

Equation 28, if carried out numerically, will give a full load torque equal to 3 per unit (17). It is common standard to choose three-phase full load equal to 1 per unit. Hence, Eq. 28 must be divided by 3:

$$T_e = \frac{1}{3}(\lambda_d i_q - \lambda_q i_d) \quad (29)$$

Using relations 9a and 9d, we get:

$$T_e = \frac{1}{3}\{(L_q i_q)i_d + (kM_F i_q)i_F + (kM_D i_q)i_D$$
$$-(L_q i_d)i_q - (kM_{Q1} i_d)i_{Q1} - (kM_{Q2} i_d)i_{Q2}\} \quad (30)$$

Note that ω in Eqs. 8a, 8d, and 22 is the generator rotor angular velocity, i.e., ω_5 in Eq. 26. Note also that in the equations developed for the electrical system, the time is in per unit. So, it is essential to have the same time base for the overall system. The time base chosen is one second. To convert per unit time to seconds, the following definition is consistent with the per unit system adopted, i.e.,

$$t_u \triangleq \omega_B t, \; t \text{ in seconds} \tag{31}$$

Furthermore, v_d and v_q in Eqs. 8a and 8d can be eliminated by incorporating their values from Eqs. 22a and 22b.

Putting Eqs. 8, 22, 26, and 27 in matrix form, we obtain a first order non-linear differential equation of the form:

$$\underline{A}\,\dot{\underline{X}} = \underline{f}\,(\underline{X}) + \underline{T} \tag{32a}$$

where

$\underline{A}$: a 20 x 20 symmetric non-singular constant coefficient matrix,

$f(\underline{X})$: a 20 x 20 matrix,

$\underline{T}$: a column matrix of size 20, and

$\underline{X} = \{i_d, i_F, i_D, i_q, i_{Q1}, i_{Q2}, v_{cd}, v_{cq}, \omega_1, \omega_2, \omega_3, \omega_4, \omega_5, \omega_6, \delta_1, \delta_2, \delta_3, \delta_4, \delta_5, \delta_6\}$, a column matrix of size 20.

These matrices are shown in detail form in Eq. 32b.

$$
\begin{bmatrix}
(L_d+L_e)/\omega_B & kM_F/\omega_B & kM_D/\omega_B & & & & & \\
kM_F/\omega_B & L_F/\omega_B & M_R/\omega_B & & & & & \\
kM_D/\omega_B & M_R/\omega_B & L_D/\omega_B & & & & & \\
 & & & (L_q+L_e)/\omega_B & kM_{Q1}/\omega_B & kM_{Q2}/\omega_B & & \\
 & & & kM_{Q1}/\omega_B & L_{Q1}/\omega_B & M_Q/\omega_B & & \\
 & & & kM_{Q2}/\omega_B & M_Q/\omega_B & L_{Q2}/\omega_B & & \\
 & & & & & & 1/\omega_B & \\
 & & & & & & & 1/\omega_B
\end{bmatrix}
$$

$$
\begin{bmatrix}
-2H_1 & & & & & & & & & & & \\
 & -2H_2 & & & & & & & & & & \\
 & & -2H_3 & & & & & & & & & \\
 & & & -2H_4 & & & & & & & & \\
 & & & & -2H_5 & & & & & & & \\
 & & & & & -2H_6 & & & & & & \\
 & & & & & & 1/\omega_B & & & & & \\
 & & & & & & & 1/\omega_B & & & & \\
 & & & & & & & & 1/\omega_B & & & \\
 & & & & & & & & & 1/\omega_B & & \\
 & & & & & & & & & & 1/\omega_B & \\
 & & & & & & & & & & & 1/\omega_B
\end{bmatrix}
\begin{bmatrix}
\dot{i}_d \\ \dot{i}_F \\ \dot{i}_D \\ \dot{i}_q \\ \dot{i}_{Q1} \\ \dot{i}_{Q2} \\ \dot{v}_{cd} \\ \dot{v}_{cq} \\ \dot{\omega}_1 \\ \dot{\omega}_2 \\ \dot{\omega}_3 \\ \dot{\omega}_4 \\ \dot{\omega}_5 \\ \dot{\omega}_6 \\ \dot{\delta}_1 \\ \dot{\delta}_2 \\ \dot{\delta}_3 \\ \dot{\delta}_4 \\ \dot{\delta}_5 \\ \dot{\delta}_6
\end{bmatrix} =
$$

(32b)

$$
\begin{bmatrix}
-(R_e + r) & & -\omega_5\times(L_q+L_e) & -\omega_5\times kM_{Q1} & -\omega_5\times kM_{Q2} & -1 \\
& -r_F & & & & \\
& & -r_D & & & \\
\omega_5\times(L_d+L_e) & \omega_5\times kM_F & \omega_5\times kM_D & -(R_e+r) & & -1 \\
& & & -r_{Q1} & & \\
& & & & -r_{Q2} & \\
X_c & & & & & -\omega_5 \\
& & X_c & & & \omega_5 \\
& & & & & d_1 \\
& & & & & d_2 \\
& & & & & d_3 \\
\frac{1}{3}L_d i_q & \frac{1}{3}kM_F i_q & \frac{1}{3}kM_D i_q & -\frac{1}{3}(L_q i_d) & -\frac{1}{3}(kM_{Q1} i_d) & -\frac{1}{3}(kM_{Q2} i_d) \\
& & & & & 1 \\
& & & & & 1 \\
& & & & & 1
\end{bmatrix}
$$

$$
\begin{bmatrix}
 & & & & & & & & \\
 & & & & & & & & \\
 & & & & & & & & \\
 & & & & & & & & \\
 & & & & & & & & \\
 & & & & & & & & \\
 & & & & & & & & \\
 & & & & & & & & \\
 & & & K_{12} & -K_{12} & & & & \\
 & & & -K_{12} & K_{12}+K_{23} & -K_{23} & & & \\
 & & & & -K_{23} & K_{23}+K_{34} & -K_{34} & & \\
d_4 & & & & & -K_{34} & K_{34}+K_{45} & -K_{45} & \\
 & d_5 & & & & & -K_{45} & K_{45}+K_{56} & -K_{56} \\
 & & d_6 & & & & & -K_{56} & K_{56} \\
 & & & & & & & & \\
 & & & & & & & & \\
 & & & & & & & & \\
1 & & & & & & & & \\
 & 1 & & & & & & & \\
 & & 1 & & & & & &
\end{bmatrix}
\begin{bmatrix} i_d \\ i_F \\ i_D \\ i_q \\ i_{Q1} \\ i_{Q2} \\ v_{cd} \\ v_{cq} \\ \omega_1 \\ \omega_2 \\ \omega_3 \\ \omega_4 \\ \omega_5 \\ \omega_6 \\ \delta_1 \\ \delta_2 \\ \delta_3 \\ \delta_4 \\ \delta_5 \\ \delta_6 \end{bmatrix}
+
\begin{bmatrix} \sqrt{3}V_\infty \sin\delta_5 \\ v_F \\ 0 \\ -\sqrt{3}V_\infty \cos\delta_5 \\ 0 \\ 0 \\ 0 \\ 0 \\ -(T_{m1}+d_1) \\ -(T_{m2}+d_2) \\ -(T_{m3}+d_3) \\ -(T_{m4}+d_4) \\ -d_5 \\ -d_6 \\ -1 \\ -1 \\ -1 \\ -1 \\ -1 \\ -1 \end{bmatrix}
\tag{32b}
$$

D. Methods of Analysis

Equation 32 is non-linear: the function $\underline{f}(\underline{X})$ has product non-linearities and the forcing function $\underline{T}$ has trigonometric functions.

The system described by Eq. 32 will be analyzed for two situations: when subjected to small perturbations, and under the influence of major disturbances.

1. Small perturbations

Equation 32 is linearized about a quiescent operating state $\underline{X}_0$ to obtain the set:

$$\underline{\dot{\Delta X}} = \underline{A}\ \underline{\Delta X} + \underline{\Delta U} \tag{33}$$

where $\underline{A}$ is a square matrix, the elements of which depend upon the system parameters and the initial operating state.

The stability of the system described by Eq. 33 is examined from the nature of the eigenvalues of the A-matrix. A special digital computer program available at Iowa State University is used for this analysis.

2. Major disturbances

For this case, the non-linear system described by Eq. 32 is simulated in its entirety on the Iowa State University's analog computer. This analog computer is an Electronic Associates, Model EAI8800. It has 8-channel hot-pen recorder.

In the transient analysis, two disturbances are investigated:

1) A step change in mechanical torque inputs;

2) A three-phase fault at bus B through an inductive reactance to ground (see Fig. 4).

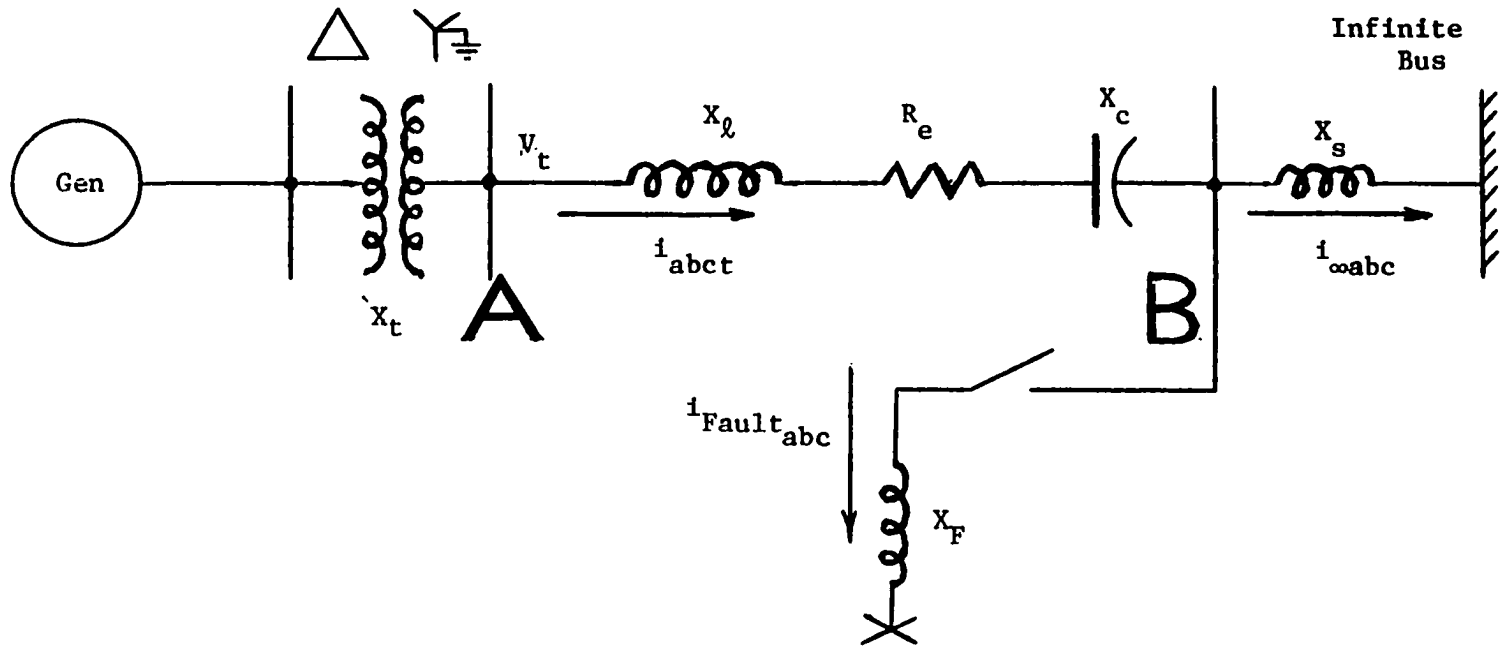

Figure 4. IEEE proposed test system for fault studies.

V. LINEARIZED EQUATIONS AND ANALOG COMPUTER'S EQUATIONS

A. Linearized Equations for Eigenvalue Analysis

In Eq. 32, there are five non-linear terms, namely (ωi), (ωv_c), $\sin\delta$, (ii), and $\cos\delta$.

Using the following relation for each state variable:

$$X \triangleq X_0 + \Delta X \tag{33}$$

where

X_0: initial or steady state value of X,

ΔX: incremental value of X.

The procedure for linearization is illustrated below.

$$\begin{aligned}\omega i &= (\omega_0 + \Delta\omega)(i_0 + \Delta i) \\ &= \omega_0 i_0 + \omega_0 \Delta i + i_0 \Delta\omega + \Delta\cdot\Delta - \text{terms}\end{aligned} \tag{34}$$

Neglecting the higher order terms, we get:

$$\Delta(\omega i) = \omega_0 \Delta i + i_0 \Delta\omega \tag{35a}$$

Similarly, we obtain

$$\Delta(i_d i_q) = i_{d0}\Delta i_q + i_{q0}\Delta i_d \tag{35b}$$

$$\Delta(\omega v_c) = \omega_0 \Delta v_c + v_{c0}\Delta\omega \tag{35c}$$

For trigonometric functions, we have:

$$\sin\delta = \sin(\delta_0 + \Delta\delta) = \sin\delta_0 \cdot \cos\Delta\delta + \cos\delta_0 \cdot \sin\Delta\delta$$

Since $\Delta\delta$ is normally small (in radians), we assume that

$$\sin\Delta\delta \simeq \Delta\delta \text{ and } \cos\Delta\delta \simeq 1$$

Therefore,

$$\Delta(\sin\delta) \simeq \cos\delta_0 \cdot \Delta\delta \tag{36a}$$

Similarly, we obtain:

$$\Delta(\cos\delta) \simeq -\sin\delta_0 \cdot \Delta\delta \tag{36b}$$

Replacing all state-variables in Eq. 32 by their initial and incremental values as obtained in relations 35a, b, and c, and 36a and b, the linearized form of Eq. 32b is obtained. It is shown in Eq. 38, with Δ-prefix omitted for convenience.

B. Analog Computer's Equations

1. Complete electromechanical system model

Defining (17,25)

$$\frac{1}{L_{MD}} \triangleq \frac{1}{L_{AD}} + \frac{1}{\ell_d} + \frac{1}{\ell_F} + \frac{1}{\ell_D}$$

$$\frac{1}{L_{MQ}} \triangleq \frac{1}{L_{AQ}} + \frac{1}{\ell_q} + \frac{1}{\ell_{Q1}} + \frac{1}{\ell_{Q2}}$$

And using relations:

$$\lambda_{AD} = L_{MD}\left(\frac{\lambda_d}{\ell_d} + \frac{\lambda_F}{\ell_F} + \frac{\lambda_D}{\ell_D} - \frac{\Delta\lambda_{AD}}{L_{AD}}\right)^{1} \tag{a}$$

$$\lambda_{AQ} = L_{MQ}\left(\frac{\lambda_q}{\ell_q} + \frac{\lambda_{Q1}}{\ell_{Q1}} + \frac{\lambda_{Q2}}{\ell_{Q2}}\right) \tag{b} \quad (37)$$

And using time in seconds, we obtain the following analog computer's equations from Eqs. 8 and 30:

---

[1] λ_{AD} accounts for saturation in the d-axis, computed as a function of the saturated value of λ_{AD}. It is, however, omitted in this dissertation.

$$
\begin{bmatrix}
(L_d+L_e)/\omega_B & kM_F/\omega_B & kM_D/\omega_B & & & & & \\
kM_F/\omega_B & L_F/\omega_B & M_R/\omega_B & & & & & \\
kM_D/\omega_B & M_R/\omega_B & L_D/\omega_B & & & & & \\
 & & & (L_q+L_e)/\omega_B & kM_{Q1}/\omega_B & kM_{Q2}/\omega_B & & \\
 & & & kM_{Q1}/\omega_B & L_{Q1}/\omega_B & M_Q/\omega_B & & \\
 & & & kM_{Q2}/\omega_B & M_Q/\omega_B & L_{Q2}/\omega_B & & \\
 & & & & & & 1/\omega_B & \\
 & & & & & & & 1/\omega_B
\end{bmatrix}
$$

$$
\begin{bmatrix}
-2H_1 & & & & & & & & & & & & \\
 & -2H_2 & & & & & & & & & & & \\
 & & -2H_3 & & & & & & & & & & \\
 & & & -2H_4 & & & & & & & & & \\
 & & & & -2H_5 & & & & & & & & \\
 & & & & & -2H_6 & & & & & & & \\
 & & & & & & 1/\omega_B & & & & & & \\
 & & & & & & & 1/\omega_B & & & & & \\
 & & & & & & & & 1/\omega_B & & & & \\
 & & & & & & & & & 1/\omega_B & & & \\
 & & & & & & & & & & 1/\omega_B & & \\
 & & & & & & & & & & & 1/\omega_B &
\end{bmatrix}
\begin{bmatrix}
\dot{i}_d \\ \dot{i}_F \\ \dot{i}_D \\ \dot{i}_q \\ \dot{i}_{Q1} \\ \dot{i}_{Q2} \\ \dot{v}_{cd} \\ \dot{v}_{cq} \\ \dot{\omega}_1 \\ \dot{\omega}_2 \\ \dot{\omega}_3 \\ \dot{\omega}_4 \\ \dot{\omega}_5 \\ \dot{\omega}_6 \\ \dot{\delta}_1 \\ \dot{\delta}_2 \\ \dot{\delta}_3 \\ \dot{\delta}_4 \\ \dot{\delta}_5 \\ \dot{\delta}_6
\end{bmatrix} = \tag{38}
$$

$$
\begin{bmatrix}
-(R_e+r) & & -\omega_{50}\times(L_q+L_e) & -\omega_{50}\times kM_{Q1} & -\omega_{50}\times kM_{Q2} & -1 \\
& -r_F & & & & \\
& & -r_D & & & \\
\omega_{50}\times(L_d+L_e) & \omega_{50}\times kM_F & \omega_{50}\times kM_D & -(R_e+r) & & -1 \\
& & & & -r_{Q1} & \\
& & & & & -r_{Q2} \\
X_c & & & & & -\omega_{50} \\
& & X_c & & & \omega_{50}
\end{bmatrix}
$$

$$
\begin{bmatrix}
\frac{1}{3}(L_d i_{q0}-\lambda_{q0}) & \frac{1}{3}kM_F i_{q0} & \frac{1}{3}kM_D i_{q0} & \frac{1}{3}(\lambda_{d0}-L_q i_{d0}) & -\frac{1}{3}kM_{Q1} i_{d0} & -\frac{1}{3}kM_{Q2} i_{d0}
\end{bmatrix}
$$

$$
\left.\begin{array}{cccccccccccc}
 & & & & -\hat{\lambda}_{q0} & & & & & & \sqrt{3}V_\infty \cos\delta_{50} & \\
 & & & & & & & & & & & \\
 & & & & & & & & & & & \\
 & & & & \hat{\lambda}_{d0} & & & & & & \sqrt{3}V_\infty \sin\delta_{50} & \\
 & & & & & & & & & & & \\
 & & & & & & & & & & & \\
 & & & & -v_{cq0} & & & & & & & \\
 & & & & v_{cd0} & & & & & & & \\
d_1 & & & & & & K_{12} & -K_{12} & & & & \\
 & d_2 & & & & & -K_{12} & K_{12}+K_{23} & -K_{23} & & & \\
 & & d_3 & & & & & -K_{23} & K_{23}+K_{34} & -K_{34} & & \\
 & & & d_4 & & & & & -K_{34} & K_{34}+K_{45} & -K_{45} & \\
 & & & & d_5 & & & & & -K_{45} & K_{45}+K_{56} & -K_{56} \\
 & & & & & d_6 & & & & & -K_{56} & K_{56} \\
1 & & & & & & & & & & & \\
 & 1 & & & & & & & & & & \\
 & & 1 & & & & & & & & & \\
 & & & 1 & & & & & & & & \\
 & & & & 1 & & & & & & & \\
 & & & & & 1 & & & & & &
\end{array}\right]
\begin{bmatrix} i_d \\ i_F \\ i_D \\ i_q \\ i_{Q1} \\ i_{Q2} \\ v_{cd} \\ v_{cq} \\ \omega_1 \\ \omega_2 \\ \omega_3 \\ \omega_4 \\ \omega_5 \\ \omega_6 \\ \delta_1 \\ \delta_2 \\ \delta_3 \\ \delta_4 \\ \delta_5 \\ \delta_6 \end{bmatrix}
+
\begin{bmatrix} 0 \\ v_F \\ 0 \\ 0 \\ 0 \\ 0 \\ 0 \\ 0 \\ -T_{m1} \\ -T_{m2} \\ -T_{m3} \\ -T_{m4} \\ 0 \\ 0 \\ 0 \\ 0 \\ 0 \\ 0 \\ 0 \\ 0 \end{bmatrix}
\qquad (38)
$$

where $\lambda_{d0} = L_d i_{d0} + kM_F i_{F0} + kM_D i_{D0}$ $\quad \hat{\lambda}_{d0} = (L_d+L_e) i_{d0} + kM_F i_{F0} + kM_D i_{D0}$

$\lambda_{q0} = L_q i_{q0} + kM_{Q1} i_{Q10} + kM_{Q2} i_{Q20}$ $\quad \hat{\lambda}_{q0} = (L_q+L_e) i_{q0} + kM_{Q1} i_{Q10} + kM_{Q2} i_{Q20}$

$$\lambda_d = \omega_B \int \left[\frac{r}{\ell_d} (\lambda_{AD} - \lambda_d) - \omega_5 \lambda_q - v_d \right] dt \qquad \text{(a)}$$

$$\lambda_F = \omega_B \int \left[\frac{r_F}{\ell_F} (\lambda_{AD} - \lambda_F) + v_F \right] dt \qquad \text{(b)}$$

$$\lambda_D = \omega_B \int \left[\frac{r_D}{\ell_D} (\lambda_{AD} - \lambda_D) \right] dt \qquad \text{(c)} \quad (39)$$

$$\lambda_q = \omega_B \int \left[\frac{r_D}{\ell_q} (\lambda_{AQ} - \lambda_q) + \omega_5 \lambda_d - v_q \right] dt \qquad \text{(a)}$$

$$\lambda_{Q1} = \omega_B \int \left[\frac{r_{Q1}}{\ell_{Q1}} (\lambda_{AQ} - \lambda_{Q1}) \right] dt \qquad \text{(b)}$$

$$\lambda_{Q2} = \omega_B \int \left[\frac{r_{Q2}}{\ell_{Q2}} (\lambda_{AQ} - \lambda_{Q2}) \right] dt \qquad \text{(c)} \quad (40)$$

$$i_d = \frac{1}{\ell_d} (\lambda_d - \lambda_{AD}) \qquad \text{(a)}$$

$$i_q = \frac{1}{\ell_q} (\lambda_q - \lambda_{AQ}) \qquad \text{(b)}$$

$$T_e = \lambda_d i_q - \lambda_q i_d \qquad \text{(c)} \quad (41)$$

Note that Eqs. 39 and 40 contain the voltages v_d and v_q. These are given in Eqs. 22a and 22b, which contain derivatives of i_d and i_q. To avoid differentiating i_d and i_q, we follow the following procedure (see Reference 25). We assume that a large resistance R is placed at the generator terminal. Thus,

$$v_d = (i_d - i_{dt})R \qquad \text{(a)}$$

$$v_q = (i_q - i_{qt})R \qquad \text{(b)} \quad (42)$$

where i_{dt} and i_{qt} are dq-component transmission line currents, and R is arbitrarily large (50 to 100 per unit). Then, from Eq. 22 we obtain:

$$i_{dt} = \omega_B \int \frac{1}{L_e} \{v_d - R_e i_{dt} - \omega_5 L_e i_{qt} - v_{cd} + \sqrt{3}V_\infty \sin \delta_5\} \, dt \quad (a)$$

$$i_{qt} = \omega_B \int \frac{1}{L_e} \{v_q - R_e i_{qt} + \omega_5 L_e i_{dt} - v_{cq} + \sqrt{3}V_\infty \cos \delta_5\} \, dt \quad (b) \quad (43)$$

where infinite bus voltages $\sqrt{3}V_\infty \sin \delta_5$ and $\sqrt{3}V_\infty \cos \delta_5$ are generated by a Resolver (26). From Eqs. 22c and 22d, we have:

$$v_{cd} = \omega_B \int [X_c i_{dt} - \omega_5 v_{cq}] \, dt \quad (a)$$

$$v_{cq} = \omega_B \int [X_c i_{qt} + \omega_5 v_{cd}] \, dt \quad (b) \quad (44)$$

From Eqs. 26 and 27, we have:

$$\omega_1 = \frac{1}{2H_1} \int \{T_{m1} - d_1 \Delta\omega_1 - K_{12}(\delta_1 - \delta_2)\} \, dt \quad (a)$$

$$\omega_2 = \frac{1}{2H_2} \int \{T_{m2} - d_2 \Delta\omega_2 - K_{12}(\delta_2 - \delta_1) - K_{23}(\delta_2 - \delta_3)\} dt \quad (b)$$

$$\omega_3 = \frac{1}{2H_3} \int \{T_{m3} - d_3 \Delta\omega_3 - K_{23}(\delta_3 - \delta_2) - K_{34}(\delta_3 - \delta_4)\} dt \quad (c)$$

$$\omega_4 = \frac{1}{2H_4} \int \{T_{m4} - d_4 \Delta\omega_4 - K_{34}(\delta_4 - \delta_3) - K_{45}(\delta_4 - \delta_5)\} dt \quad (d)$$

$$\omega_5 = \frac{1}{2H_5} \int \{-\frac{T_e}{3} - d_5 \Delta\omega_5 - K_{45}(\delta_5 - \delta_4) - K_{56}(\delta_5 - \delta_6)\} dt \quad (e)$$

$$\omega_6 = \frac{1}{2H_6} \int \{-d_6 \Delta\omega_6 - K_{56}(\delta_6 - \delta_5)\} \, dt \quad (f)$$

where

$$\Delta\omega_i = \omega_i - 1 \quad (g)$$

$$\delta_i = \omega_B \int (\omega_i - 1) \, dt \qquad i = 1, 2, \ldots, 6 \quad (h) \quad (45)$$

2. Reduced mechanical system model

For modal analysis, the electrical system's equations remain unchanged, except for the value of the generator rotor impedances which must be adjusted to reflect the effect of a given mode (5,13).

For the mechanical system, however, Eqs. 45 are reduced according to Eq. 7b as follows:

$$\omega_E = \frac{1}{2H_E} \int \{T_a - \varepsilon \Delta\omega_E - K_E \delta_E\} \, dt \qquad (a)$$

$$\delta_E = \omega_B \int [\omega_E - 1] \, dt \qquad (b) \qquad (46)$$

where, in per unit, we have:

$$\left(\frac{1}{\omega_B}\right) \dot{\delta}_E = \omega_E - 1 \triangleq \Delta\omega_E$$

$$\left(\frac{1}{\omega_B}\right) \ddot{\delta}_E = \dot{\omega}_E$$

and

$$\varepsilon \triangleq \varepsilon_M \omega_B$$

and T_a is defined by Eq. 6.

It is customary to refer the modal equivalent mass inertia constant, H_E, and the modal equivalent spring constant, K_E, to the generator rotor mass (13). When this is followed, it is essential to interpret δ_E as incremental value contributed to the generator rotor angular deviation by the mode of oscillation in question. The contribution factor of each mode to the generator rotor angular displacement is governed by Eq. 5. If there are no subsynchronous oscillations, the deviation of the generator rotor angle (δ_5) is the same as δ_E of the mode 0.

This model therefore is convenient for studying any particular mode of oscillation. Furthermore, in working with the analog computer, it is convenient to include mode 0 in addition to the mode chosen. This is done to establish the system's initial conditions which are usually computed beforehand using mode 0 for electromechanical effect.

The analog computer patching diagrams for the electrical and for the two models of the mechanical system are shown in Figs. 5 and 6 respectively. Figure 6b shows the reduced model of the mechanical system under the influence of mode 2.

3. Three-phase fault simulation

For Fig. 4, we can derive the following equations:

$$\underline{v}_{abc} = \underline{R}_e \underline{i}_{abct} + \underline{L} \dot{\underline{i}}_{abct} + \underline{v}_{cabc} + \underline{L}_s \dot{\underline{i}}_{\infty abc} + \underline{v}_{\infty abc} \tag{47}$$

and

$$\underline{L}_f (\dot{\underline{i}}_{abct} - \dot{\underline{i}}_{\infty abc}) = \underline{L}_s \dot{\underline{i}}_{\infty abc} + \underline{v}_{\infty abc} \tag{48}$$

From Eq. 48, we write

$$\dot{\underline{i}}_{\infty abc} = \left(\frac{1}{L_s + L_f}\right) \{\underline{L}_f \dot{\underline{i}}_{abct} - \underline{v}_{\infty abc}\} \tag{49}$$

Substituting Eq. 49 in Eq. 47, we get:

$$\underline{v}_{abc} = \underline{R}_e \underline{i}_{abct} + \left[L + \frac{L_s L_f}{L_s + L_f}\right] \dot{\underline{i}}_{abct} + \underline{v}_{cabc} + \left[\frac{L_f}{L_s + L_f}\right] \underline{v}_{\infty abc} \tag{50}$$

Comparing Eq. 50 with Eq. 10, we draw the following conclusions pertaining to the simulation of a 3ϕ-fault:

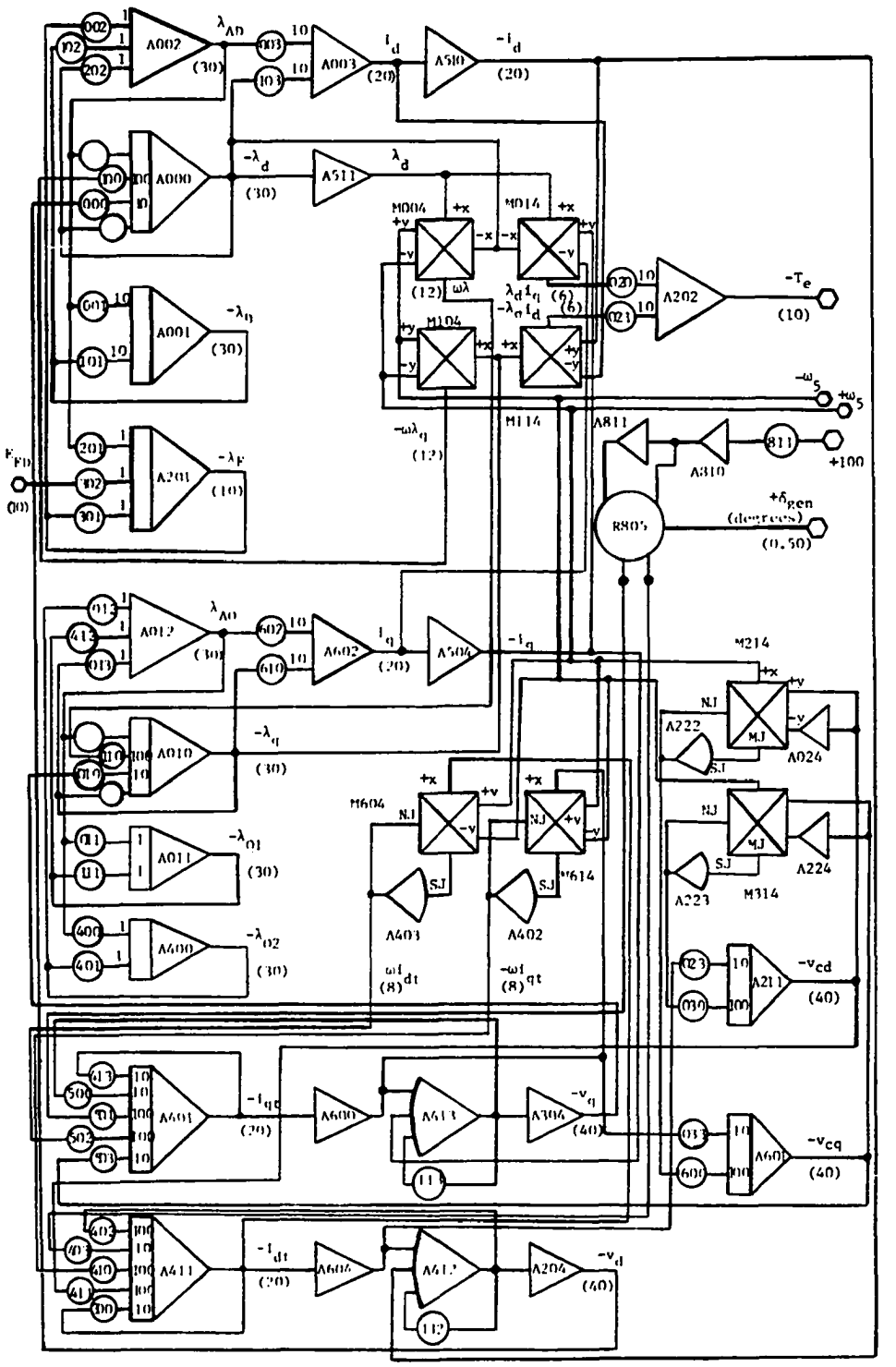

Figure 5. Patching diagram for the electrical system: A synchronous generator connected to an infinite bus via a series compensated transmission line.

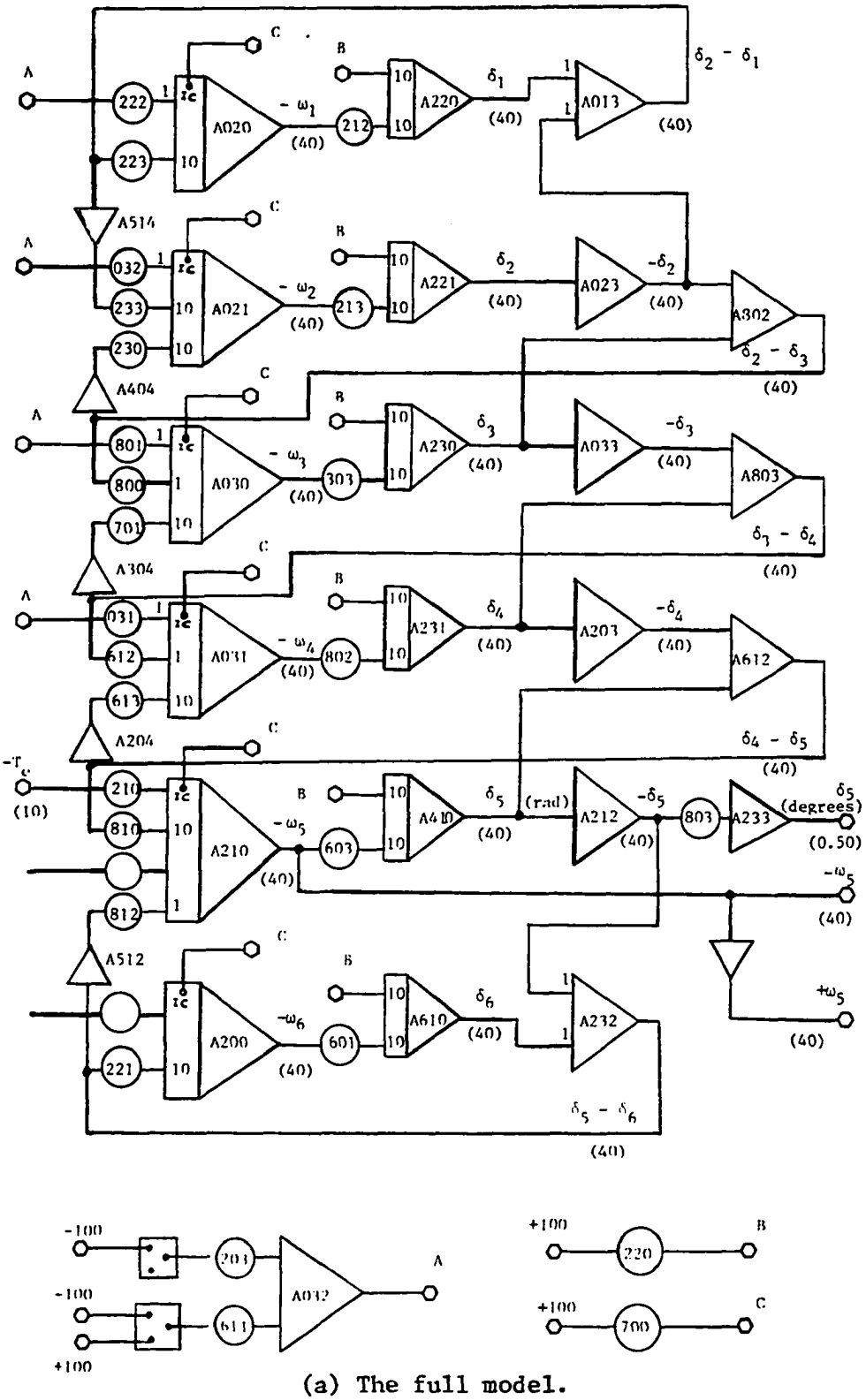

(a) The full model.

Figure 6. Patching diagram for the mechanical system:

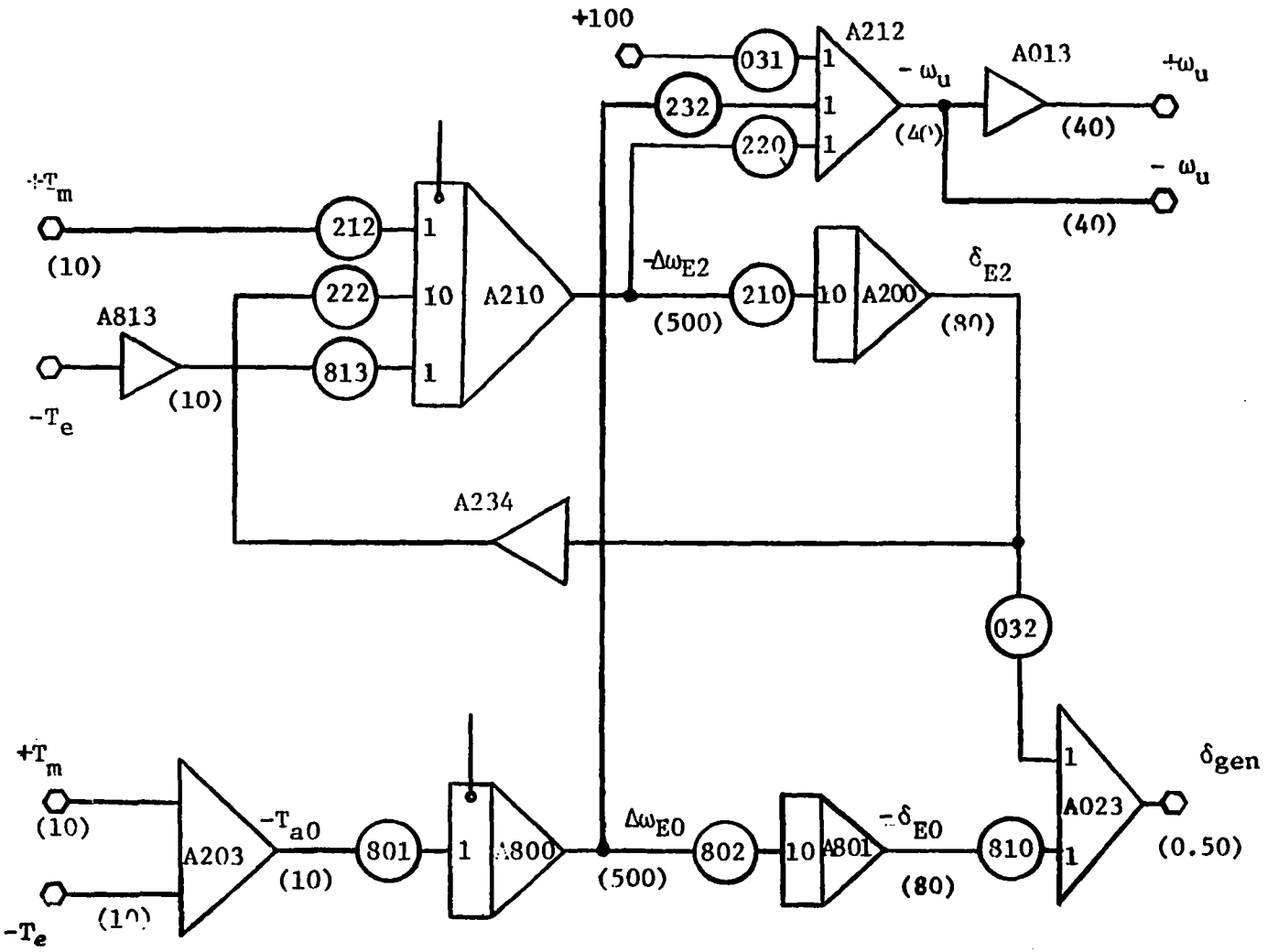

(b) The reduced model for Modal Analysis.

Figure 6. (continued)

(a) L_e becomes $\left[L + \frac{L_s L_f}{L_s + L_f}\right]$, $L = X_t + X_\ell$ in p.u.;

(b) The coefficient of $\underline{v}_{abc}$, which was unity, becomes $\left[\frac{L_f}{L_s + L_f}\right]$;

(c) To simulate the fault, the values of potentiometers which are affected by the above coefficients are changed accordingly;

(d) The validity of Eq. 50 can be checked by letting L_f equal to infinity to obtain the no-fault condition.

Patching diagrams for pertinent components and logic control for fault application and clearing are shown in Fig. 7.

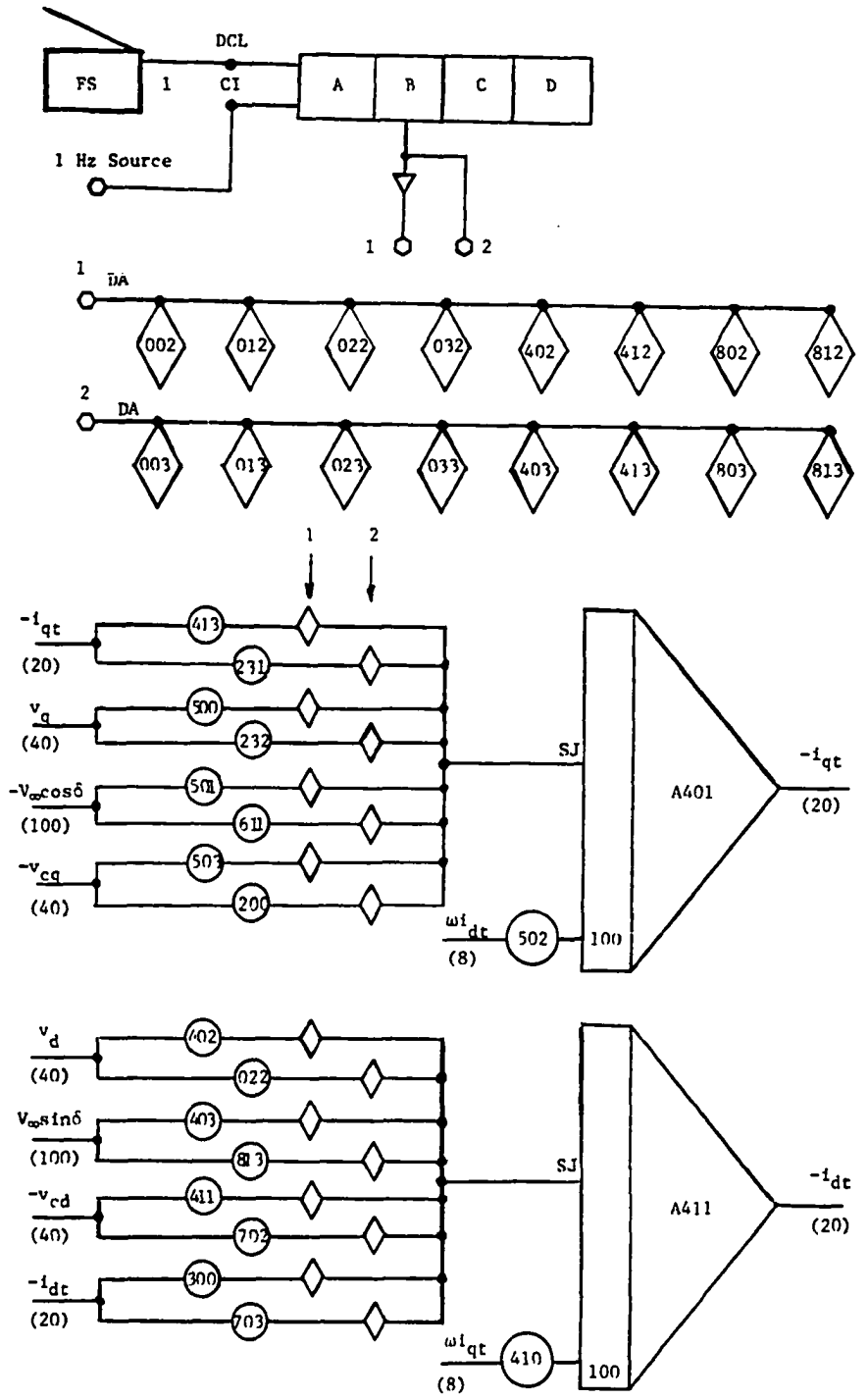

Figure 7. Patching diagram for three-phase fault simulation and logic patching.

VI. NUMERICAL RESULTS

The values of the system parameters used are given in Appendix D. The armature resistance r is neglected.

A. Dynamic Stability Analysis: Effect of Variation of System Parameters

For the small perturbation case, the generator is operated at light load (0.01 pu power), with 90% lagging power factor. The generator terminal voltage is maintained constant at 1.00 pu. The electrical system is also simplified by omitting the d-axis damper winding (D-circuit) and one of the two q-axis damper windings (Q2-circuit), and by assuming that the system's inherent damping is proportional to the generator rotor speed deviation (25). In so doing, the matrix Eq. 32b is reduced to 18th order.

1. Effect of the variation of X_c on the modal decrement factors

The main purpose of this analysis is to have a general picture of the extent of the effects of subsynchronous resonance upon a given system, and to identify the various critical modes as line compensation changes.

The computation of eigenvalues is carried out by adjusting the system initial values for each value of X_c chosen (see Table 1). Note that the impedances of the generator rotor circuits are maintained constant for convenience.

To concentrate on SSR effects, all mechanical damping coefficients are neglected here. The eigenvalues obtained are shown in Table 2.

Table 1. The system initial conditions.[a]

i_{d0} = -0.008685 pu i_{q0} = +0.017173 pu i_{F0} = 1.052198 pu	λ_{d0} = 1.731103 pu λ_{q0} = 0.029366 pu	$\hat{\lambda}_{d0}$ = 1.725024 pu $\hat{\lambda}_{q0}$ = 0.041387 pu

X_c (pu)	δ_0 (degrees)	V_∞ (pu)	$\sqrt{3}V_\infty\cos\delta_0$ (pu)	$\sqrt{3}V_\infty\sin\delta_0$ (pu)	v_{cd0} (pu)	$-v_{cq0}$ (pu)
0.05	1.35	0.996673	1.725810	0.040614	-0.000859	0.000434
0.10	1.32	0.996911	1.726242	0.039777	-0.001717	0.000869
0.20	1.26	0.997391	1.727114	0.037987	-0.003435	0.001737
0.287	1.21	0.997808	1.727869	0.036495	-0.004929	0.002492
0.30	1.20	0.997871	1.727984	0.036196	-0.005152	0.002606
0.371	1.16	0.998212	1.728600	0.035002	-0.006372	0.003221
0.40	1.15	0.998351	1.728849	0.034603	-0.006869	0.003474
0.42	1.14	0.998448	1.729023	0.034259	-0.007213	0.003648
0.4235	1.13	0.998465	1.729054	0.034199	-0.007272	0.003680
0.45	1.12	0.998592	1.729282	0.033808	-0.007728	0.003909
0.50	1.09	0.998833	1.729717	0.032885	-0.008587	0.004343
0.55	1.06	0.999075	1.730152	0.032026	-0.009445	0.004777
0.60	1.03	0.999316	1.730585	0.031168	-0.010304	0.005212
0.65	1.00	0.999558	1.731022	0.030216	-0.011162	0.005646
0.70	0.97	0.999800	1.731454	0.029450	-0.012021	0.006080

[a] P_0=0.01 pu, PF=0.90 lagging. Z_r=0.0076 + j0.0408 pu, Z_Q=0.00998 + j0.04556 (pu). V_t=1.00 pu.

Table 2. Eigenvalues obtained with the initial conditions of Table 1.

Mode Identification	X_c=0pu	X_c=.05pu	X_c=.10pu	X_c=.20pu	X_c=.40pu
Electrical Network	-8.652338 ± j377.0	-4.6724 ± j467.12	-4.781274 ± j504.55	-4.910003 ± j557.46	-5.055100 ± j632.26
		-3.763983 ± j286.66	-3.413968 ± j249.12	-3.08390 ± j196.92	-.542853 ± j120.97
Mode 5	± j298.20	± j298.20	± j298.20	± j298.20	± j298.20
Mode 4	-.000689 ± j203.00	+.001290 ±j 203.02	+.007091 ± j203.07	+.404950 ± j202.16	-.001458 ± j202.88
Mode 3	-.001463 ± j160.62	-.001095 ± j160.63	-.000569 ± J160.65	+.005910 ± j160.74	+.003265 ± j160.46
Mode 2	-.000760 ± j127.02	-.000765 ± j127.03	-.000801 ± j127.03	-.000796 ± j127.04	+.046826 ± j126.68
Mode 1	-.014224 ± j99.13	-.015292 ± j99.16	-.016984 ± j99.20	-.021880 ± j99.31	-.087134 ± j100.36
Mode 0 or Inertial Oscillation	-1.826965 ± j7.75	-1.946400 ± j7.97	-2.081489 ± j8.20	-2.412050 ± j8.72	-3.499558 ± j10.18
Rotor Circuits Inverse Time-constants	-4.875695	-5.069224	-5.287783	-5.822785	-7.574879
	-2.711976	-2.714139	-2.716776	-2.722223	-2.733641

X_c=.45pu	X_c=.50pu	X_c=.60pu	X_c=.70pu
-5.080951 ± j647.75	-5.104292 ± j662.40	-5.145059 ± j689.65	-5.179803 ± j714.70
+3.953181 ± j103.20	+4.504033 ± j95.10	+4.506142 ± j65.38	+10.460010 ± j42.12
± j298.20	± j298.20	± j298.20	± j298.20
-.002282 ± j202.89	-.002878 ± j202.90	-.003798 ± j202.92	-.004655 ± j202.93
-.000079 ± j160.50	-.001582 ± j160.52	-.003195 ± j160.55	-.004404 ± j160.57
+.002448 ± j126.93	+.000005 ± j126.97	-.001240 ± j127.00	-.001931 ± j127.00
-3.719987 ± j102.33	-3.236279 ± j95.70	-.040703 ± j98.30	-.042444 ± j98.70
-3.938110 ± j10.67	-4.501536 ± j11.23	-6.301594 ± j12.58	-9.763517 ± j13.54
-8.272365	-9.155820	-11.855730	-16.754630
-2.736620	-2.739668	-2.745920	-2.752422

From the data of Table 2, a plot of the decrement factors versus the series capacitive reactance (or line compensation) is shown in Fig. 8.

From Fig. 8, a graph of the mechanical system natural frequencies (f_m) versus the series capacitance (X_c) is obtained. Three zones of interest are shown: a zone of Torsional Interaction, a zone of Self-excitation, and a zone of Combined Effect of SSR (see Fig. 9).

2. Effect of the variation of d_1 and d_5 on the modal decrement factors

The system is being operated at light load and under the influence of mode 3, i.e., the capacitive reactance X_c is chosen equal to 0.287 pu. The mechanical damping is first introduced at the HP-turbine (d_1) with all other d's equal to zero. Then the location of the mechanical damping is shifted to the generator rotor mass (d_5).

Eigenvalues obtained for different values of d_1 and d_5 are shown in Tables 3 and 4 respectively.

3. Effect of the variation of the line resistance R_e on mode 3

The system is operated at light load and under the influence of mode 3. All mechanical damping coefficients are zero. The line resistance R_e is varied from 0.02 pu to 0.873 pu. Eigenvalues obtained are shown in Table 5.

4. Effect of reducing field circuit resistance r_F on mode 1

The system is operated at light load, and under the influence of mode 1, i.e., X_c is equal to 0.50 pu.

The graph of Fig. 9 indicates that, at this value of line compensation, the generator is self-excited and is also subjected to torsional interaction in mode 2, while mode 1 is very well damped. The rotor circuits' impedances

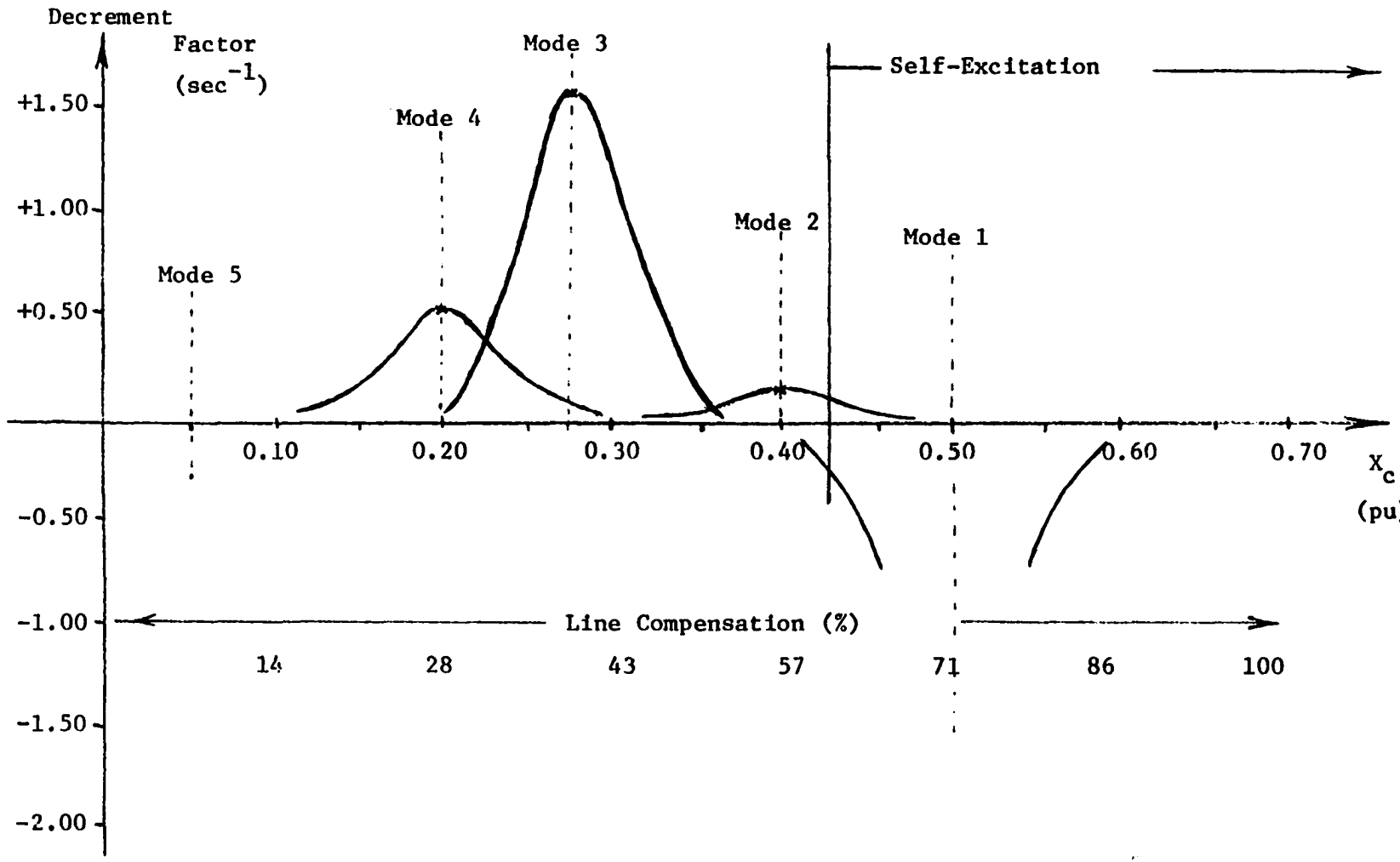

Figure 8. Decrement factor vs. X_c (or line compensation).

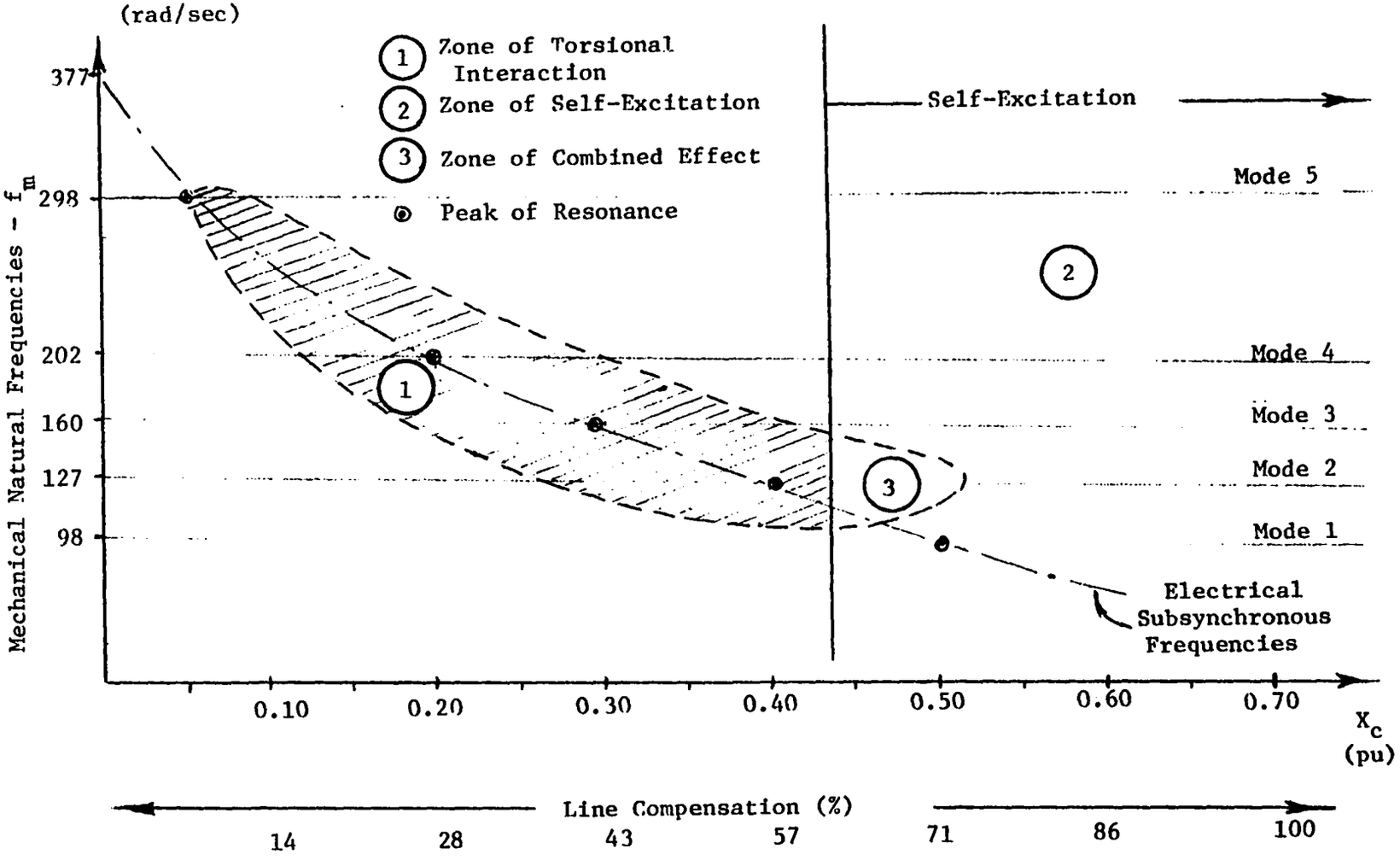

Figure 9. Zones of influence of subsynchronous resonance.

Table 3. Effect of changing d_1.[a]

Mode Identification	d_1=0	d_1=.50	d_1=1.50	d_1=2.05	d_1=2.16	d_1=2.20
Electrical Network	-4.98±j593.20 -3.45±j160.48	-4.98±j593.20 -3.67±j160.50	-4.98±j593.20 -4.24±j160.53	-4.98±j593.20 -4.63±j160.54	-4.98±j593.20 -4.72±j160.54	-4.98±j593.20 -4.75±j160.54
Mode 5	±j298.20	-.345 ±j298.20	-1.034 ±j298.15	-1.413 ±j298.12	-1.489 ±j298.20	-1.516 ±j298.12
Mode 4	+.005 ±j202.81	-.057 ±j202.81	-.181 ±j202.80	-.249 ±j202.78	-.262 ±j202.78	-.267 ±j202.78
Mode 3	+1.546 ±j160.58	+1.115 ±j160.55	+.380 ±j160.49	+.054 ±j160.45	-.005 ±j160.45	-.026 ±j160.44
Mode 2	-.000110 ±j127.08	-.042 ±j127.08	-.125 ±j127.08	-.171 ±j127.08	-.180 ±j127.08	-.183 ±j127.08
Mode 1	-.030 ±j99.49	-.231 ±j99.49	-.634 ±j99.50	-.855 ±j99.52	-.899 ±j99.52	-.915 ±j99.52
Mode 0 or Inertial Oscillation	-2.792 ±j9.28	-2.845 ±j9.29	-2.950 ±j9.31	-3.007 ±j9.33	-3.019 ±j9.33	-3.023 ±j9.33
Rotor Circuits' Inverse Time-constants	-6.437 -2.727	-6.437 -2.712	-6.437 -2.682	-6.437 -2.665	-6.437 -2.662	-6.437 -2.661

[a] P_0=0.01 pu, PF=0.90 Lag. Other d's are zero. X_c=.287 pu.

Table 4. Effect of changing d_5.[a]

Mode Identification	$d_5 = 0$	$d_5 = 50.$	$d_5 = 70.$	$d_5 = 76.75$	$d_5 = 77.15$	$d_5 = 80.$
Electrical Network	-4.98±j593.20	-4.98±j593.20	-4.98±j593.20	-4.98±j593.20	-4.98±j593.20	-4.98±j593.20
	-3.45±j160.48	-4.19±j160.20	-4.57±j160.0	-4.70±j159.90	-4.72±j159.90	-4.78±j159.90
Mode 5	±j298.20	-.0011 ±j298.20	-.0015 ±j298.20	-.0016 ±j298.20	-.00165 ±j298.20	-.0017 ±j298.20
Mode 4	+.005 ±j202.81	-3.111 ±j202.30	-4.265 ±j201.80	-4.635 ±j201.60	-4.656 ±j201.60	-4.809 ±j201.50
Mode 3	+1.546 ±j160.58	+.444 ±j160.67	+.103 ±j160.68	+.000639 ±j160.68	-.005 ±j160.68	-.0464 ±j160.68
Mode 2	-.000110 ±j127.08	-.466 ±j127.00	-.636 ±j126.90	-.689 ±j126.90	-.692 ±j126.90	-.714 ±j126.90
Mode 1	-.030 ±j99.49	-4.773 ±j99.25	-6.726 ±j99.00	-7.397 ±j98.90	-7.437 ±j98.88	-7.722 ±j98.82
Mode 0 or Inertial Oscillation	-2.792 ±j9.28	-7.564 ±j10.00	-9.443 ±j9.90	-10.084 ±j9.80	-10.122 ±j9.78	-10.394 ±j9.73
Rotor Circuits' Inverse Time-constants	-6.437	-6.437	-6.437	-6.437	-6.437	-6.437
	-2.727	-1.643	-1.398	-1.330	-1.326	-1.300

[a] P_0=0.01 pu, PF=0.90 Lag. Other d's are zero. X_c=.287 pu.

Table 5. Effect of changing R_e.[a]

Mode Identification	R_e = 0.02 pu	R_e = 0.45 pu	R_e = 0.50 pu	R_e = 0.62 pu	R_e = 0.853 pu	R_e 0.873 pu
Electrical	-4.98 ±j293.20	-97.81 ±j569.64	-108.59 ±j563.73	-134.41 ±j545.96	-184.21 ±j488.63	-188.42 ±j481.16
Network	-3.45 ±j160.48	-97.18 ±j181.92	-108.26 ±j187.77	-134.80 ±j205.53	-186.42 ±j263.02	-190.91 ±j270.51
Mode 5	±j298.20	±j298.20	±j298.20	±j298.20	±j298.20	±j298.20
Mode 4	+.005 ±j202.81	+.022 ±j202.90	+.017 ±j202.90	+.006 ±j202.90	-.008 ±j202.89	-.009 ±j202.89
Mode 3	+1.546 ±j160.58	+.033 ±j160.57	+.026 ±j160.57	+.014 ±j160.56	+.0001 ±j160.55	-.0006 ±j160.55
Mode 2	-.000110 ±j127.08	+.011 ±j127.01	+.009 ±j127.01	+.005 ±j127.01	+.001 ±j127.01	+.001 ±j127.01
Mode 1	-.030 ±j99.94	+.114 ±j99.05	+.096 ±j99.02	+.060 ±j98.96	+.015 ±j98.90	+.012 ±j98.89
Mode 0 or Inertial Oscillation	-2.792 ±j9.28	-1.157 ±j8.21	-.952 ±j7.99	-.537 ±j7.43	-.0003 ±j6.43	+.0322 ±j6.35
Rotor Circuits' Inverse Time-constants	-6.437	-5.639	-5.507	-5.204	-4.690	-4.650
	-2.727	-2.733	-2.734	-2.738	-2.748	-2.749

[a] P_0=0.01 pu, PF=0.90 Lag., all d's are zero. X_c=0.287 pu.

are adjusted to reflect mode 1 oscillation. The full model for the mechanical system is used with all damping coefficients (d's) neglected.

Then, the field circuit resistance (r_F) is reduced from 0.00587 pu to 0.000005 pu.

Similar analysis is also carried out with the reduced model for the mechanical system corresponding to mode 1. Table 6 shows the eigenvalues obtained using the full model for the mechanical system, and Table 7 shows those obtained using the reduced model.

B. Transient Stability Analysis: Effect of SSR on System Components

For this case, the generator is operated at high load (P_0 = 0.90 pu), and under the conditions of mode 2, i.e., X_c is equal to 0.371 pu, and the generator rotor circuits and fault impedances are given in Appendix D, (see parameters for transient analysis). The mechanical system is simulated with the full model, with the damping coefficients (d's) neglected.

However, in the absence of additional mechanical damping (other than damping provided by the damper windings), the system, being unstable, cannot be simulated on the analog computer for a reasonable length of time. For this reason, an arbitrary value of mechanical damping is introduced to bring the system to a relatively less unstable state.

The analysis is carried out with the following assumptions:

a) Constant field voltage;

b) A step change of 10% in mechanical torque-inputs;

Table 6. Effect of reducing r_F, using the full model for the mechanical system.[a]

Mode Identification	r_F = 0.00587 pu	r_F = 0.00100 pu	r_F = 0.000010 pu	r_F = 0.000005 pu
Electrical Network	-4.943604±j661.70 +4.222482±j95.85	-4.731003±j661.71 +3.547243±j96.47	-4.687779±j661.71 +3.443921±j96.60	-4.687561±j661.71 +3.443424±j96.60
Mode 5	±j298.20	±j298.20	±j298.20	±j298.20
Mode 4	-0.002971±j202.90	-0.001085±j202.90	-0.000839±j202.90	-0.000838±j202.90
Mode 3	-0.000600±j160.52	+0.001667±j160.52	+0.002128±j160.52	+0.002130±j160.52
Mode 2	+0.001245±j126.96	+0.003948±j126.97	+0.004497±j126.97	+0.004500±j126.97
Mode 1	-3.975783±j95.54	-4.849761±j94.87	-5.061864±j94.76	-5.062959±j94.76
Mode 0 or Inertial Oscillation	-3.980215±j11.67	-3.961703±j11.68	-3.957788±j11.68	-3.957769±j11.68
Rotor Circuits' Inverse Time-constants	-6.848212 -2.312183	-1.163511 -2.319532	-0.011652 -2.316598	-0.005829 -2.316591

[a] P_0=0.01 pu, PF=0.90 Lag. X_c=0.50 pu. No mechanical damping.

Table 7. Effect of reducing r_F, using the reduced model for the mechanical system.[a]

Mode Identification	r_F = 0.00587 pu	r_F = 0.001000 pu	r_F = 0.000010 pu	r_F = 0.000005 pu
Electrical	-4.943489±j661.61	-4.730831±j661.62	-4.687573±j661.62	-4.687354±j661.62
Network	+4.248955±j95.98	+3.580586±j96.57	+3.478195±j96.68	+3.477692±j96.68
Mode 1	-4.028524±j95.67	-4.883861±j95.04	-5.091728±j94.94	-5.092790±j94.94
Rotor Circuits' Inverse Time-constants	-6.846544 -10.225280	-1.166600 -10.229620	-0.011662 -10.229830	-0.005831 -10.229830

[a] P_0=0.01 pu, PF=0.90 Lag. X_c=0.50 pu. No mechanical damping.

c) A three-phase fault arbitrarily applied at bus B (see Fig. 4), regardless of the value of line voltage at the moment of fault initiation;

d) Simultaneous clearing of fault on all three phases.

Figure 10a illustrates the behavior of the system with no mechanical damping introduced. The amplification of mode 2 oscillation at 127 rad/sec (20.2 Hz) due to torsional interaction is clearly shown.

When a damping coefficient is applied at the exciter rotor ($d_6 = 0.345$), the torsional oscillation is very well damped out as shown in Fig. 10b.

Figure 11 illustrates the various system parameters before, during, and after a three-phase fault is applied for 0.075 second. A damping coefficient of $d_5 = 1.74$ is introduced at the generator rotor mass. This value of damping is not enough to damp out the oscillation due to torsional interaction.

The same analysis is carried out for a damping coefficient d_5 equal to 59.06, and the resulting system behavior is shown in Fig. 12a. Note that the oscillation due to torsional interaction is then well damped. Figure 12b shows the torques experienced by various sections of the shaft. Particularly serious stress cycles are observed during the fault and thereafter.

Figure 13 illustrates the effect of the fault duration upon the various components of the system subjected to torsional interaction.

C. Discussions of Results

From the results obtained in the above stability analyses, the following remarks are in order:

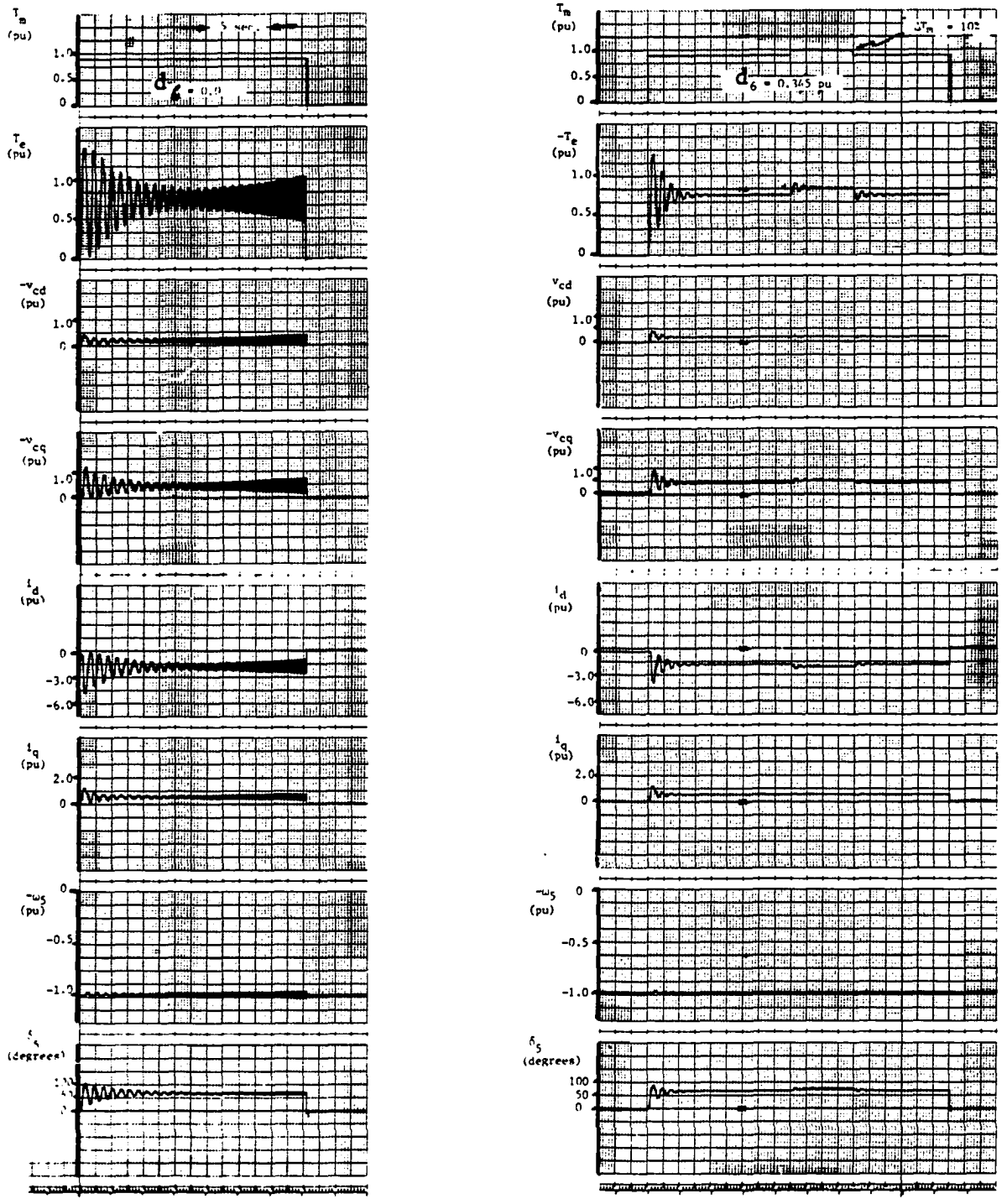

Figure 10. System's dynamic responses:

(a) No damping.

(b) With damping $d_6 = 0.345$.

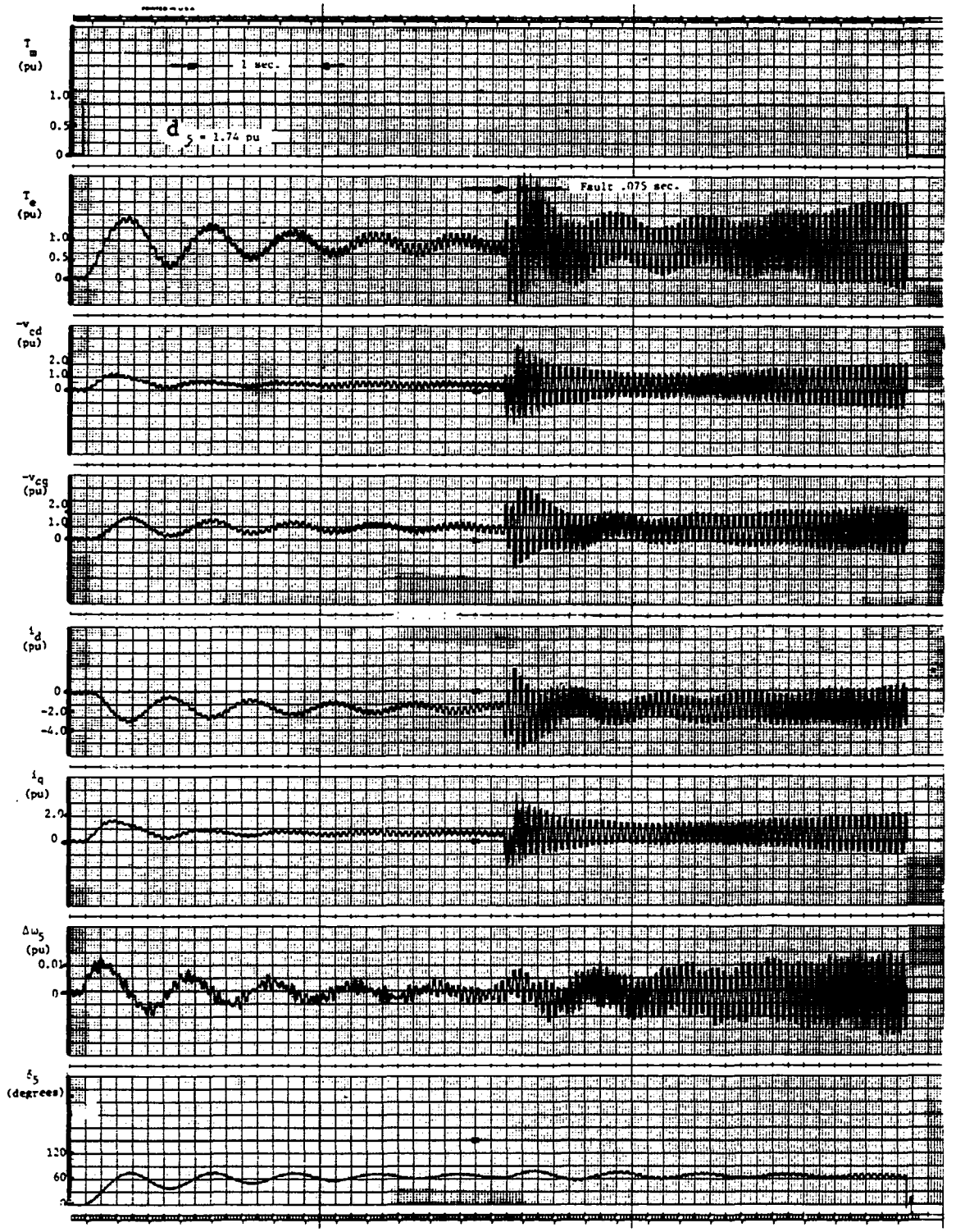

Figure 11. Transient responses before, during, and after a three-phase fault is applied.

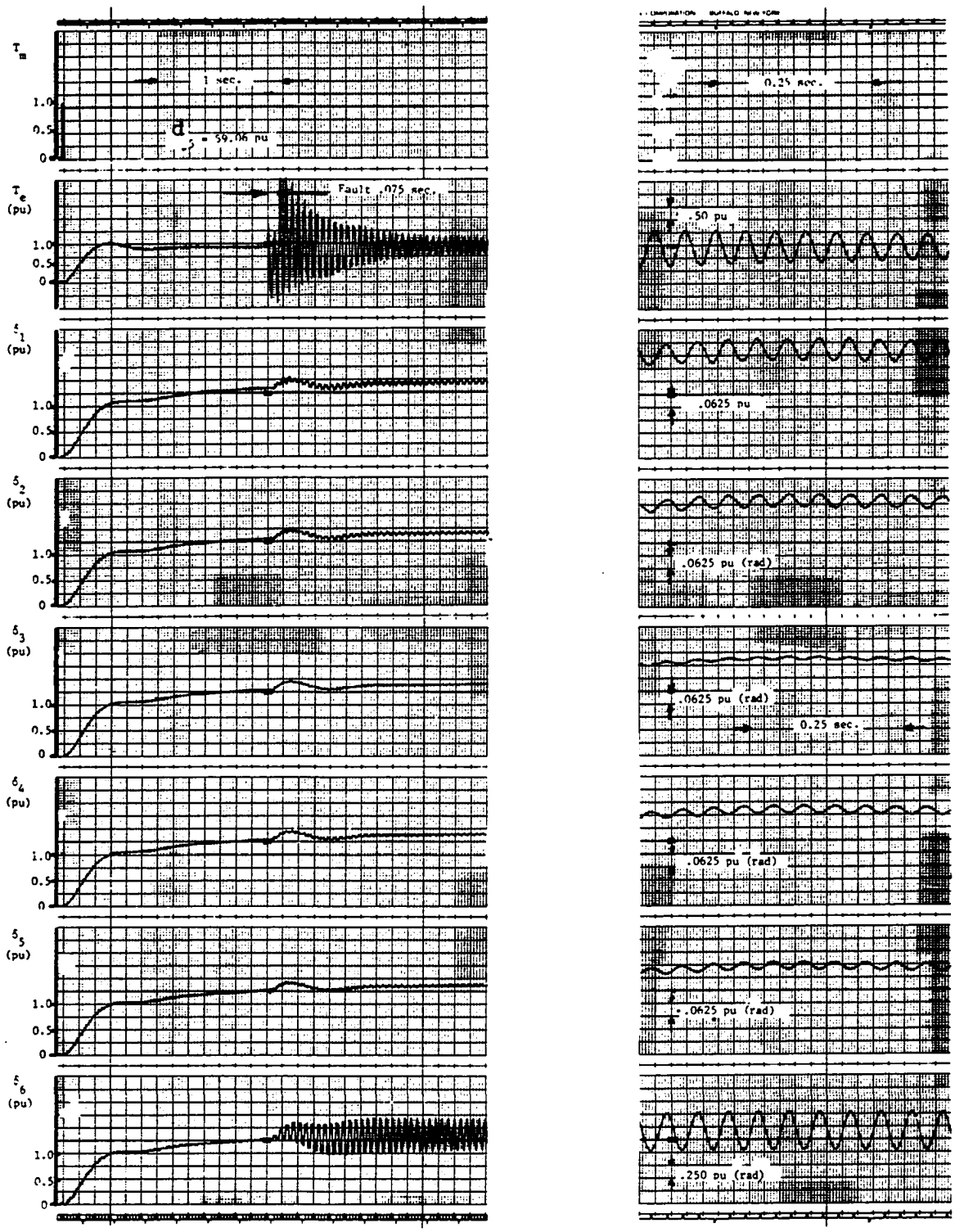

(a) With d_5 = 59.06.

Figure 12. Transient responses.

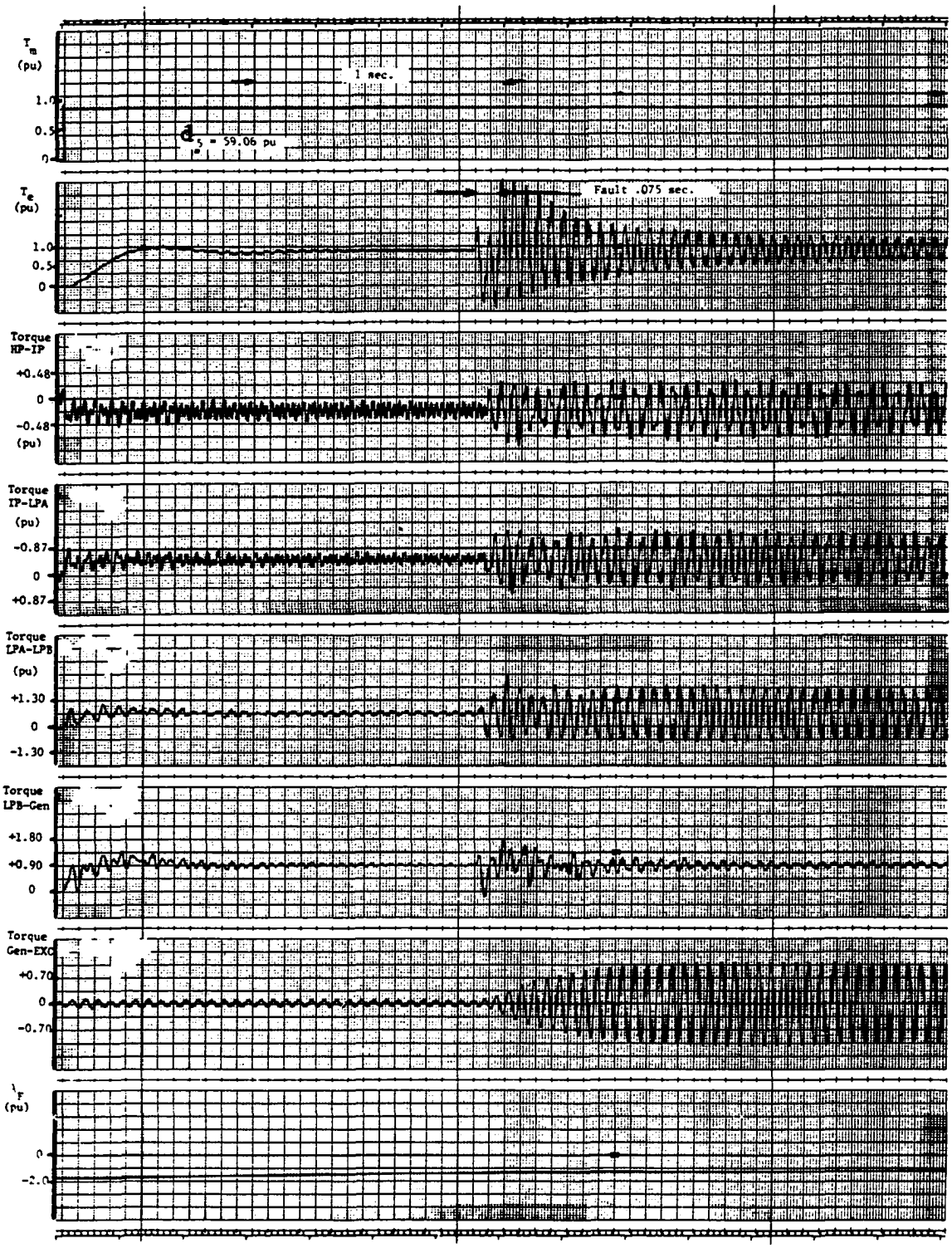

(b) Transient torques of the shaft.

Figure 12. (continued)

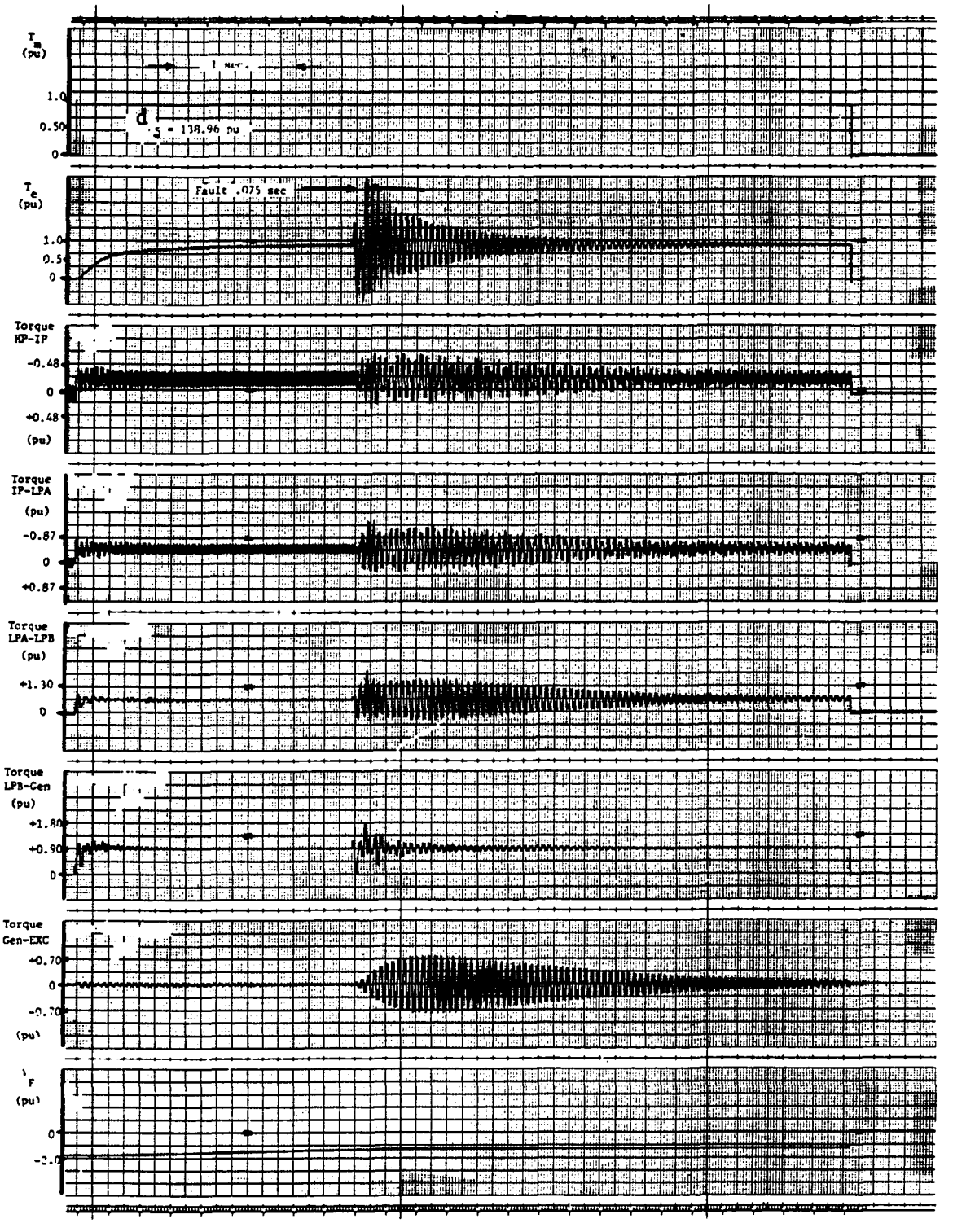

(a) Fault for 0.075 sec.

Figure 13. Effect of fault duration.

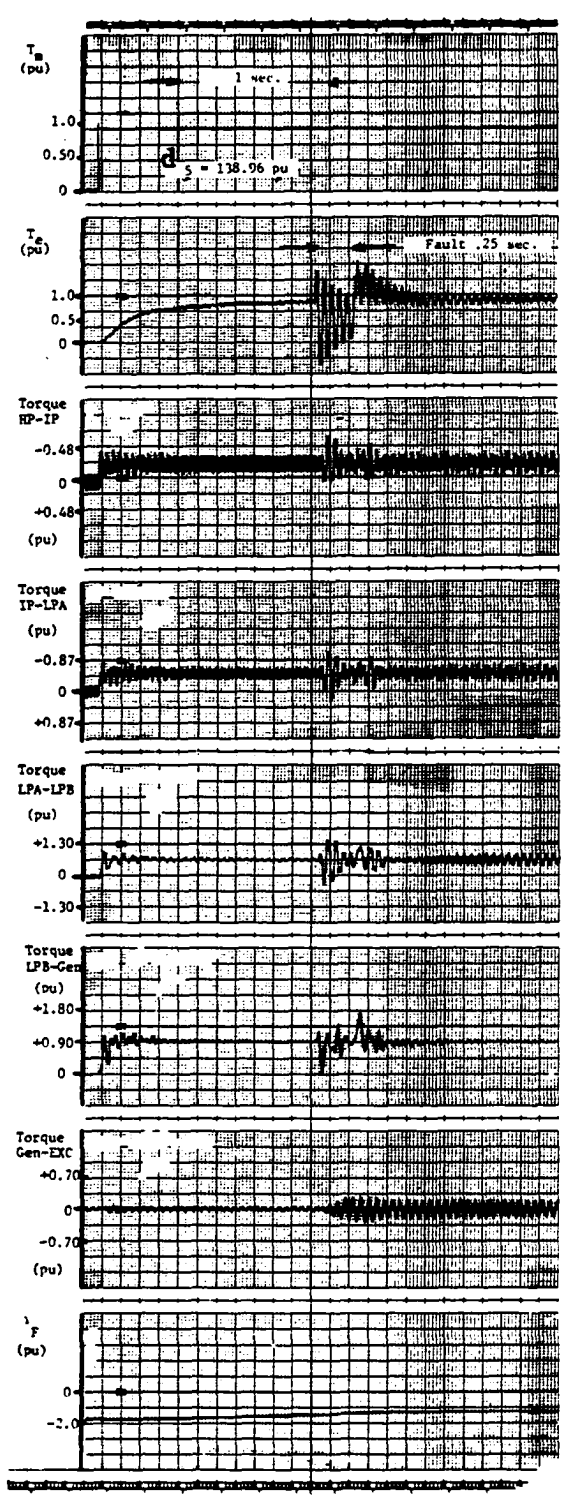

(b) Fault for 0.25 sec.

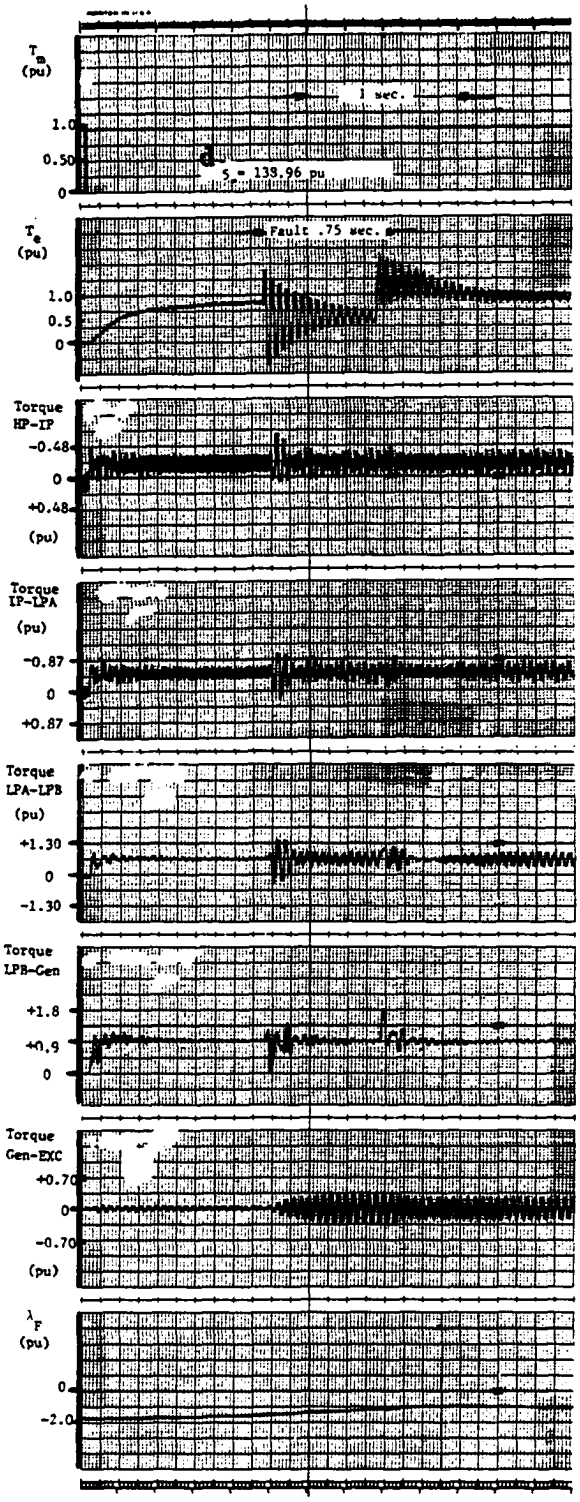

(c) Fault for 0.75 sec.

Figure 13. (continued)

1) Self-excitation is characterized by the decrement factor of the subsynchronous component of the electrical network.

2) Torsional Interaction is characterized by the decrement factor of the mechanical system's modes of oscillation.

3) Hunting is characterized by the decrement factor of mode 0 (inertial oscillation).

4) Self-excitation and torsional interaction can either occur separately or simultaneously, while hunting depends on the armature (or line) real or apparent resistance,[1] regardless of the presence of series capacitors.

5) A mode, whose frequency falls within the self-excitation zone, will be well damped.[2] For example, mode 1, as shown in Tables 1, 2, 3, and 5, is very well damped, because its peak is in the self-excitation zone (see Fig. 9).

Concerning the damping of subsynchronous oscillations, we note the following:

1) Mechanical damping will definitely help damp out subsynchronous resonance effects, including hunting. The magnitude of the needed

---

[1]The hunting phenomenon is shown to be a function of the ratio of armature resistance to the net system reactance (27). Thus, the presence of series capacitance tends to accentuate hunting. Apparent resistance refers to that which might be caused by excitation control system or by any other supplementary control circuits as discussed in Chapter VII.

[2]Eli Katz, Department of Water and Power, Los Angeles, California, private communication, 1976.

damping depends on where it is applied. For instance, a value of $d_1 = 2.16$ is needed to reduce the decrement factor of mode 3 from +1.546 to -0.005 (see Table 3); while a value of $d_5 = 77.15$ is needed to reduce that decrement factor by the same amount (see Table 4). From the many computations performed, some of which are not displayed here, we observe that the following relation holds:

$$d_i \delta_i^2 = d_j \delta_j^2 , \quad i,j = 1, 2, \ldots, 6.$$

where δ_i is the relative angular deviation of the mass i for a given mode of oscillation (see Appendix B). For instance, in this case (mode 3),

$$d_1 = 2.16 \qquad \delta_1 = 1.0 \qquad \delta_5 = 0.166$$

thus,

$$d_5 = \left(\frac{\delta_1}{\delta_5}\right)^2 d_1 = \left(\frac{1}{0.166}\right)^2 2.16 = 78.39$$

which is very close to the value of $d_5 = 77.15$ referred to previously.

Therefore, mode shapes are convenient graphical representations showing where mechanical damping, if it can be developed, could be applied most efficiently for a given mode of torsional oscillation.

2) Increasing the line resistance results in damping out self-excitation and torsional interaction. However, the synchronous generator will be more susceptible to hunting (as confirmed by Ref. 27). Furthermore, increasing the line resistance has the effect of shifting self-excitation zone farther toward higher line

compensation as observed in Table 5. For example, mode 1 has a negative decrement factor at R_e = 0.02 pu. When R_e is increased to 0.45 pu, mode 1 has a positive decrement factor, indicating that the peak of mode 1 is outside the zone of self-excitation.

3) Reducing the field circuit resistance will help damp out self-excitation, but does not cure torsional interaction and hunting.

From the studies of the three-phase fault, two significant remarks can be made:

1) For a given fault duration, the maximum magnitude of the torsional stress on each section of the shaft decreases with increased mechanical damping. However, the level of damping does not affect the maximum magnitude of the electrical developed torque (T_{emax}) during the fault or at the moment the fault is cleared. This latter remark is consistent with the fact that T_{emax} depends on the operating conditions and on the circuit configuration, but not on damping.

2) Our results indicate that, for a fixed level of damping, an increase in the duration of the three-phase fault reduces the post-fault level of torsional stress experienced by the shaft. This result could be significant in the sense that it may offer an added criterion for a minimum clearing time of the fault, below which excessive shaft stresses may occur. We note, however, that these results are not conclusive since longer unbalanced faults may result in more severe shaft stresses. This type of faults was not investigated in this work.

Concerning the choice of models (full and reduced models) for the mechanical system, we can make the following remarks:

1) Comparing the eigenvalues obtained in Tables 6 and 7, it is noted that both models give essentially the same results. Except for one of the inverse time-constants, the discrepancy is less than 1%.

2) The two resulting inverse time-constants have the following characteristics:

   - One time constant (τ'_d) is dependent upon the parameters of the electrical system's external circuit. It is defined as the effective field time constant (23). It can be seen that this time constant remains unaffected by the choice of the mechanical system models;
   - The other time constant depends upon the mechanical moment of inertia and damping. It can be defined as the effective inertial time constant. It differs from one reduced mechanical model to another and from one level of mechanical damping to another.

3) Considering the eigenvalues computed (in the first column of Tables 6 and 7), namely -3.975783 + j95.54 and +4.222482 + j95.85, we would not be certain as to decide which eigenvalue belongs to mode 1 without the help of Fig. 9. A wrong decision in this case would lead us to think that the system is undergoing a torsional interaction, while it is self-excitation that occurs here with X_c = 0.50 pu.

Two additional and important remarks must be made about mathematical modeling of a system and its actual physical behavior.

1) The results of the eigenvalues method of analysis, as shown in Tables 2, 5, and 6, have consistently indicated that mode 5 has negligible decrement factor. Mathematically, this would mean that mode 5 is always critically stable, i.e., oscillates with constant magnitude. Even at X_c = 0.05 pu where the electrical network subsynchronous frequency is very close to that of mode 5, it is observed that the decrement factor of this mode remains negligible, meaning that this mode cannot be excited by a perturbation applied at the generator rotor mass. This fact has been confirmed by an experiment reported upon in Ref. 19. The mode shapes of Figure 2 show that mode 5 has indeed a node at the generator rotor mass. Reference 19 makes an analogy of this situation with a person trying to close a door by pushing at the hinge (which is a node), rather than at the handle. Consequently, mode 5 can only be excited by a perturbation in the mechanical inputs.

2) In Fig. 12b, we particularly note that, if mode 2 oscillation is not damped out, the stress on the shaft section between the generator rotor and the exciter rotor keeps increasing even after the disturbance is cleared. It was this particular section of the shaft that sustained the most damage at the Mohave generating station (7,8).

The consistency in the results obtained from the mathematical model and the actual experiments performed on the real system has been demonstrated.

VII. REMEDIAL MEASURES

A. Previously Proposed Solutions

In the previous chapter, it was shown that for a given power system, with a series-compensated transmission line, there are regions of operation where instability may occur due to self-excitation, torsional interaction, or hunting (see Fig. 9).

For the power system proposed by the IEEE SSR Task Force, this can happen with line compensation higher than 10%. While the actual system at Mohave has 35% series compensation, it has been successfully operated since 1972. Any potential subsynchronous oscillations were quickly damped out (8). This does not necessarily contradict the findings of this dissertation, since the studies conducted here are carried out for the worse possible conditions: no mechanical damping, no shaft damping, and no modal damping.

We recall that when subsynchronous resonance occurred at the Mohave Generating Station, the line compensation was set at 70%. At that level of line compensation, there is always a possibility of self-excitation and/or torsional interaction following a disturbance. The machine manufacturers were then requested to add amortisseur windings at the pole face to reduce the field resistance. This has been successful in eliminating the self-excitation part of the subsynchronous resonance (13).

Modern power systems, with low armature and line resistances, are not likely to experience hunting.

Therefore, the problem of concern at Mohave has been that of torsional interaction. Because of this problem, the electric network at the Mohave region has been operated at a reduced level of line compensation.

1. Protective schemes

One protective measure adopted has been the use of spark-gaps installed across the series capacitors to shunt them out in the event of subsynchronous resonance (13). However, when a fault occurs, a high voltage is developed across the gaps. Without a selective control, the capacitors would be shunted out. Since, during a severe perturbation, it is of primary interest to have series capacitors help raise the system transient stability limit (3), this scheme thus appears to act against the purpose of using the series capacitors in the first place.

Another protective scheme, which has been developed and is presently used at Mohave Generating Station, is the subsynchronous overcurrent relay. This relay detects the presence of subsynchronous oscillations. Whenever the level of subsynchronous current reaches a preset value, it trips out the protected generator (28).

The spark-gaps and the subsynchronous overcurrent relay serve as excellent backup protective devices for subsynchronous resonance. They do not, however, control or damp out these oscillations.

2. Suggested SSR control schemes

Reference 29 suggests the shunting of series capacitors with a resistance. The drawbacks of this solutions are: loss of energy, decrease of transient stability limit, and the tendency toward hunting.

Another solution is the insertion of a subsynchronous filter at the neutral of the main power transformer (29,30,31). This solution, which would neither cause a decrease in the system transient stability limit, nor increase the likelihood of hunting, is very appealing. Its drawbacks are: it increases the needed insulation level of the transformer neutral BIL and requires a large area of the substation. Furthermore, its practicality can be limited by its narrow bandwidth. During a major disturbance resulting in a frequency excursion, the filter may become ineffective due to de-tuning.

Reference 30 suggests the use of Supplementary Excitation Damper Control (SEDC). This technique consists of injecting a properly phased sinusoidal signal into the voltage regulator. This signal is derived from the rotor motion by sensors. Though logical, this technique has not been demonstrated. With basically the same idea, Ref. 32 demonstrates that a properly designed AVR, such as current compensating or adaptive AVR (automatic voltage regulator), could enhance the damping of subsynchronous oscillation. The scheme investigated in this dissertation, while different from these schemes, is inspired by them.

B. New Solution Investigated Using Stabilizing Signal

A direct and simple method to damp out torsional oscillations in a power system is to generate a voltage of equal magnitude and opposite phase in series with that produced by any oscillating motion of the rotor at any of the frequencies corresponding to torsional resonance frequencies.

This principle has in fact been advanced by Ref. 31, and it can be justified by the fact that any disturbed motion of the generator rotor produces a subsynchronous voltage as shown in Appendix A.

This point will be demonstrated by numerical results obtained through eigenvalue analysis of the system shown in Fig. 14 (see Section 2 of this chapter).

While the principle is simple, the technique of injecting the necessary opposing voltage in the synchronous generator is complex.

1. Conventional PSS scheme

For this analysis, we will consider a simple mathematical model to represent the synchronous machine connected to an infinite bus. This model was used by deMello and Concordia (33) in their study of the effect of excitation system upon the stability of a power system (see also Chapter 6 of Ref. 17). It is valid for small signal analysis. For this model, the linearized system equations are given as follows:

$$\Delta T_e = K_1 \Delta\delta + K_2 \Delta E'_q \qquad \text{(a)}$$

$$\Delta E'_q = \frac{K_3}{1 + K_3 \tau'_{d0} s} \Delta E_{FD} - \frac{K_3 K_4}{1 + K_3 \tau'_{d0} s} \Delta\delta \qquad \text{(b)}$$

$$\Delta V_t = K_5 \Delta\delta + K_6 \Delta E'_q \qquad \text{(c)} \qquad (51)$$

where K_1 - K_6 are constants that depend on the machine and network parameters, and on the initial operating conditions; E'_q is a stator voltage that corresponds to the d-axis field flux linkage. E_{FD} is a stator voltage that corresponds to a given value of field voltage v_F, and τ'_{d0} is the field open-circuit time constant.

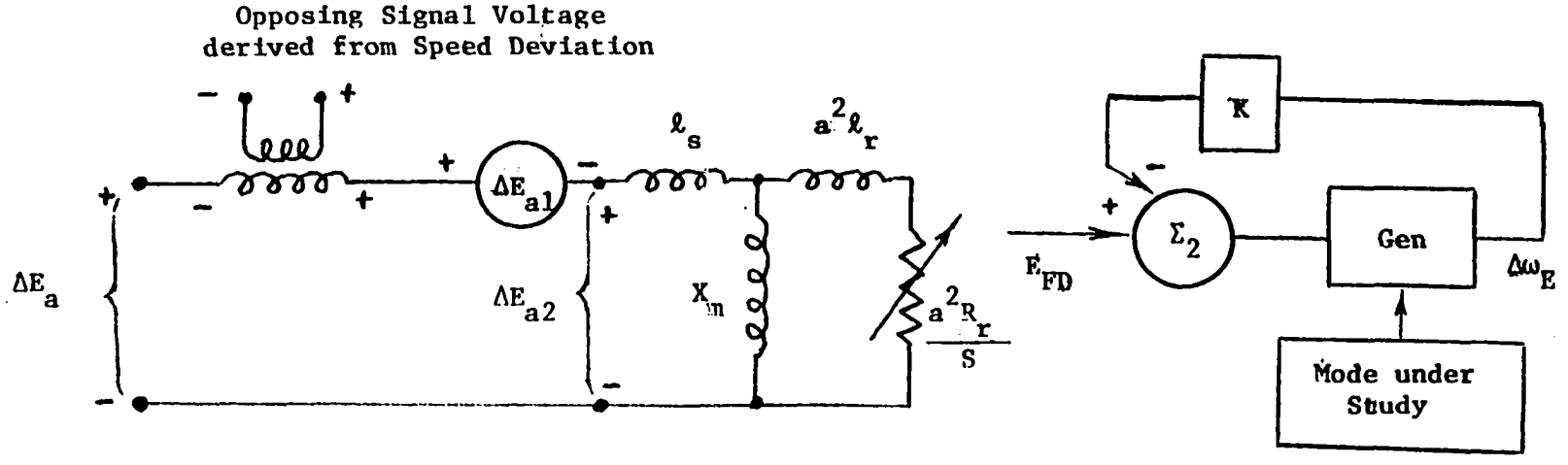

Figure 14. Generator subjected to SSR with signal voltage fed back in series but in opposing phase with voltage produced by subsynchronous motion of the generator rotor:
(a) Circuit diagram.[1]
(b) Block diagram.

[1]See Appendix A.

Following a procedure similar to that used by deMello and Concordia, that electrical developed torque is examined when the machine is subjected to a sinusoidal input. In the transfer function for ΔT_e, the substitution of s by $j\omega$ is made. The resulting expression for ΔT_e includes real and imaginary terms. The former constitutes the component of the synchronizing torque, while the latter gives the component of the damping torque.

In the study of negative damping situations in power systems, a stabilizing signal is introduced in the excitation system to enhance the system damping. This signal is derived from the speed deviation of the synchronous machine and is fed back to the input of the excitation system via a Power System Stabilizer (PSS) circuit (see Chapter 8 of Ref. 17). Figure 15 illustrates the scheme for an IEEE Type-1 excitation system (34).

2. Development of the desired control scheme

Referring to Fig. 14, which gives a schematic representation of the proposed scheme for controlling SSR, we note that the feedback point (Σ_2) is introduced at a point on the generator stator. If the feedback signal is to be injected in the generator rotor, an appropriate compensating signal must be used. From physical consideration, the appropriate point for introducing the control signal should be at the input (Σ_1) of the excitation system (34). The scheme would then be similar to that given in Fig. 15, except for the fact that this control circuit is designed to damp out subsynchronous modes instead of damping out the inertial mode as the conventional PSS.

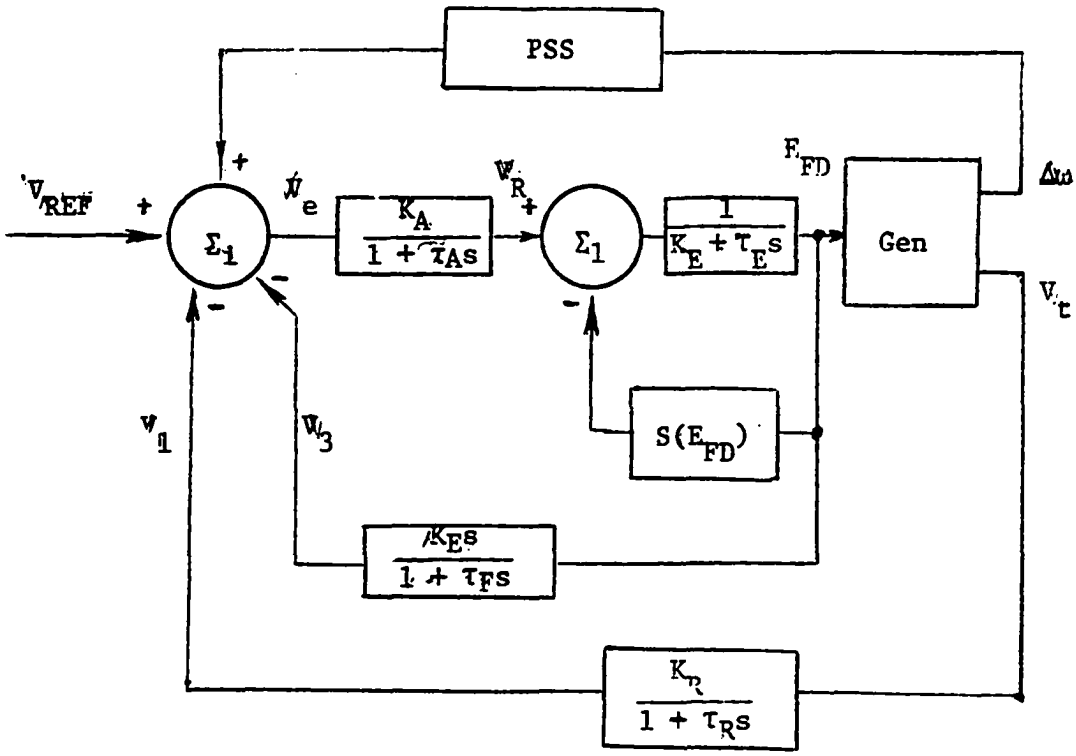

Figure 15. Generator with Type-I Exciter and Power System Stabilizer (PSS).

The procedure to be followed for designing the control circuit will thus be similar to that normally used for designing the PSS scheme. Because of this similarity, one obvious question presents itself: why would the PSS provide a positive damping torque for the inertial oscillations, which are actually of mode 0, and not be effective for the subsynchronous oscillations?

The main difference is that, at higher frequencies, the various stages of the system shown in Fig. 15 induce more phase-lag, even though the negative damping torque introduced by the excitation control is considerably reduced in magnitude (35).

In the light of this reasoning, the author arrives at the following procedure to develop a positive damping torque for modes other than mode 0:

(a) The transfer function will have the same form as that developed for inertial oscillations (PSS), and will simply be called Stabilizing Control Circuit (SCC);

(b) The amount of phase-lead needed will be determined by the system operating conditions and the subsynchronous frequencies of concern; and

(c) The pick-up speed deviation will be that produced solely by the modes in question.

The power system under investigation with excitation system and Stabilizing Control Circuit is shown in Fig. 16.

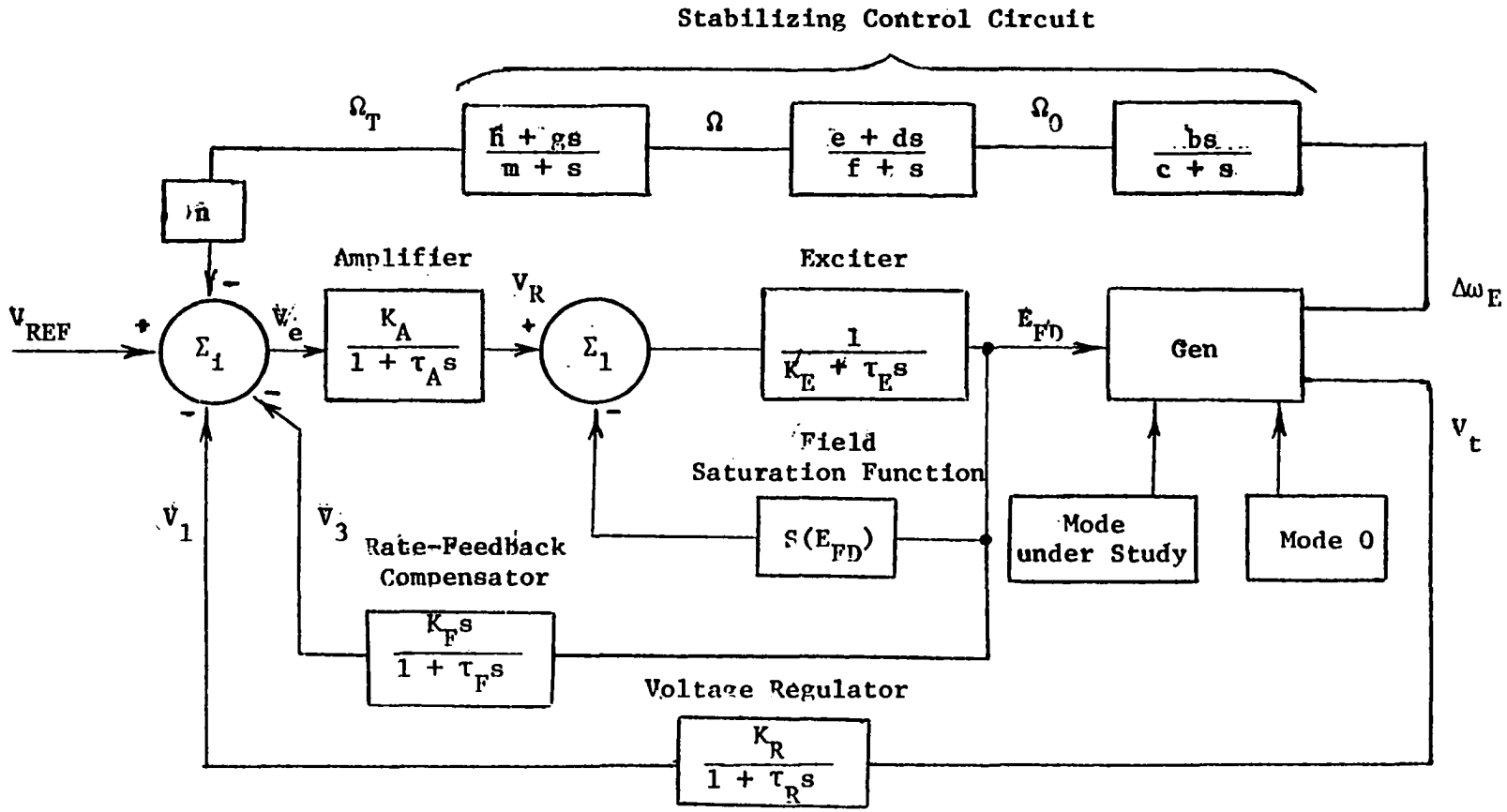

Figure 16. Generator subjected to SSR with excitation control and Stabilizing Control Circuit.

3. Tests conducted

a. Eigenvalue analysis For the following studies, the reduced model of the mechanical system is adopted. H_E and K_E are chosen to reflect the influence of mode 2. This choice of the reduced model is dictated by the lack of components needed for the system simulation on the existing analog computer. The generator model is that of Fig. 3b. IEEE Type-1 Exciter is used (see Fig. 16). The value of its parameters are listed in Appendix D.

The governing linearized equations for this excitation system can be derived as follows (see also Ref. 17):

$$-\left(d_0 \frac{K_R}{\tau_R}\frac{L_e}{\omega_B}\right)\dot{i}_d - \left(q_0 \frac{K_R}{\tau_R}\frac{L_e}{\omega_B}\right)\dot{i}_q + \dot{V}_1 =$$

$$\frac{K_R}{\tau_R}(d_0R_e - q_0\omega_0L_e)\, i_d + \frac{K_R}{\tau_R}(d_0\omega_0L_e + q_0R_e)\, i_q$$

$$+\frac{K_R}{\tau_R}(d_0 i_{q0}L_e - q_0 i_{d0}L_e)\omega - \sqrt{3}\,\frac{K_R}{\tau_R}V_\infty(d_0\cos\delta_0 + q_0\sin\delta_0)\delta$$

$$+\left(\frac{K_R}{\tau_R}d_0\right)v_{cd} + \left(\frac{K_R}{\tau_R}q_0\right)v_{cq} - \frac{1}{\tau_R}V_1 \qquad \text{(a)}$$

$$\dot{V}_3 = -\left[\frac{K_F(K_E + S'_E)}{\tau_E\tau_F}\right]E_{FD} - \frac{1}{\tau_F}V_3 + \frac{K_F}{\tau_E\tau_F}V_R \qquad \text{(b)}$$

$$\dot{V}_R = -\frac{K_A}{\tau_A}V_1 - \frac{K_A}{\tau_A}V_3 - \frac{1}{\tau_A}V_R + \frac{K_A}{\tau_A}V_{REF} \qquad \text{(c)}$$

$$\dot{E}_{FD} = \frac{1}{\tau_E}V_R - \left(\frac{K_E + S'_E}{\tau_E}\right)E_{FD} \qquad \text{(d)} \qquad (52)$$

where

$$d_0 = \frac{1}{3}\frac{v_{d0}}{v_{t0}} \qquad q_0 = \frac{1}{3}\frac{v_{q0}}{v_{t0}}$$

$$S'_E = \frac{\partial S(E_{FD})}{\partial E_{FD}}\bigg|_{E_{FD0}} = A_{EX}B_{EX}e^{B_{EX}E_{FD0}}$$

and

$$\frac{kM_F}{\omega_B}\dot{i}_d + \frac{L_F}{\omega_B}\dot{i}_F = -r_F i_F + \sqrt{3}\frac{r_F}{L_{AD}}E_{FD} \tag{53}$$

All variables are in per unit, except time in seconds.

For the system of Fig. 14, Eq. 53 becomes:

$$\frac{kM_F}{\omega_B}\dot{i}_d + \frac{L_F}{\omega_B}\dot{i}_F = -r_F i_F + \sqrt{3}\frac{r_F}{L_{AD}}E_{FD} + K\Delta\omega_{E2} \tag{54}$$

The system initial conditions are the same as those of Chapter VI for 90% load and 90% lagging power factor (see Appendix D).

Table 8 shows the effect of $\Delta\omega_{E2}$-feedback upon the decrement factor of mode 2.

The results obtained in Table 8 confirm that torsional oscillations can be damped out by an opposing voltage applied in series with that produced by the rotor motion due to a disturbance.

The next test is conducted for the system of Fig. 16. In this case, $\Delta\omega_{E2}$ is fedback at Σ_i through a transfer function of the form:

$$\frac{\Omega T}{\Delta\omega_{E2}} = \left[\frac{bs}{c+s}\right]\left[\frac{e+ds}{f+s}\right]\left[\frac{h+gs}{m+s}\right] \tag{55}$$

Three more state-variables are needed to represent this Stabilizing Control Circuit:

Table 8. Effect of $\Delta\omega_{E2}$-feedback.

Mode Identification	K = 0	K = 5.0	K = 12.5
Electrical	-4.7156±j623.6	-4.7154±j623.6	-4.7151±j623.6
Network	-3.0233±j130.0	-2.804±j130.0	-2.533±j130.4
Mode 2	+0.384±j127.5	+0.1478±j127.3	-0.1487±j127.0
Exciter	-10.192±j27.3	-10.192±j27.3	-10.193±j27.3
	-1.683±j0.76	-1.686±j0.76	-1.691±j0.76
Rotor Circuits'	-100.0	-100.0	-100.0
Inverse	-31.194	-31.154	-31.094
Time-	-4.3729	-4.3727	-4.3725
Constants	-20.470	-20.470	-20.470

$$-b\dot{\Delta\omega}_{E2} + \dot{\Omega}_0 = -c\Omega_0 \qquad (a)$$

$$-d\dot{\Omega}_0 + \dot{\Omega} = e\Omega_0 - f\Omega \qquad (b)$$

$$-g\dot{\Omega} + \dot{\Omega}_T = h\Omega - m\Omega_T \qquad (c) \quad (56)$$

and

$$V_R = -\left[\frac{K_F(K_E + S_E')}{\tau_E\tau_F}\right] E_{FD} - \frac{1}{\tau_F} V_3 + \frac{K_F}{\tau_E\tau_F} V_{REF} - n\Omega_T \qquad (57)$$

In the study of the control circuits, parametric expressions are essential.

In dealing with large systems, however, the derivation of parametric expressions can be very tedious. With the advent of digital computers, many design and analysis methods are preferably carried out numerically.

To determine the proper values for the constants in Eq. 56, the eigenvalue method is used to make several trial runs. From these runs, a set of values for the constants of the Stabilizing Control Circuit to damp out the torsional oscillation caused by subsynchronous resonance at 127 rad/sec (mode 2) has been found. Equation 55 becomes:

$$\frac{\Omega_T}{\Delta\omega_{E2}} = \left[\frac{282.75s}{125 + s}\right]\left[\frac{52500 + 5650s}{15074 + s}\right]\left[\frac{2.115 + 5.65s}{14213 + s}\right] \qquad (58)$$

Eigenvalues computed for the system of Fig. 16 with different value of input gain (n) to the summer Σ_i are tabulated in Table 9. Note that the mode 0 is included in the mechanical model.

b. Analog computer studies The transfer function of Eq. 58 is put in a form suitable for analog computation:

$$\Omega_0 = \frac{c}{a}\int\Omega_0 dt - b\Delta\omega_{E2} \qquad (a)$$

Table 9. Effect of Stabilizing Control Circuit.

Mode Identification	n = 0	n = 5.0	n = 6.0	n = 7.0	n = 10.0
Electrical	-4.710±j623.6	-4.707±j623.6	-4.706±j623.6	-4.706±j623.6	-4.704±j623.6
Network	-3.078±j129.6	-2.663±j129.0	-2.614±j128.5	-2.662±j128.3	-2.800±j128.0
Mode 2	+0.4385±j127.4	+0.0145±j128.2	-0.0371±j128.5	-0.0308±j128.7	+0.1403±j129.3
Mode 0 (Inertial Oscillation)	-0.6293±j10.4	-0.6295±j10.4	-0.6295±j10.4	-0.6295±j10.4	-0.6295±j10.4
Exciter	-9.614±j27.2	-9.608±j27.2	-9.606±j27.2	-9.605±j27.2	-9.601±j27.2
	-1.354±j1.0	-1.354±j1.0	-1.354±j1.0	-1.354±j1.0	-1.354±j1.0
Stabilizing	-1.42×10^4	-1.42×10^4	-1.42×10^4	-1.42×10^4	-1.42×10^4
Control	-1.51×10^4	-1.51×10^4	-1.51×10^4	-1.51×10^4	-1.51×10^4
Circuit	-1.25×10^2	-1.25×10^2	-1.25×10^2	-1.25×10^2	-1.25×10^2
Rotor Circuits'	-99.940	-99.940	-99.940	-99.940	-99.940
Inverse	-30.920	-30.913	-30.911	-30.910	-30.908
Time-	-5.326	-5.326	-5.326	-5.326	-5.326
Constants	-20.470	-20.470	-20.470	-20.470	-20.470

$$\Omega = \frac{f}{a}\int\Omega dt - d\Omega_0 - \frac{e}{a}\int\Omega_0 dt \qquad (b)$$

$$\Omega_T = \frac{m}{a}\int\Omega_T dt - g\Omega - \frac{h}{a}\int\Omega dt \qquad (c) \quad (59)$$

where

$b = 282.75$ $\quad c = 125$

$d = 5650.$ $\quad e = 52500.$

$f = 15074.$ $\quad g = 5.65$

$h = 2.115$ $\quad m = 14213.$

and a is time scaling factor of 40.

Analog patching diagram for Eq. 59 is shown in Fig. 17. The simultaneous inclusion of mode 2 and mode 0 for the mechanical system is governed by the relations (see Eqs. 5 and 6 and also Appendix B):

$$\delta_{gen} = [1 \quad -1] \begin{bmatrix} \delta_{E0} \\ \delta_{E2} \end{bmatrix} \qquad (a)$$

$$\omega_{gen} = [1 \quad -1] \begin{bmatrix} \omega_{E0} \\ \omega_{E2} \end{bmatrix} \qquad (b)$$

and

$$T_{a0} = \sum_{i=1}^{4} T_{mi} - T_e \qquad (c)$$

$$T_{a2} = 2.9385T_{m1} + 1.7273T_{m2} + 0.4011T_{m3} - 1.0561T_{m4} + T_e \qquad (d) \quad (60)$$

Analog patching diagram for Eq. 60 is shown in Fig. 6b. The excitation system patching diagram is shown in Fig. 18. All potentiometers' coefficients are given in Appendix E. Due to lack of analog

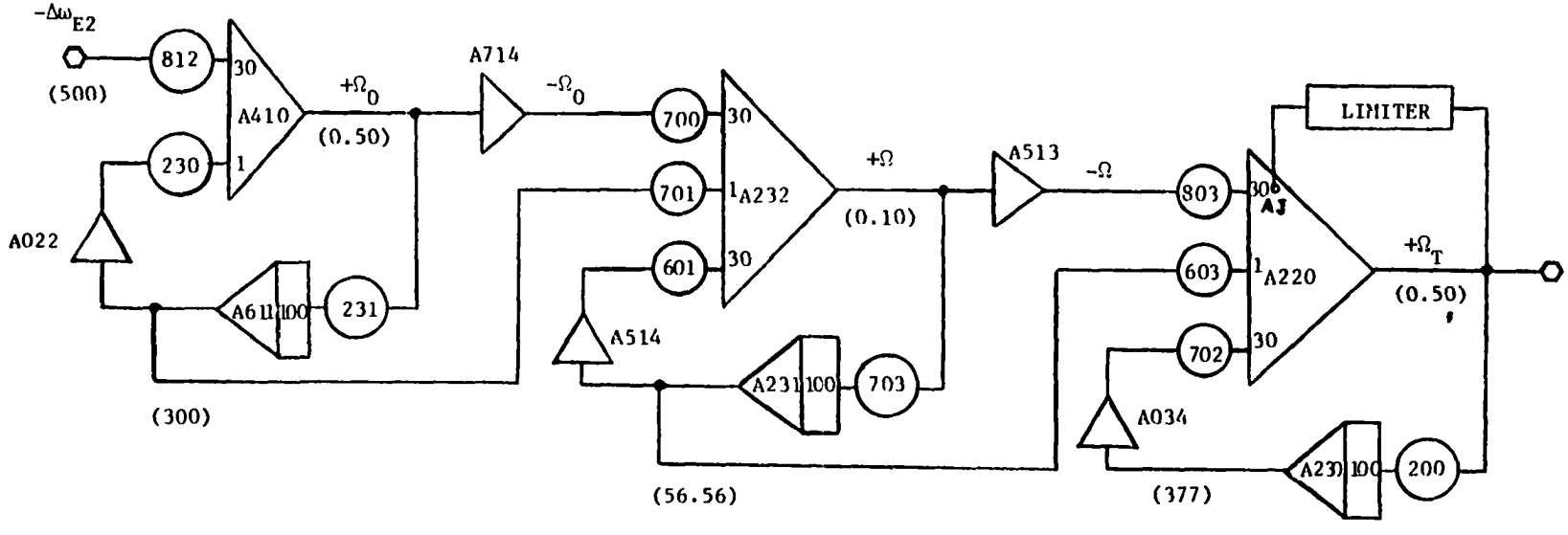

Figure 17. Patching diagram for SCC.

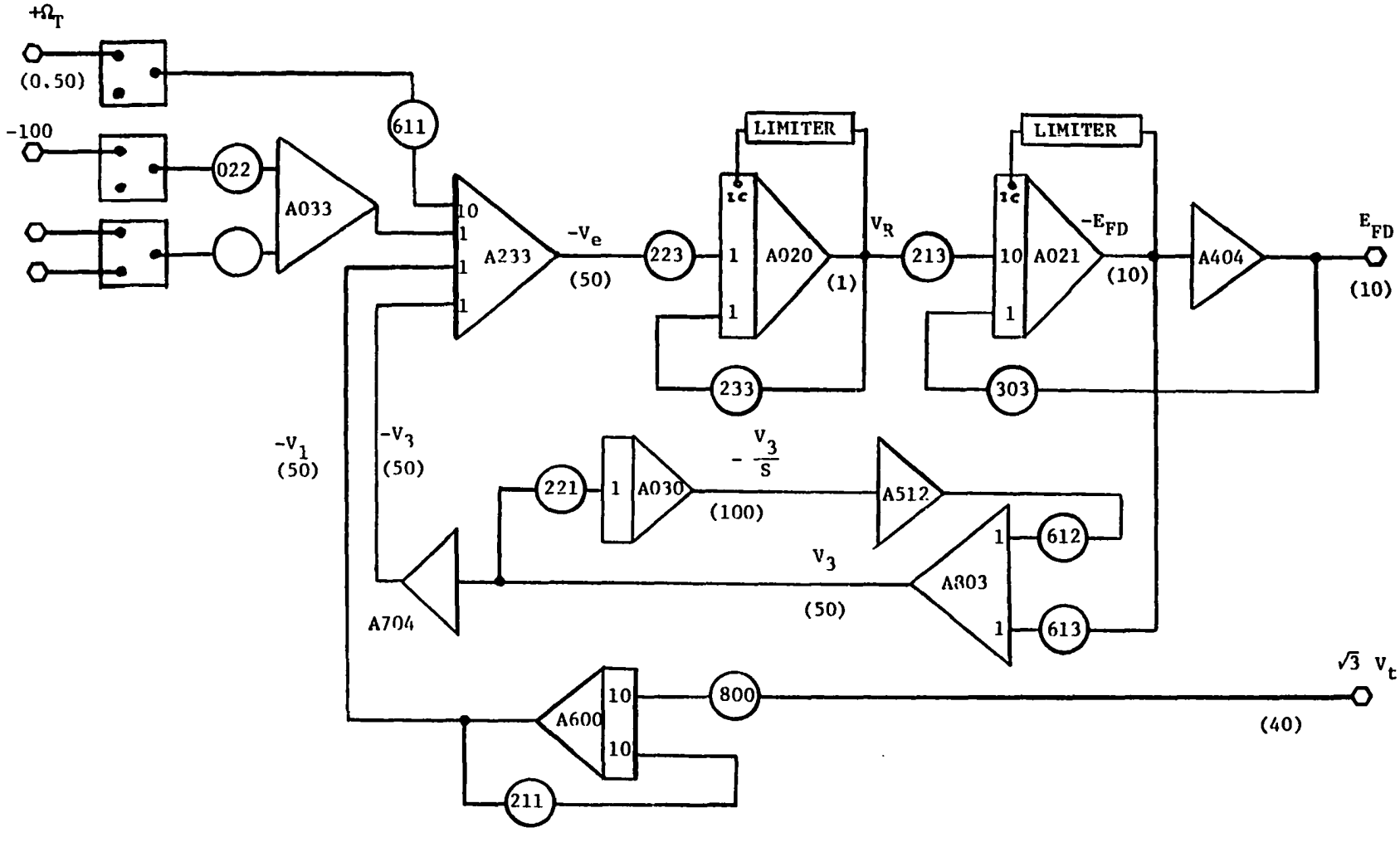

(a) IEEE Type-I Exciter.

Figure 18. Patching diagram for excitation system.

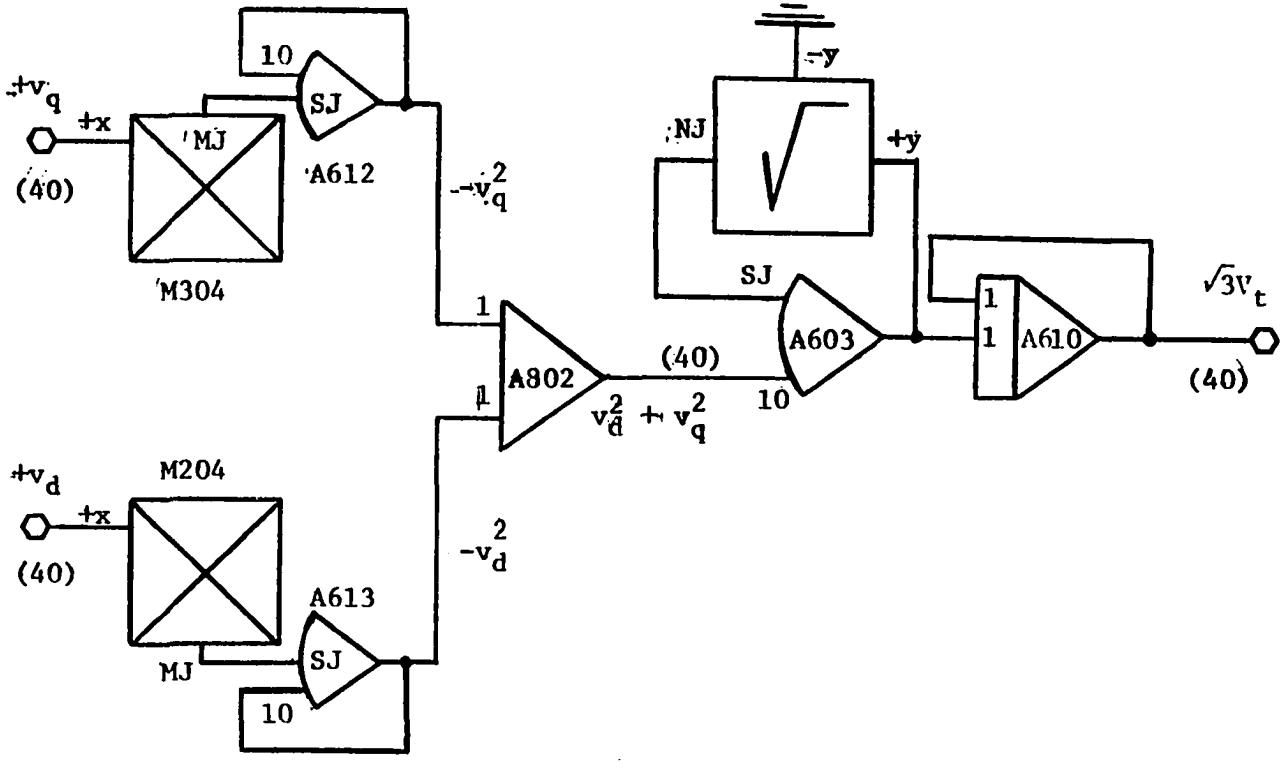

(b) Generation of generator terminal voltage V_t.

Figure 18. (continued)

components, 3ϕ-fault simulation for this case is not carried out. The perturbation is thus limited to the change in the mechanical input torque.

Figure 19 illustrates transient behavior of the system subject to torsional interaction with excitation control only. Note that the system is unstable under the influence of torsional interaction (mode 2).

Figure 20 shows the system's behavior when Stabilizing Control Circuit is closed during the operation and then opened for a short lapse of time, and then reclosed to damp out the torsional oscillation.

Figure 21 illustrates the condition in which the Stabilizing Control Circuit cannot bring the system back to stability if it is reclosed too late.

Figure 22 shows the effect of the gain (n) upon the damping of the torsional oscillation. Note the magnitude of n in the analog computer's results and that of n in the eigenvalue analysis.

Figure 23 illustrates a sample of the output of the close-loop Stabilizing Control Circuit used.

C. Discussions of Results

From the results obtained in Section B above, it is obvious that sub-synchronous oscillations can be successfully damped out using Supplementary Signals introduced at the input of the excitation system.

A simple computation of phase-lead at ω = 0.34 pu (127 rad/sec) introduced by the transfer function of Eq. 58 shows that:

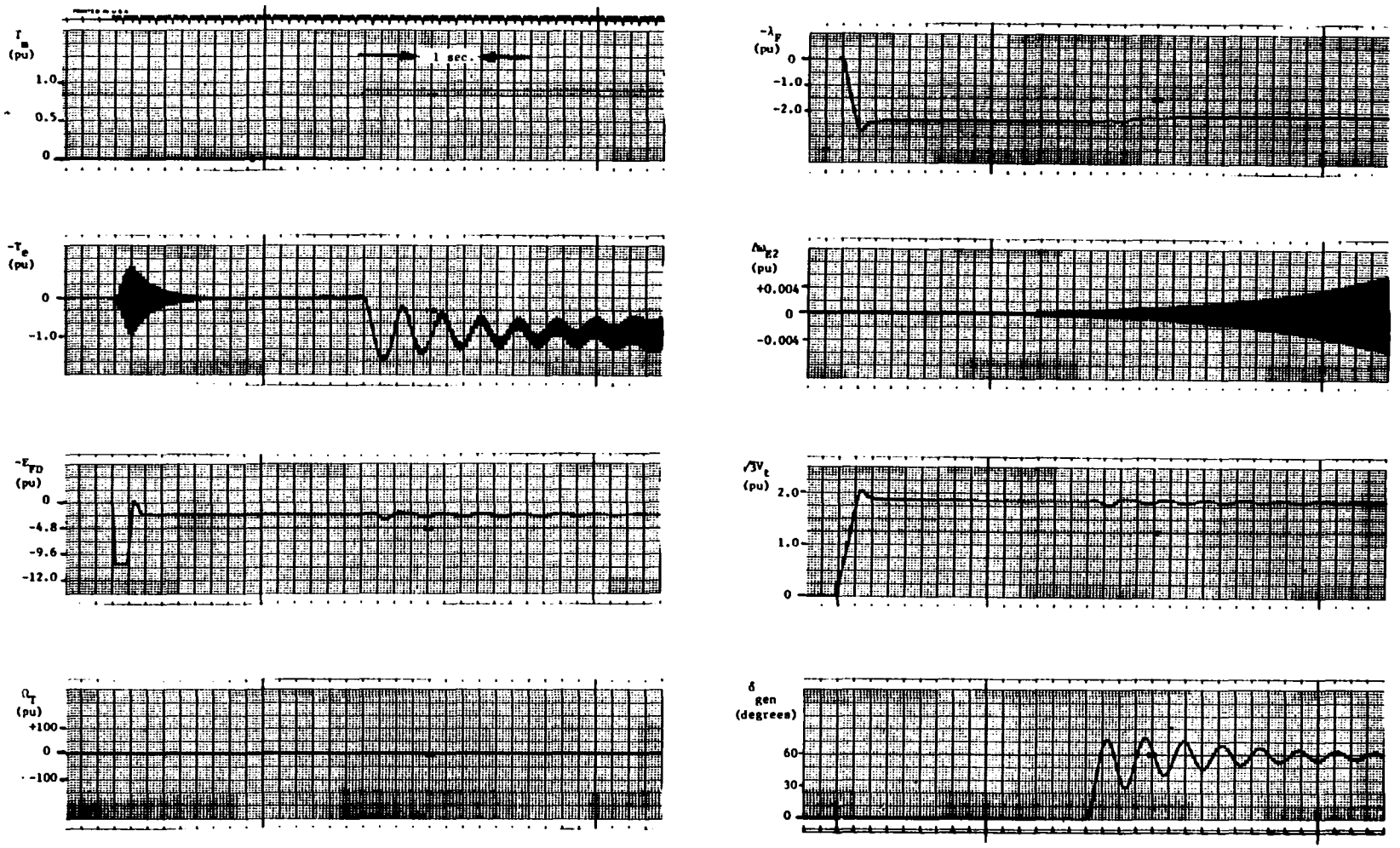

Figure 19. Transient responses with excitation system alone.

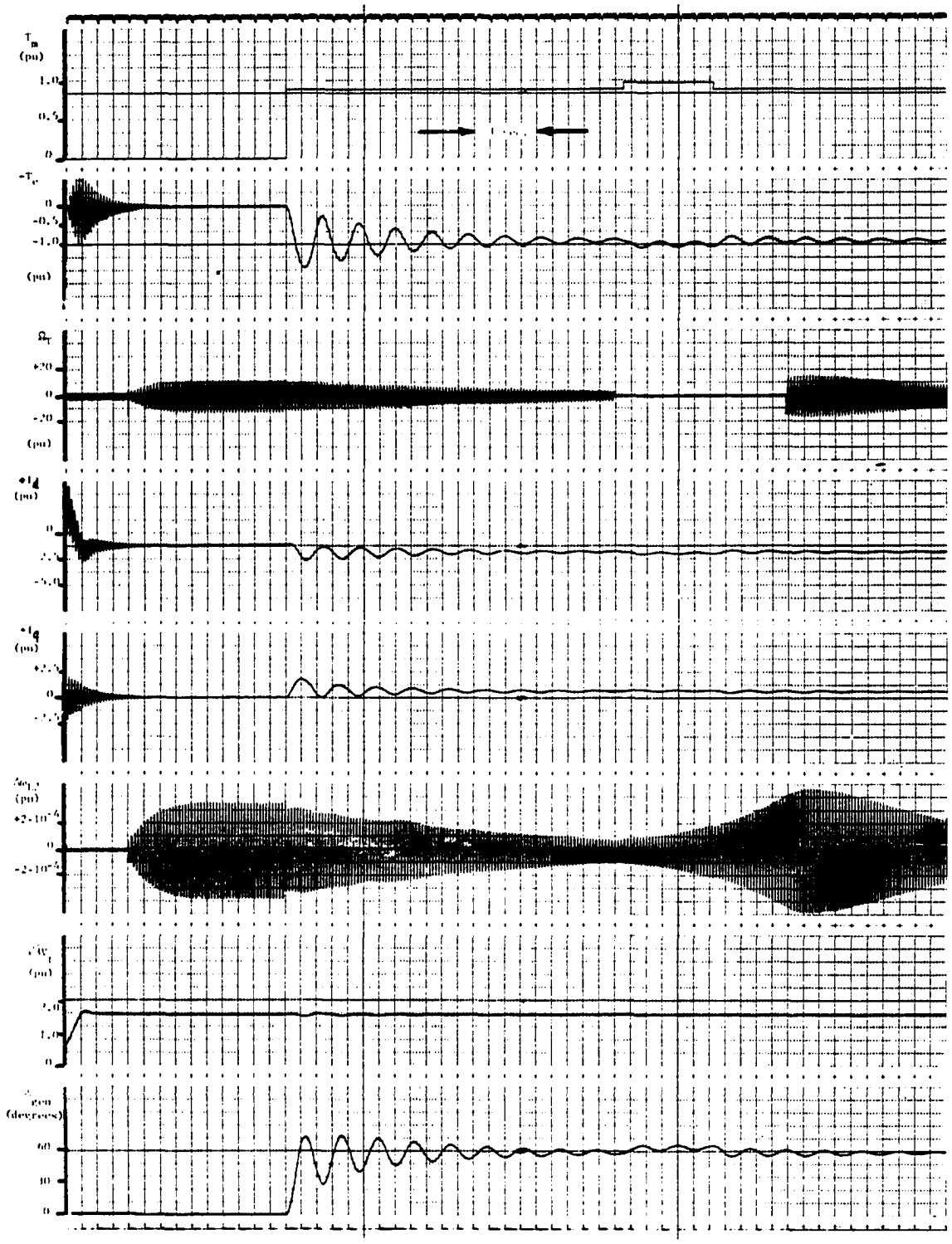

Figure 20. Transient responses with SCC added and n = 0.09316.

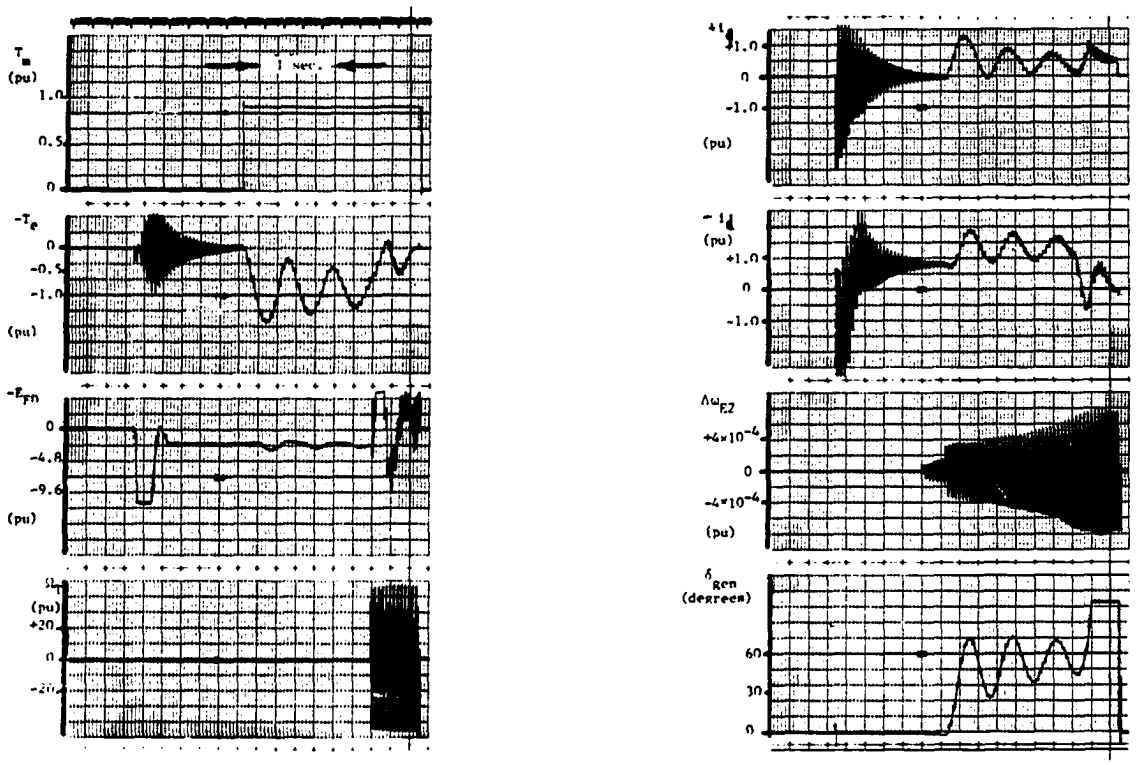

Figure 21. System instability due to retarded reclosure of SCC.

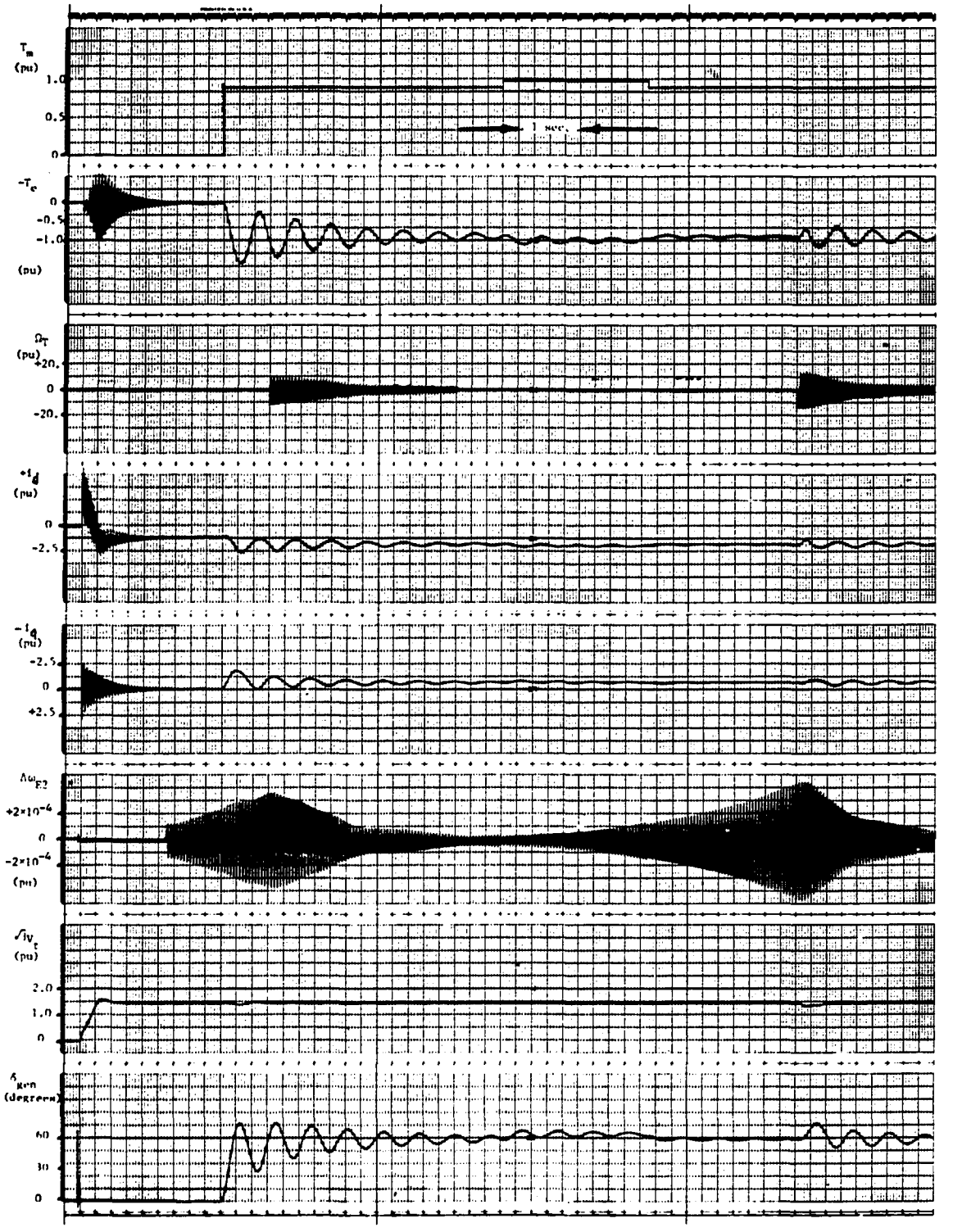

(a) With n = 2 × 0.09316.

Figure 22. Transient responses.

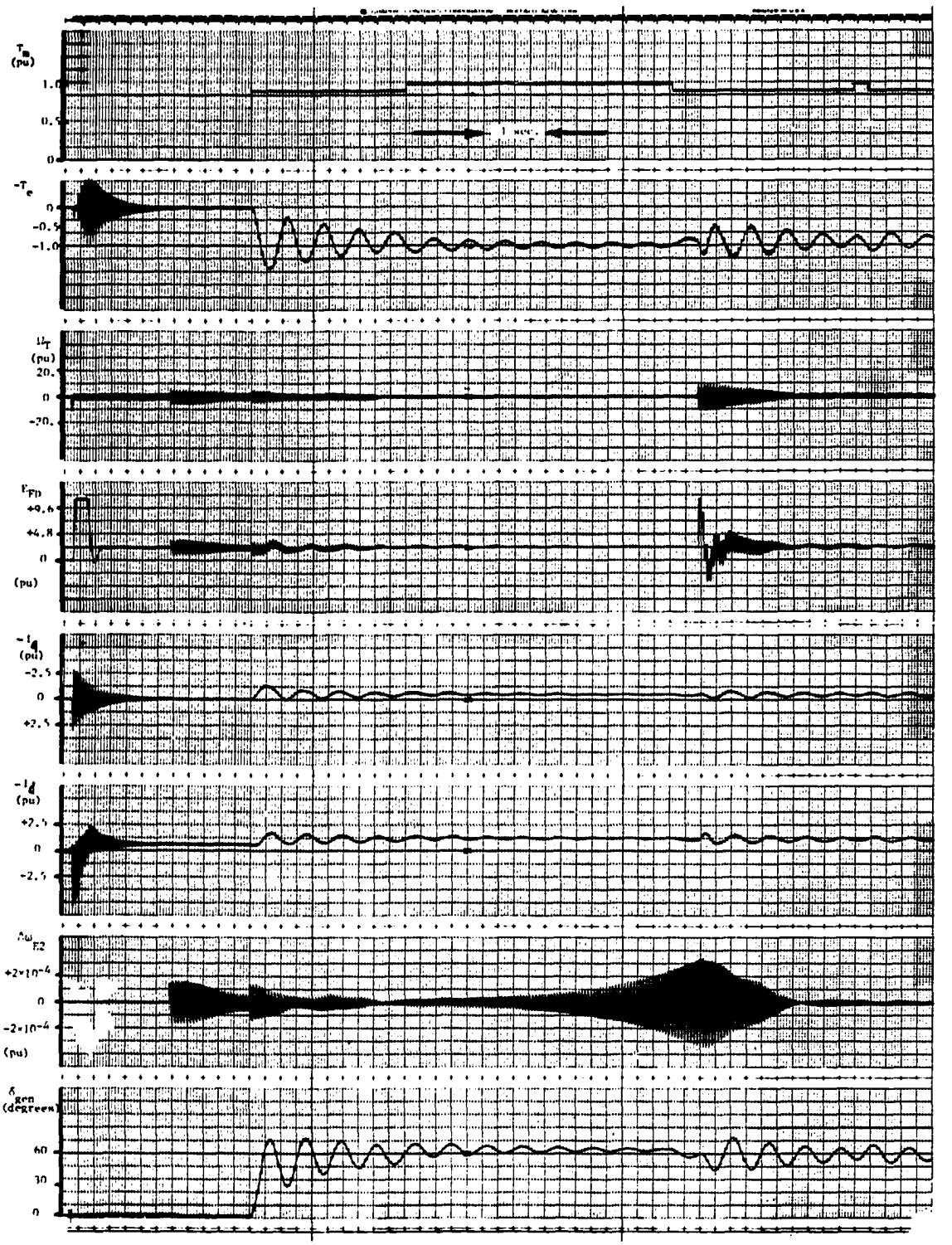

(b) With n = 3 × 0.09316.

Figure 22. (continued)

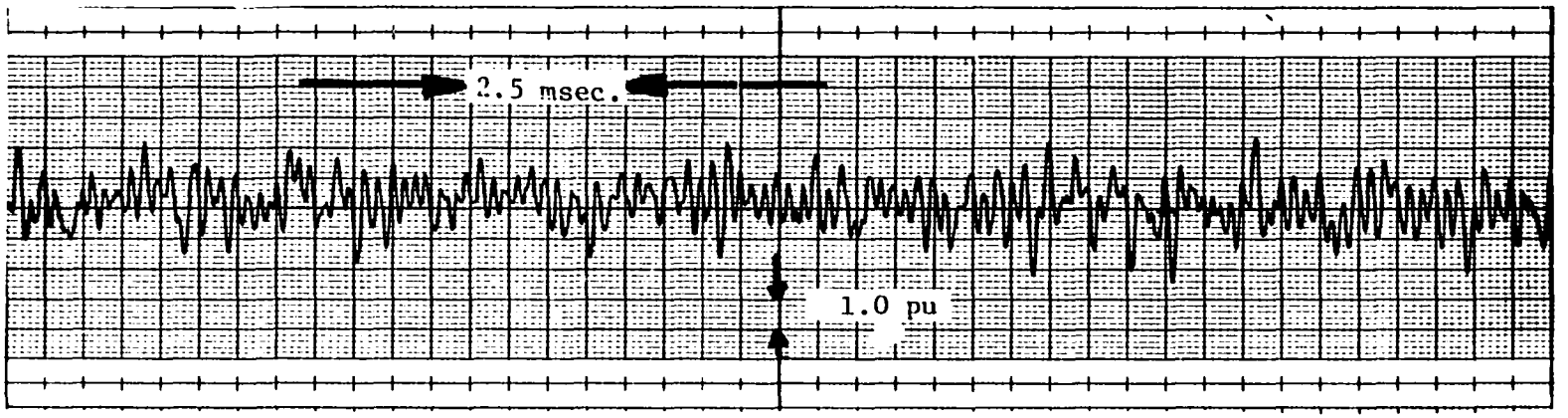

Figure 23. Output signal of the Stabilizing Control Circuit during normal close-loop operation.

$$\left.\frac{\Omega_T}{\Delta\omega_{E2}}\right|_{\omega = 0.34} = \left[\frac{96.135/90°}{125/.16°}\right]\left[\frac{52535/2.1°}{15074/0°}\right]\left[\frac{2.86/42.25°}{14213/0°}\right]$$

$$\approx 5 \times 10^{-4}/134.2°$$

Thus a phase-lead of 134.2° is needed. This amount of phase-lead is similar to the amount of phase-lag (of 134°) between the generator rotor speed deviation and the electrical developed torque computed by Ref. 35 for a typical power system at a frequency of oscillation of 20 Hz, using a linearized model for the generator.

Comparing the eigenvalues and recorded analog computer's results, when no SCC applied, the following values are noted:

Components	Eigenvalue Method	Analog Computer
Frequency of mode 2	127.4 rad/sec (20.3 Hz)	20.2 Hz
Decrement Factor of mode 2	+ 0.4385 sec^{-1}	+ 0.498 sec^{-1}
Frequency of Inertial Oscillation	10.4 rad/sec (1.7 Hz)	1.6 Hz
Decrement Factor of Inertial Oscillation	-0.6293 sec^{-1}	- 0.598 sec^{-1}

When the SCC is included, the analog computer shows that a gain of n = 0.09316 is sufficient to reduce the decrement factor of mode 2 from + 0.498 sec^{-1} to - 0.3917 sec^{-1}. The eigenvalue method shows, however, that a gain of n = 6.0 is needed to bring the decrement factor of mode 2 from + 0.4385 sec^{-1} to only - 0.0371 sec^{-1}, and any higher gain would make the system unstable again.

This discrepancy can be explained by the fact that when the SCC is inserted during the system operation (this can only be done with analog computer), the system operating conditions at that moment change from those used in the eigenvalue method, and this change may not be considered as "small" perturbations. This point is made clear by considering Fig. 20: the SCC is inserted from the start with no major perturbation. Note that this same SCC has hardly any damping effect upon the oscillation of mode 2 as suggested by eigenvalue analysis.

A special note about the effect of the voltage regulator gain upon the stability of the system should be made: In formulating a state-variable relation for the voltage regulator (see Eq. 52a), and including this equation into Eq. 32a, we note that the line resistance (R_e) will be modified by a coefficient which is proportional to the regulator gain (K_R) in the product-matrix ($\underline{A}^{-1}\underline{f}(\underline{X})$). Hence, increasing K_R is equivalent to adding more line resistance, giving to the system an <u>apparent increase of line resistance</u>. From Chapter 6 (Section C), it is recalled that this has the effect of pushing the system toward hunting. This instability is consistent with the analysis carried out in Ref. 33, in which it is found that increased voltage regulator gain makes damping torque more negative (for high load operation).

Eigenvalues obtained for this case, where K_R is increased from 1 to 100 (without SCC) are shown below:

Mode Identification	$K_R = 1$	$K_R = 10$	$K_R = 100$
Electrical Network	-4.710±j623.6 -3.078±j129.6	-4.710±j623.6 -3.126±j129.6	-4.710±j623.6 -3.593±j129.0
Mode 2	+0.4385±j127.4	+0.4479±j127.4	+0.5205±j127.3
Mode 0	-0.6293±j10.4	-0.2053±j10.9	-0.3960±j11.0

Note that increasing K_R helps damp out self-excitation but makes inertial oscillation and torsional interaction worse. The difference between the apparent increase in the line resistance, introduced by the voltage regulator, and the actual increase of R_e is that the latter would damp out torsional oscillations as well.

In Fig. 22b, we note that the re-insertion of the SCC makes the field voltage (E_{FD}) swing bewteen -3.5 pu and +12.5 pu, and the system will still be stabilized. This is because the generator field flux linkage (λ_F) changes much slower than the change in field voltage. However, if the re-insertion of the SCC causes the field voltage to swing beyond a certain range, as illustrated by Fig. 21 where the SCC is inserted too late, the system cannot be brought back to stability[1].

The eigenvalues shown in Table 9, and analog computer's recorded curves show that the SCC does not seem to have an appreciable effect on the system normal operating conditions as far as the system inertial oscillation is concerned.

---

[1]One important operational feature of these tests is that it is preferable to have the SCC on all the time.

However, more studies about the effect of the SCC upon other modes should be considered before its permanent presence in the system can be justified.

VIII. CONCLUSIONS AND RECOMMENDATIONS

If the series compensated transmission lines are here to stay, appropriate protective and control mechanisms have to be developed and perfected. The effect of subsynchronous resonance upon the power system, especially upon the shafts of the generating units, is too costly to offset any benefit derived from the presence of series capacitors.

This dissertation attempts to add a small contribution to the many made by researchers in the field of analysis and solution of the problem. If the Stabilizing Control Circuit under study can be implemented and proven successful in practice, controlling SSR would then be achieved at a reasonable cost.

The whole concept of power system stability and contingency plans have to be revised in order to cope with the phenomena of subsynchronous resonance.

(1) In the planning stage: More coordination between the machine manufacturers and the network designers is needed to avoid excessive number of possible SSR occurrences.

(2) In the stage of expansion of an existing system: Careful analysis should be made to determine if conditions favorable to the occurrence of SSR are present. Proper measures are then taken, such as protective devices for the generating units, switching schemes to be avoided or modified, SSR control schemes to be used, etc.

As an extension of the work carried out in this dissertation, we see the following as areas worthy of further investigations:

1. In deriving the transfer function for the Stabilizing Control Circuit, the author has used a well-known principle, applied by trial-and-error with the aid of the digital computer. A systematic method of deriving the transfer function is needed. This can be carried out by formulating a reliable simplified model of the electrical system (such as in Section B of Chapter VII), and by observing the effect of various parameters upon the resulting damping torque expression at the frequencies of interest.
2. The effect of the choice of the excitation system upon the performance of the Stabilizing Control Circuit has not been looked into in detail. In this dissertation, IEEE Type-1 Exciter is used. But for this particular SCC to have a proper damping effect, the exciter time constant (τ_E) must be arbitrarily made small (0.05 second). In other words, it appears that the so-called fast exciters have better characteristics as far as the damping of subsynchronous oscillations is concerned.
3. It is to be noted that the pick-up speed deviation (for the SCC) is that caused solely by the mode under study. The design of transducers for this signal has not been investigated. Nonetheless, it is an essential element of the control scheme itself.
4. In the area of analysis, the problem of relating the mechanical damping coefficients, the shaft damping coefficients, and the modal damping coefficients, is yet to be resolved. We need to

study how the amplitudes of the various modes depend upon one another in a real system.

5. In the study of the system's transient behavior, the following are suggested for further investigations:
   (a) Use of the full model for the mechanical system with excitation and stabilization controls.
   (b) The effect of three-phase and/or unbalanced faults upon torsional stresses of the shaft and other system's components.
   (c) The effect of the presence of limiters in the excitation and stabilization systems upon the power system stability.
   (d) For a given power system, the number of SCC needed to cover an entire range of SSR frequencies, and how one SCC affects the performance of others.
   (e) Coordination of the control circuits' performance to obtain optimal results.
   (f) The effect of field saturation upon the efficiency of SCC to damp out subsynchronous oscillations.
6. Finally, the study of the phenomena of SSR for other types of mechanical systems (such as cross-compound steam turbines), a group of similar and/or dissimilar generating units, and induction machines, deserves particular attention as well.

IX. REFERENCES

1. Butler, J. W. and Concordia, C. "Analysis of Series Capacitor Application Problems." AIEE Transactions 56 (August 1937): 975-88.

2. Brener, G. D., Rustebakke, H. M., Gibley, R. A., and Simmons, H. O. "The Use of Series Capacitors to Obtain Maximum EHV Transmission Capability." IEEE Transactions PAS Nov. 1964. Reprinted in "Stability of Large Electric Power Systems," pp. 365-75. Edited by Richard T. Byerly and Edward W. Kimbark. IEEE Press, 1974.

3. Kimbark, E. W. "Improvement of System Stability by Switched Series Capacitors." IEEE Transactions PAS Feb. 1966. Reprinted in "Stability of Large Electric Power Systems," pp. 387-84. Edited by Richard T. Byerly and Edward W. Kimbark. IEEE Press, 1974.

4. Rustebakke, H. M. and Concordia, C. "Self-excitation in a Transmission System Using Series Capacitors." IEEE Transactions PAS-89, No. 7 (Sept./Oct. 1970): 1504-10.

5. Kilgore, L. A., Elliott, L. C., and Taylor, E. R. "The Prediction and Control of Self-excited Oscillations Due to Series Capacitors in Power Systems." IEEE Transactions PAS-90, No. 3 (May/June 1971): 1305-11.

6. Maneatis, J. A., Hubacher, E. J., Rothenbuhler, W. N., and Sabath, J. "500 kV Series Capacitor Installations in California." IEEE Transactions PAS-90, No. 3 (May/June 1971): 1138-49.

7. Gold, S. H. "Power System Oscillations Which Resulted in the Second Failure of Generator Rotor of Mohave Generating Station Unit No. 1." A report of Southern California Edison Company, February 1972.

8. Hall, M. C. and Hodges, D. A. "Experience With 500 kV Subsynchronous Resonance and Resulting Turbine Generator Shaft Damage at Mohave Generating Station." Paper presented at IEEE PES 1976 Winter Meeting and Tesla Symposium. Reprinted in "Analysis and Control of Subsynchronous Resonance," pp. 22-25. Edited by IEEE SSR Task Force under Special Publication No. 76 CH 1066-0-PWR.

9. Bowler, C. E. J., Ewart, D. N., and Concordia, C. "Self-exciter Torsional Frequency Oscillations With Series Capacitors." IEEE Transactions PAS-92, No. 5 (Sept./Oct. 1973): 1688-95.

10. Kilgore, L. A., Ramey, D. G., and Hall, M. C. "Simplified Transmission and Generation System Analysis Procedures for Subsynchronous Resonance Problems." Paper presented at IEEE PES, 1976 Winter Meeting and Tesla Symposium. Reprinted in "Analysis and Control of Subsynchronous Resonance," pp. 6-11. Edited by IEEE SSR Task Force under Special Publication No. 76 CH 1066-0-PWR.

11. IEEE SSR Task Force. "Analysis and Control of Subsynchronous Resonance." Special Publication No. 76 CH 1066-0-PWR. IEEE Power Engineering Society, 1976 Winter Meeting and Tesla Symposium. IEEE Service Center, Piscataway, New Jersey.

12. IEEE SRR Task Force. "Proposed Terms and Definitions for Subsynchronous Resonance in Series Compensated Transmission Systems." Paper presented at IEEE PES, 1976 Winter Meeting and Tesla Symposium. Reprinted in "Analysis and Control of Subsynchronous Resonance," pp. 55-58. Edited by IEEE SSR Task Force under Special Publication No. 76 CH 1066-0-PWR.

13. Katz, E. "Proposed Test Cases for Subsynchronous Resonance Studies." Paper presented at IEEE PES, Summer Power Meeting, San Francisco, California, July 20-25, 1975.

14. Hall, M. C., Daniels, R. L., and Ramey, D. G. "A New Technique for Subsynchronous Resonance Analysis and an Application to the Kaiparowits System." Paper presented at IEEE PES, 1976 Winter Meeting and Tesla Symposium. Reprinted in "Analysis and Control of Subsynchronous Resonance," pp. 46-50. Edited by IEEE SSR Task Force under Special Publication No. 76 CH 1066-0-PWR.

15. IEEE Committee Report. "Dynamic Models for Steam and Hydro Turbines in Power System Studies." IEEE Transactions PAS Nov./Dec. 1973. Reprinted in "Stability of Large Electric Power Systems," pp. 128-36. Edited by Richard T. Byerly and Edward W. Kimbark. IEEE Press, 1974.

16. Quay, R. and Placek, R. J. "Cyclic Fatique of Turbine-Generator Shafts." Paper presented at IEEE PES, 1976 Winter Meeting and Tesla Symposium. Reprinted in "Analysis and Control of Subsynchronous Resonance," pp. 121-21. Edited by IEEE SSR Task Force under Special Publication No. 76 CH 1066-0-PWR.

17. Anderson, P. M. and Fouad, A. A. "Power System Control and Stability." Ames, Iowa: Iowa State University Press, 1977.

18. Tropper, A. M. "Matrix Theory for Electrical Engineers." Reading, Massachusetts: Addison-Wesley Publishing Co., Inc., 1962.

19. Walker, D. N. and Schwalb, A. L. "Results of Subsynchronous Resonance Test at Novajo." Paper presented at IEEE PES, 1976 Winter Meeting and Tesla Symposium. Reprinted in "Analysis and Control of Subsynchronous Resonance," pp. 37-45. Edited by IEEE SSR Task Force under Special Publication No. 76 CH 1066-0-PWR.

20. Bowler, C. E. J. "Understanding Subsynchronous Resonance." Paper presented at IEEE PES, 1976 Winter Meeting and Tesla Symposium. Reprinted in "Analysis and Control of Subsynchronous Resonance," pp. 66-73. Edited by IEEE SSR Task Force under Special Publication No. 76 CH 1066-0-PWR.

21. Bolotin, V. V. "The Dynamic Stability of Elastic Systems." Translated from Russian by V. I. Weingarten, L. B. Greszczuk, K. N. Trirogoff, and K. D. Gallegos. London: Holden-Day, Inc., 1964.

22. Adkins, B. and Harley, R. G. "The General Theory of Alternating Current Machines: Application to Practical Problems." London: Cahpman and Hall, 1975.

23. Concordia, C. "Synchronous Machines—Theory and Performance." New York: John Wiley & Sons, Inc., 1951.

24. Ballance, J. W. and Goldberg, S. "Subsynchronous Resonance in Series Compensated Transmission Lines." Paper No. T73 167-4 presented at the IEEE PES, Winter Meeting, New York, N.Y., Jan. 28-Feb. 2, 1973.

25. Robb, D. D. and Krause, P. C. "Dynamic Simulation of Generator Faults Using Combined abc and Odq Variables." IEEE Transactions PAS-94 (Nov./Dec. 1975): 2084-91.

26. Electronic Associates, Inc. 8800 System Reference Handbook. West Long Branch, New Jersey: Electronic Associates, Inc., 1967.

27. Wagner, C. F. "Effect of Armature Resistance Upon Hunting of Synchronous Machines." AIEE Transactions 49 (July 1930): 1011-20.

28. Ning, T. S. "Subsynchronous Overcurrent Relay for Generators Connected to a Series Compensated Power System." Paper presented at IEEE PES, 1976 Winter Meeting and Tesla Symposium. Reprinted in "Analysis and Control of Subsynchronous Resonance," pp. 74-76. Edited by IEEE SSR Task Force under Special Publication No. 76 CH 1066-0-PWR.

29. Concordia, C., Tice, J. B., and Bowler, C. E. J. "Subsynchronous Torques on Generating Units Feeding Series-Capacitor Compensated Lines." Paper presented at American Power Conference, Chicago, Illinois, May 8-10, 1973.

30. Farmer, R. G., Katz, E., and Schwalb, A. L. "Navajo Project Report on SSR Analysis and Solutions." Paper presented at IEEE PES, 1975 Summer Power Meeting, San Francisco, California, July 20-25, 1975.

31. Kilgore, L. A., Ramey, D. G., and South, W. H. "Dynamic Filter and Other Solutions to the SSR Problems." Paper presented at American Power Conference, Chicago, Illinois, April 21-23, 1975.

32. Suzuki, H., Fujiwara, R., and Vemura, K. "Analysis and Control for SSR Problem." Paper presented at IEEE PES, 1976 Summer Power Meeting, Portland, Oregon, July 18-23, 1976.

33. deMello, F. P., and Concordia, C. "Concepts of Synchronous Machine Stability as Affected by Excitation Control." IEEE Transactions, PAS, April 1969. Reprinted in "Stability of Large Electric Power Systems," pp. 189-200. Edited by Richard T. Byerly and Edward W. Kimbark. IEEE Press, 1974.

34. IEEE Committee Report. "Computer Representation of Excitation Systems." IEEE Transactions, PAS-87 (June 1968): 1460-64.

35. Watson, W., and Coultes, M. E. "Static Exciter Stabilizing Signals on Large Generators—Mechanical Problems." IEEE Transactions, PAS, Jan./Feb. 1973. Reprinted in "Stability of Large Electric Power Systems," pp. 354-360. Edited by Richard T. Byerly and Edward W. Kimbark. IEEE Press, 1974.

X. ACKNOWLEDGMENTS

The author would like to express his sincere gratitude to all the members of his committee, Dr. A. A. Fouad, Dr. D. D. Robb, Dr. H. W. Hale, Dr. G. W. Smith, and Dr. J. L. Cornette. A special note of thanks is given to the major advisor, Dr. Fouad, for his great understanding, sincere concern, and valuable guidance and suggestions, not only in the academic field, but in the domain of the author's personal problems as well. Special thanks are also extended to Dr. Robb for making many excellent documents available to the author, and to Dr. Richard Horton for his valuable aid with the EAI8800 analog computer.

The author would like to extend his deepest appreciation to the Mekong Committee, through which many nations have contributed a much needed financial support to make the completion of his program of studies possible.

Last, but not least, thanks are also due to Jo Kline for her patience, her eagerness, and ability in putting the author's handwriting into type.

As this dissertation is being submitted to the Thesis Office, Dr. Robb finds himself unavailable to serve as committee member due to circumstances beyond his control.

The author would like to express his special gratitude to Dr. Aly Mahmoud for agreeing to fill in as a committee member on such a short notice.

XI. APPENDIX A. EXISTENCE OF SUBSYNCHRONOUS FREQUENCIES AND INDUCTION GENERATOR ACTION

From Chapter IV (Equation 8), the voltage equations for a synchronous machine (generator) in 0dq-frame are given as follows:

$$v_0 = -ri_0 - \dot{\lambda}_0 \quad \text{(a)}$$

$$v_d = -ri_d - \dot{\lambda}_d - \omega\lambda_q \quad \text{(b)}$$

$$v_q = -ri_q - \dot{\lambda}_q + \omega\lambda_d \quad \text{(c)} \qquad \text{(A-1)}$$

From Chapter IV (Equation 11), we get:

$$\underline{v}_{abc} = \underline{P}^{-1}\underline{v}_{0dq} \qquad \text{(A-2)}$$

Carrying out matrix multiplication for (A-2), we get:

$$v_a = \frac{1}{\sqrt{3}} v_0 + \sqrt{\frac{2}{3}} \{\cos\theta v_d + \sin\theta v_q\} \quad \text{(a)}$$

$$v_b = \frac{1}{\sqrt{3}} v_0 + \sqrt{\frac{2}{3}} \{\cos(\theta - 2\Pi/3)v_d + \sin(\theta - 2\Pi/3)v_q\} \quad \text{(b)}$$

$$v_c = \frac{1}{\sqrt{3}} v_0 + \sqrt{\frac{2}{3}} \{\cos(\theta + 2\Pi/3)v_d + \sin(\theta + 2\Pi/3)v_q\} \quad \text{(c)} \qquad \text{(A-3)}$$

Assuming balanced operating conditions, and negligible armature resistance, we get for v_a:

$$v_a = \sqrt{\frac{2}{3}} \{\cos\theta v_d + \sin\theta v_q\} \qquad \text{(A-4)}$$

Linearizing Eq. A-4 about a quiescent operating point, we get:

$$\Delta v_a = \sqrt{\frac{2}{3}}\{\Delta\omega(\sin\theta_0\lambda_{d0} - \cos\theta_0\lambda_{q0}) + \Delta\theta(\cos\theta_0 v_{q0} - \sin\theta_0 v_{d0}) + \cos\theta_0(\Delta\dot{\lambda}_d - \omega_0\Delta\lambda_q) + \sin\theta_0(\Delta\dot{\lambda}_q + \omega_0\Delta\lambda_d)\} \qquad \text{(A-5)}$$

Which is put in the form:

$$\Delta v_a = \Delta E_{a1} + \Delta E_{a2} \qquad \text{(A-6)}$$

Where

$$\Delta E_{a1} = \sqrt{\frac{2}{3}} \{\Delta\omega[\sin\theta_0\lambda_{d0} - \cos\theta_0\lambda_{q0}] + \Delta\theta[\cos\theta_0 v_{q0} - \sin\theta_0 v_{d0}]\} \tag{A-7}$$

$$\Delta E_{a2} = \sqrt{\frac{2}{3}} \{\cos\theta_0[\Delta\dot{\lambda}_d - \omega_0\Delta\lambda_q] + \sin\theta_0[\Delta\dot{\lambda}_q + \omega_0\Delta\lambda_d]\} \tag{A-8}$$

1) First, consider the voltage-component ΔE_{a1}. At steady-state, we have

$$v_{d0} = -\omega_0\lambda_{q0},$$

and

$$v_{q0} = \omega_0\lambda_{d0} \tag{A-9}$$

Assuming the perturbation in the motion of the generator rotor is sinusoidal with an amplitude A (radians) and a frequency μ (rad/sec), then

$$\Delta\theta = A\sin\mu t,$$

and

$$\Delta\omega = \mu A\cos\mu t \tag{A-10}$$

Substituting Eqs. A-9 in Eq. A-7, we get:

$$\Delta E_{a1} = \sqrt{\frac{2}{3}} \{\Delta\omega[\sin\theta_0\lambda_{d0} - \cos\theta_0\lambda_{q0}] + \Delta\theta\omega_0[\cos\theta_0\lambda_{d0} + \sin\theta_0\lambda_{q0}]$$

or

$$\Delta E_{a1} = \sqrt{\frac{2}{3}} \{[\Delta\omega\sin\theta_0 + \Delta\theta\omega_0\cos\theta_0]\lambda_{d0} + [-\Delta\omega\cos\theta_0 + \Delta\theta\omega_0\sin\theta_0]\lambda_{q0} \tag{A-11}$$

To express Eq. A-11 in complex form, we adopt the following system of axes:

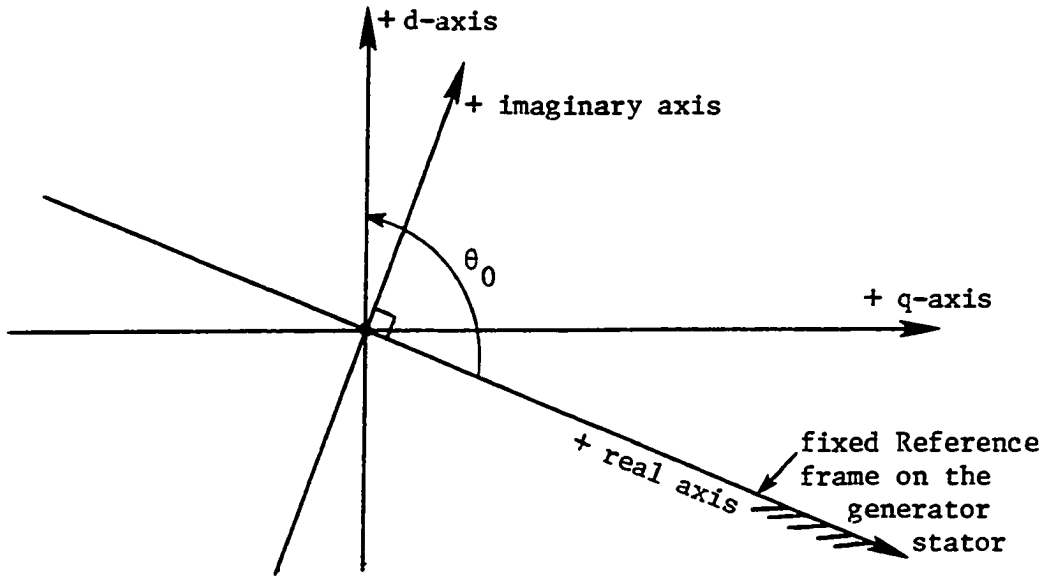

Eq. A-11 can be written as follows:

$$\Delta E_{a1} = \sqrt{\frac{2}{3}} \{[\Delta\omega \frac{\sin\theta_0}{j} + \Delta\theta\omega_0 \frac{\cos\theta_0}{j}](j\lambda_{d0}) + [-\Delta\omega\cos\theta_0 + \Delta\theta\omega_0\sin\theta_0]\lambda_{q0}\}$$

Using the relation $\cos\theta_0 = j\sin\theta_0$ (according to the system of axes chosen), we obtain:

$$\Delta E_{a1} = \sqrt{\frac{2}{3}} \{[\Delta\omega(-\cos\theta_0) + \Delta\theta\omega_0(\sin\theta_0)](j\lambda_{d0}) + [-\Delta\omega\cos\theta_0 + \Delta\theta\omega_0\sin\theta_0]\lambda_{q0}\}$$

$$= \sqrt{\frac{2}{3}} \{-\Delta\omega\cos\theta_0[\lambda_{q0} + j\lambda_{d0}] + \Delta\theta\omega_0\sin\theta_0[\lambda_{q0} + j\lambda_{d0}]\}$$

or

$$\Delta E_{a1} = \sqrt{\frac{2}{3}} [\lambda_{q0} + j\lambda_{d0}](-\Delta\omega\cos\theta_0 + \Delta\theta\omega_0\sin\theta_0) \qquad \text{(A-12)}$$

Substituting Eq. A-10 in Eq. A-12, we get:

$$\Delta E_{a1} = \sqrt{\frac{2}{3}} [\lambda_{q0} + j\lambda_{d0}]A[-\mu\cos\mu t\cos\theta_0 + \omega_0\sin\mu t\sin\theta_0] \quad (a)$$

Through trigonometric manipulations, and noting that

$$\theta_0 = \omega_0 t \quad (b) \quad (A\text{-}13)$$

$$\Delta E_{a1} = \sqrt{\frac{1}{6}} A[\lambda_{q0} + j\lambda_{d0}]\{(\omega_0 - \mu)\cos(\omega_0 - \mu)t - (\omega_0 + \mu)\cos(\omega_0 + \mu)t\}$$

Defining

$$\Delta E_{a1} \triangleq \Delta E_{SUB} + \Delta E_{super} \quad (A\text{-}14)$$

then

$$\Delta E_{SUB} = \sqrt{\frac{1}{6}} A(\omega_0 - \mu)[\lambda_{q0} + j\lambda_{d0}]\cos(\omega_0 - \mu)t \quad (a)$$

$$\Delta E_{super} = -\sqrt{\frac{1}{6}} A(\omega_0 + \mu)[\lambda_{q0} + j\lambda_{d0}]\cos(\omega_0 + \mu)t \quad (b) \quad (A\text{-}15)$$

Thus the voltage-component ΔE_{a1}, which is caused by the disturbed motion of the generator rotor, is composed of two components: ΔE_{SUB} which is due to the subsychronous frequency $(\omega_0 - \mu)$; and ΔE_{super} which is due to the supersynchronous frequency $(\omega_0 + \mu)$.

2) Next, consider the voltage-component ΔE_{a2}. For a constant field voltage, $\Delta\lambda_d$ and $\Delta\lambda_q$ can be expressed in the form (23)

$$\Delta\lambda_d \approx x_d(p)\Delta i_d \quad (a)$$

$$\Delta\lambda_q \approx x_q(p)\Delta i_q \quad (b) \quad (A\text{-}16)$$

where $x_d(p)$ and $x_q(p)$ are termed operational impedances, and p is time-derivative operator. Therefore, $x_d(p)$ and $x_q(p)$ can be

expressed in function of frequency of operation by making a substitution of $(j\omega)$ for p.

At a given frequency, these impedances are thus complex constants, and can be denoted as Z_d and Z_q, respectively.

Equation A-8 thus becomes at steady-state:

$$\Delta E_{a2} = \sqrt{\frac{2}{3}} \{-\omega_0 Z_q \Delta i_q \cos\omega_0 t + \omega_0 Z_d \Delta i_d \sin\omega_0 t\} \qquad \text{(A-17)}$$

From the theory developed for induction machines[1], where the stator and rotor terminal voltages are expressed as a function of the stator and rotor currents, and by adopting the direction of current flow to be the same as that for synchronous generator, we have:

$$\Delta v_{as} = \sqrt{\frac{2}{3}} \{-\omega_B[(Ls + L_{sm})\Delta i_q s + \frac{3}{2} Ls_r \Delta i_{qr}]\cos\omega_B t + \omega_B[(Ls + Ls_m)\Delta i_d s + \frac{3}{2} Ls_r \Delta i_{dr}]\sin\omega_B t\} \qquad \text{(a)}$$

$$\Delta v_{ar} = \sqrt{\frac{2}{3}} \{-S\omega_B[\frac{3}{2} Ls_r \Delta i_q s + (L_r + L_{rm})\Delta_i qr]\cos S\omega_B t - R_r \Delta i_{dr} \cos S\omega_B t + S\omega_B[\frac{3}{2} Ls_r \Delta i_d s + (L_r + L_{rm})\Delta i_{dr}]\sin S\omega_B t - R_r \Delta i_{qr} \sin S\omega_B t\} \qquad \text{(b)} \quad \text{(A-18)}$$

where

ω_B: Base angular velocity (line frequency)

S: Slip defined as $(\omega_B - \omega_r)/\omega_B$

ω_r: Rotor anguiar velocity

R_r: Rotor circuit resistance

---

[1] David D. Robb, Department of Electrical Engineering, Iowa State University. Induction Machines class notes, Winter Quarter, 1975.

L_s: Stator self-inductance

L_{sm}: Stator mutual inductance

L_r: Rotor self-inductance

L_{rm}: Rotor mutual inductance

L_{sr}: Mutual inductance between stator and rotor windings.

The quantities in Eq. A-18 can be transformed to the abc-frame, and at steady-state a T-equivalent circuit for the induction machine can be obtained as shown below:

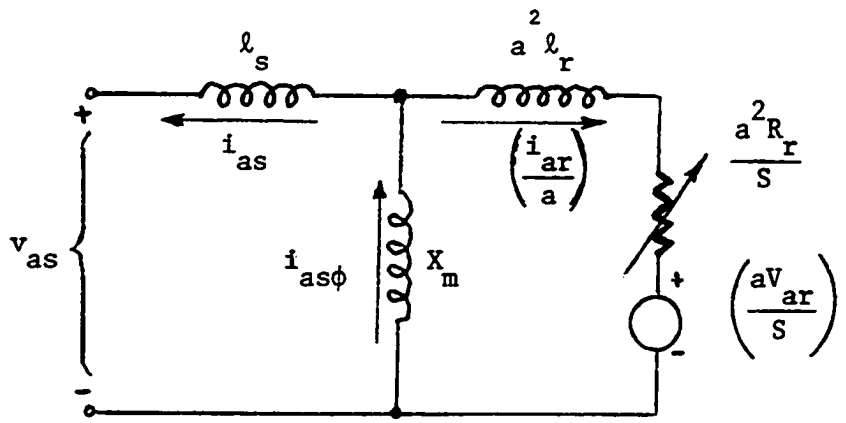

where

$$i_{as\phi} = i_{as} + \left(\frac{i_{ar}}{a}\right), \text{ magnetizing current.}$$

$$\ell_s = L_s + L_{sm} - \frac{3}{2} aL_{sr}$$

$$X_m = \frac{3}{2} aL_{sr}$$

$$\ell_r = L_r + L_{rm} - \frac{3}{2} \frac{L_{sr}}{a}$$

and $a \triangleq$ Effective winding-turns ratio of stator to rotor coils.

In Eq. A-18a, if we express all quantities in per unit, ω_B is to be replaced by ω_0 (see Eq. A-13b), and the rotor currents are referred to the stator side in their respective axes. Then Eq. A-18a will have the form

$$\Delta v_{as} = \sqrt{\frac{2}{3}} \{-\omega_0 X_{qs} \Delta i_{qs} \cos\omega_0 t + \omega_0 X_{ds} \Delta i_{ds} \sin\omega_0 t\} \qquad \text{(A-19)}$$

Neglecting subscript s denoting stator quantities, and comparing Eq. A-19 with Eq. A-17, we conclude that the voltage-component ΔE_{a2} is caused by the induction generator action.

Finally, from Eq. A-6, a steady-state model for a generator whose rotor is perturbed by a sinusoidal motion is shown below:

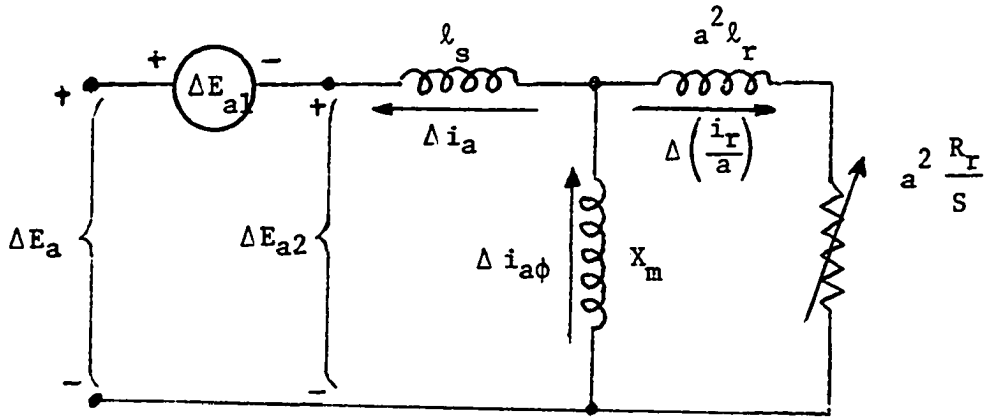

where incremental field voltage is assumed equal to zero (constant field voltage).

XII. APPENDIX B. MODES OF OSCILLATION AND MODE SHAPES

Consider an unforced and undamped mechanical system as shown below:

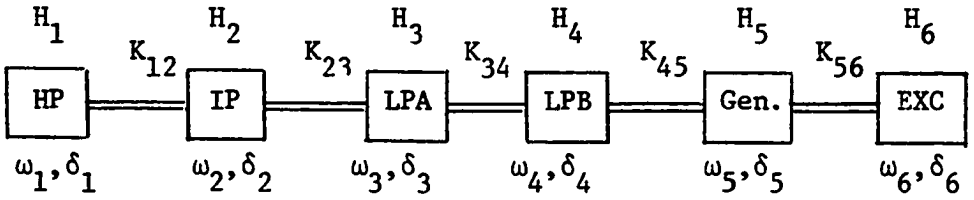

This system can be described by a set of second order differential equations that can be written in matrix form as follows (all quantities are in pu, except time in seconds and δ in radians):

$$\frac{1}{\omega_B} \underline{H}\, \ddot{\underline{\delta}} + \underline{K}\, \underline{\delta} = 0 \qquad \text{(B-1)}$$

where $\underline{H}$ = diag $[2H_1, 2H_2, 2H_3, 2H_4, 2H_5, 2H_6]$

$\underline{\delta}$ = column $[\delta_1, \delta_2, \delta_3, \delta_4, \delta_5, \delta_6]$

$$\underline{K} = \begin{bmatrix} K_{12} & -K_{12} & & & & \\ -K_{12} & (K_{12}+K_{23}) & -K_{23} & & & \\ & -K_{23} & (K_{23}+K_{34}) & -K_{34} & & \\ & & -K_{34} & (K_{34}+K_{45}) & -K_{45} & \\ & & & -K_{45} & (K_{45}+K_{56}) & -K_{56} \\ & & & & -K_{56} & K_{56} \end{bmatrix}$$

At resonance, all masses oscillate at the same frequency, ω_m, such that

$$\delta_i = X_i \sin(\omega_m t + \alpha), \quad i = 1, 2, \ldots, 6 \qquad \text{(B-2)}$$

Substitute Eq. B-2 into Eq. B-1, we get:

$$\frac{\omega_m^2}{\omega_B} \underline{H}\,\underline{X} - \underline{K}\,\underline{X} = 0$$

or

$$\underline{M}\,\underline{X} = \frac{\omega_m^2}{\omega_B}\,\underline{X} = \lambda_m \underline{X} \tag{B-3}$$

where

$$\underline{M} = \underline{H}^{-1}\underline{K},\ \lambda_m = \frac{\omega_m^2}{\omega_B}$$

or

$$\omega_m = \sqrt{\lambda_m \omega_B}\ ,\quad m = 0,\ 1,\ldots,\ 5 \tag{B-4}$$

To each λ_m corresponds an eigenvector Q_m. A transformation matrix $\underline{Q}$ is formed as follows:

$$\underline{Q} = [Q_0,\ Q_1,\ Q_2,\ Q_3,\ Q_4,\ Q_5] \tag{B-5}$$

Values of ω_m and the matrix $\underline{Q}$ are given below for the Navajo Project Test Case.

Mode m	ω_m (rad/sec)	(Hertz)
1	98.72	15.71
2	127.00	20.21
3	160.52	25.55
4	202.85	32.28
5	298.18	47.46

$$\underline{Q} = \begin{bmatrix} 1 & -.7770 & .1099 & 1 & .8638 & -.7874 \\ 1 & -.5837 & .0646 & .3422 & -.0437 & 1 \\ 1 & -.3424 & .0150 & -.2297 & -.5027 & -.1133 \\ 1 & .1117 & -.0395 & -.0954 & 1 & .0211 \\ 1 & .3731 & -.0374 & .1660 & -.6205 & -.0045 \\ 1 & 1 & 1 & -.2525 & .3768 & .0009 \end{bmatrix}$$

We note that each column of $\underline{Q}$ corresponds to a mode shape (see Fig. 2). The following matrix-operations are termed canonical transformation of $\underline{H}$ and $\underline{K}$ (18):

$$\underline{H}_E = \underline{Q}^t \underline{H}\, \underline{Q} \qquad \text{(a)}$$

$$\underline{K}_E = \underline{Q}^t \underline{K}\, \underline{Q} \qquad \text{(b)} \qquad \text{(B-6)}$$

$\underline{H}_E$ and $\underline{K}_E$ are diagonal matrices.

Any column and/or row of $\underline{Q}$ may be multiplied by a constant without altering the property of its transformation. In power system analysis, it is common practice to refer all the masses to that of the generator rotor. This is accomplished by making all the elements of row 5 of $\underline{Q}$ equal to unity. We then have:

$$\underline{Q} = \begin{bmatrix} 1 & -2.0826 & 2.9385 & 6.0241 & 1.3921 & -174.9778 \\ 1 & -1.5645 & 1.7273 & 2.0614 & -0.0704 & 222.2222 \\ 1 & -0.9177 & 0.4011 & -1.3837 & -0.8102 & -25.1778 \\ 1 & 0.2994 & -1.0561 & -0.5747 & 1.6116 & 4.6889 \\ 1 & 1 & -1 & 1 & -1 & -1 \\ 1 & 2.6802 & 26.738 & -1.5211 & 0.6073 & 0.2000 \end{bmatrix} \qquad \text{(B-7)}$$

The following data list the values of H_E and K_E computed according to Eq. B-6 for all the modes and for any particular chosen mass of reference.

Values of H_E (in pu) when referred to:

Mode	HP	IP	LPA	LPB	Gen	Exc
0	2.89408	2.89408	2.89408	2.89408	2.89408	2.89408
1	0.622682	1.10333	3.20660	30.1251	2.70044	0.375909
2	3.21041	9.29131	172.309	24.8544	27.7213	0.03878
3	0.190583	1.62749	3.61222	20.9401	6.91609	2.98917
4	2.02384	791.354	5.97488	1.51006	3.92209	10.6342
5	0.362290	0.224619	17.4978	504.521	11092.3	277307.0

Values of K_E (pu torque/rad) when referred to:

Mode	HP	IP	LPA	LPB	Gen	Exc
0	0	0	0	0	0	0
1	32.1958	57.0478	165.797	1557.62	139.626	19.4364
2	274.668	794.924	14742.0	2126.43	2371.71	3.31745
3	26.0512	222.465	493.761	2862.34	945.376	408.597
4	441.802	172751.0	1304.31	329.645	856.187	2321.43
5	170.885	105.948	8253.36	2.38×10^5	5.23×10^6	5.57×10^7

XIII. APPENDIX C. NATURE OF COUPLING BETWEEN MODES

For an unforced mechanical system as described in Appendix B, if damping terms are added to Eq. B-1 and per unit system is used for all variables except δ in radians, we would have:

$$\underline{H}\,\ddot{\underline{\delta}} + \underline{D}\,\dot{\underline{\delta}} + \underline{K}\,\underline{\delta} = 0 \qquad \text{(C-1)}$$

Defining $\underline{\delta} \triangleq \underline{Q}\,\underline{q}$, where $\underline{Q}$ is the transformation matrix obtained in Appendix B, and performing following operation:

$$\underline{Q}^t\underline{H}\,\underline{Q}\,\ddot{\underline{q}} + \underline{Q}^t\,\underline{D}\,\underline{Q}\,\dot{\underline{q}} + \underline{Q}^t\underline{K}\,\underline{Q}\,\underline{q} = 0 \qquad \text{(C-2)}$$

where $\underline{D} = \text{diag}\,[D_1, D_2, D_3, D_4, D_5, D_6]$, we would get:

$$\underline{H}_N\,\ddot{\underline{q}} + 2\,\underline{d}\,\dot{\underline{q}} + \underline{\Omega}\,\underline{q} = 0 \qquad \text{(C-3)}$$

where $\underline{H}_N = \text{diag}\,[2H_{E1}, 2H_{E2}, 2H_{E3}, 2H_{E4}, 2H_{E5}, 2H_{E6}]$

$$\underline{d} = \begin{bmatrix} d_{11} & d_{12} & d_{13} & d_{14} & d_{15} & d_{16} \\ & d_{22} & d_{23} & d_{24} & d_{25} & d_{26} \\ & & d_{33} & d_{34} & d_{35} & d_{36} \\ & & & d_{44} & d_{45} & d_{46} \\ & & & & d_{55} & d_{56} \\ & & & & & d_{66} \end{bmatrix} \text{, symmetric matrix}$$

$$\underline{\Omega} = \text{diag}\,[K_{E1}, K_{E2}, K_{E3}, K_{E4}, K_{E5}, K_{E6}]$$

We can rewrite Eq. C-3 as:

$$\ddot{\underline{q}} + 2\,\underline{\varepsilon}\,\dot{\underline{q}} + \underline{\omega}^2\underline{q} = 0 \qquad \text{(C-4)}$$

where

$$\varepsilon_{ij} = \frac{d_{ij}}{2H_{Ei}}$$

$$\omega_i^2 = \frac{K_{Ei}}{2H_{Ei}}, \quad i = 1, 2, \ldots, 6 \qquad j = 1, 2, \ldots, 6$$

Making use of approximations as defined below (21):

$$q_i = q_i^{(0)} + \mu q_i^{(1)} + \mu^2 q_i^{(2)} + \ldots \tag{C-5}$$

where μ is a parameter showing the influence of off-diagonal damping elements upon general solution for q, and superscript denotes order of approximation.

Substituting Eq. C-5 into Eq. C-4 and collecting terms with like power in μ, one would get a system of second order differential equations as follows:

$$\ddot{q}_i^{(0)} + 2\varepsilon_{ii}\dot{q}_i^{(0)} + \omega_i^2 q_i^{(0)} = 0 \tag{a}$$

$$\ddot{q}_i^{(1)} + 2\varepsilon_{ii}\dot{q}_i^{(1)} + \omega_i q_i^{(1)} = -2 \sum_{k\neq i}^{6} \varepsilon_{ik}\dot{q}_k^{(0)} \tag{b}$$

$$\ddot{q}_i^{(2)} + 2\varepsilon_{ii}\dot{q}_i^{(2)} + \omega_i^2 q_i^{(2)} = -2 \sum_{k\neq i}^{6} \varepsilon_{ik}\dot{q}_k^{(1)} \tag{c}$$

$$\vdots \tag{C-6}$$

Equation C-6a has a general solution of the form:

$$q_i^{(0)} = a_i e^{-\varepsilon_{ii} t} \cos \bar{\omega}_i t \tag{C-7}$$

where

$$\omega_i^{-2} = \omega_i^2 - \varepsilon_{ii}^2$$

Substituting Eq. C-7 into Eq. C-6b, we get:

$$\ddot{q}_i^{(1)} + 2\varepsilon_{ii}\dot{q}_i^{(1)} + \omega_i^2 q_i^{(1)} = F_i(t) \qquad \text{(C-8)}$$

where

$$F_i(t) = 2 \sum_{k\neq i}^{6} a_k \varepsilon_{ik} e^{-\varepsilon_{kk}t} [\varepsilon_{kk}\cos\bar{\omega}_k t + \bar{\omega}_k \sin\bar{\omega}_k t]$$

For $q_i(0) = 0$ and $\dot{q}_i(0) = 0$, the solution of Eq. C-8 has the general form (convolution theorem):

$$q_i^{(1)} = \frac{e^{-\varepsilon_{ii}t}}{\bar{\omega}_i} \int_0^t F_i(\tau) e^{\varepsilon_{ii}\tau} \sin\bar{\omega}_i(t-\tau)d\tau$$

or

$$q_i^{(1)} = \frac{1}{\bar{\omega}_i} \sum_{k\neq i}^{6} a_k \varepsilon_{ik} e^{-\varepsilon_{kk}t} [M_{ik}\sin\bar{\omega}_k t + N_{ik}\cos\bar{\omega}_k t]$$

where

$$M_{ik} = -\frac{\bar{\omega}_k(\bar{\omega}_k + \bar{\omega}_i) - \varepsilon_{kk}(\varepsilon_{ii} - \varepsilon_{kk})}{(\bar{\omega}_k + \bar{\omega}_i)^2 + (\varepsilon_{ii} - \varepsilon_{kk})^2} + \frac{\bar{\omega}_k(\bar{\omega}_k - \bar{\omega}_i) - \varepsilon_{kk}(\varepsilon_{ii} - \varepsilon_{kk})}{(\bar{\omega}_k - \bar{\omega}_i)^2 + (\varepsilon_{ii} - \varepsilon_{kk})^2}$$

$$N_{ik} = \frac{\bar{\omega}_k\varepsilon_{ii} + \varepsilon_{kk}\bar{\omega}_i}{(\bar{\omega}_k + \bar{\omega}_i)^2 + (\varepsilon_{ii} + \varepsilon_{kk})^2} - \frac{\bar{\omega}_k\varepsilon_{ii} - \varepsilon_{kk}\bar{\omega}_i}{(\bar{\omega}_k - \bar{\omega}_i)^2 + (\varepsilon_{ii} - \varepsilon_{kk})^2}$$

For small damping, $\bar{\omega}_i \approx \omega_i$, so that:

$$M_{ik} \approx -\frac{\omega_k}{\omega_k + \omega_i} + \frac{\omega_k}{\omega_k - \omega_i} = \frac{2\omega_i\omega_k}{\omega_k^2 - \omega_i^2}$$

$$N_{ik} \approx 0$$

And the first approximation as stated by Eq. C-5 gives:

$$q_i = q_i^{(0)} + \mu q_i^{(1)}$$

or

$$q_i(t) = a_i e^{-\varepsilon_{ii} t} \cos\omega_i t + \mu \sum_{k \neq i}^{6} \frac{a_k \varepsilon_{ik} \omega_k}{\omega_k^2 - \omega_i^2} e^{-\varepsilon_{kk} t} \sin\omega_k t \qquad \text{(C-9)}$$

Equation C-9 shows that, at least in the first approximation, the off-diagonal elements in the damping matrix $\underline{\varepsilon}$ do not influence the damping velocity of vibrations. However, the vibrations are coupled (magnitude wise).

XIV. APPENDIX D. SYSTEM PARAMETERS USED

(Line and Machine Data are from Reference 13)

Transmission Line:

$x_t = 0.14$ pu

$x_\ell = 0.50$ pu

$x_s = 0.06$ pu

$R_e = 0.02$ pu, $x_e = x_t + x_\ell + x_s + 0.70$ pu

$x_F = 0.036$ pu

Mechanical System:

Mass	Inertia H (Seconds)	Shaft Sections	Spring Constant K(pu torque/rad)
HP	0.092897	HP - IP	19.303
IP	0.155589	IP - LPA	34.929
LPA	0.858670	LPA - LPB	52.038
LPB	0.884215	LPB - Gen	70.858
Gen	0.868495	Gen - EXC	2.822
EXC	0.0342165		

For Self-Excitation Case:

Rotor Circuits pu Impedance at 60 Hz

Modes	1	2	3	4
$\ell_d = \ell_q$	0.13	0.13	0.13	0.13
r_F	0.00587	0.00686	0.00764	0.00825
ℓ_F	0.04786	0.04401	0.04080	0.03823
L_{AD}	1.66	1.66	1.66	1.66
r_Q	0.00884	0.00936	0.00998	0.01081
ℓ_Q	0.04742	0.04648	0.04556	0.04469
L_{AQ}	1.58	1.58	1.58	1.58

P_0 = 0.01 pu @ 90% lagging. For third mode, X_c = 0.287 pu.

For Transient Case (Second mode simulation, i.e., X_c = 0.371 pu):

d-axis: r_F = 0.001406 pu $\quad r_D$ = 0.004085 pu

ℓ_F = 0.062 pu $\quad \ell_D$ = 0.0055 pu

$L_{AD} = kM_F = kM_D = M_R$ = 1.66 pu $\quad L_{MD}$ = 0.00485 pu

ℓ_d = 0.13 pu

q-axis: r_{Q1} = 0.014058 pu $\quad r_{Q2}$ = 0.008223 pu

ℓ_{Q1} = 0.326 pu $\quad \ell_{Q2}$ = 0.095 pu

$L_{AQ} = kM_{Q1} = kM_{Q2} = M_Q$ = 1.58 pu $\quad L_{MQ}$ = 0.045622 pu

ℓ_q = 0.13 pu

Mechanical Input-Torques:

T_{m1} = 30% applied @ HP

T_{m2} = 26% applied @ IP

T_{m3} = 22% applied @ LPA

T_{m4} = 22% applied @ LPB

Computed Initial Conditions for Transient Analysis:

P_0 = 0.90 pu @ PF = 90% lagging

I_a lags V_t by $\psi = 25.84°$

V_t = 1.0 pu

i_{d0} = -1.5972 pu

v_{d0} = -1.1454 pu

i_{F0} = 2.5049 pu

v_{cd0} = -0.2486 pu

V_∞ = 0.8865 pu

λ_{d0} = 1.29915 pu

$\hat{\lambda}_{d0}$ = 0.1811 pu

λ_{AD0} = 1.5068 pu

λ_{D0} = 1.5068 pu

I_a = 1.0 pu

i_{q0} = 0.6701 pu

v_{q0} = 1.2992 pu

E_{FD} = 2.4007 pu

v_{cq0} = -0.5926 pu

δ_0 = 60.32°

λ_{q0} = 1.1458 pu

$\hat{\lambda}_{q0}$ = 1.6149 pu

λ_{AQ0} = 1.0588 pu

λ_{F0} = 1.6621 pu

IEEE Type-1 Exciter:

τ_A = 0.05 sec

τ_E = 0.05 sec

τ_F = 0.715 sec

τ_R = 0.01 sec

K_A = 40

K_E = -0.05

S_E' = 0.0261

K_F = 0.04

K_R = 1

$S(E_{FD}) = A_{EX}e^{B_{EX}E_{FD}}$

A_{EX} = 0.0016

B_{EX} = 1.114

XV. APPENDIX E. ANALOG COMPUTER POTENTIOMETER COEFFICIENTS

The potentiometer coefficients are computed and tabulated for various patching diagrams according to the following data:

Tables of Potentiometer Coefficients	For Analog Computer Patching Diagrams
1. Mechanical System	
a. Full Model	Figure 6(a)
b. Reduced Model for Modal Analysis	Figure 6(b)
2. Electrical System	Figure 5
3. Three-phase Fault	Figure 7
4. Excitation System	Figure 18
5. Stabilizing Control Circuit (SCC)	Figure 17

The following abbreviations are used:

OUT Var.: Output-variable of an amplifier

Pot No.: Identification number of a potentiometer

Ampl. No.: Identification number of an amplifier (prefix A omitted)

L_0: Level of an amplifier output

L_i: Level of the input to an amplifier through a particular potentiometer

In Var.: Input-variable of an amplifier

C: Value of a constant

Ampl. Gain: Gain of an amplifier

Pot Set: Value of the setting of a potentiometer

a: Time scaling factor. A value of a = 40 is used throughout. This means that a duration of 40 seconds on the analog computer is equivalent to 1 second on the real system under study, if the operation mode is on M-sec.

Due to the shortage of needed amplifiers and/or potentiometers, some of the units appear more than once on separate tables. In this case, the corresponding patching diagrams cannot be patched at the same time. For instance, if the mechanical system's full mode is used, the excitation system and the SCC cannot be simulated. If the mechanical system's reduced model for modal analysis is used, then the excitation system and the SCC can be included, but a three-phase fault connot be simulated.

(Mechanical System - Full Model)

OUT Var.	Pot No.	Ampl. No.	L_0	L_i	L_0/L_i	In Var.	CONSTANTS	C	$C \times \frac{L_0}{L_i}$	Ampl. Gain	Pot Set
$-\omega_1$	222	020	40	10	4	T_{m1}	$\frac{(0.90)(0.30)}{2H_1a}$	0.0363	0.1454	1	0.1454
-	223	-	40	40	1	$\delta_2 - \delta_1$	$\frac{K_{12}}{2H_1a}$	2.5970	2.5970	10	0.2597
$-\omega_2$	032	021	40	10	4	T_{m2}	$\frac{(0.90)(0.26)}{2H_2a}$	0.0188	0.0752	1	0.0752
-	233	-	40	40	1	$\delta_1 - \delta_2$	$\frac{K_{12}}{2H_2a}$	1.5508	1.5508	10	0.1551
-	230	-	40	40	1	$\delta_3 - \delta_2$	$\frac{K_{23}}{2H_2a}$	2.8062	2.8062	10	0.2806
$-\omega_3$	801	030	40	10	4	T_{m3}	$\frac{(0.90)(0.22)}{2H_3a}$	0.0029	0.0115	1	0.0115
-	800	-	40	40	1	$\delta_2 - \delta_3$	$\frac{K_{23}}{2H_3a}$	0.5085	0.5085	1	0.5085
-	701	-	40	40	1	$\delta_4 - \delta_3$	$\frac{K_{34}}{2H_3a}$	0.7575	0.7575	1	0.7575

(Mechanical System - Full Model continued)

OUT Var.	Pot No.	Ampl. No.	L_0	L_i	L_0/L_i	In Var.	CONSTANTS	C	$C \times \frac{L_0}{L_i}$	Ampl. Gain	Pot Set
$-\omega_4$	031	031	40	10	4	T_{m4}	$\frac{(0.90)(0.22)}{2H_4a}$	0.0028	0.0112	1	0.0112
-	612	-	40	40	1	$\delta_3 - \delta_4$	$\frac{K_{34}}{2H_4a}$	0.7357	0.7357	1	0.7357
-	613	-	40	40	1	$\delta_5 - \delta_4$	$\frac{K_{45}}{2H_4a}$	1.0006	1.0006	10	0.1001
$-\omega_5$	210	210	40	10	4	$-T_e$	$\left(\frac{1}{3}\right)\frac{1}{2H_5a}$	0.0048	0.0192	1	0.0192
-	810	-	40	40	1	$\delta_4 - \delta_5$	$\frac{K_{54}}{2H_5a}$	1.0198	1.0198	10	0.1020
-	211	-	40	200	0.20	$-\Delta\omega_5$	$\frac{D_5}{2H_5a}$, $D_5 = 7.50$	0.1079	0.0216	1	0.0216
-	812	-	40	40	1	$\delta_6 - \delta_5$	$\frac{K_{56}}{2H_5a}$	0.0406	0.0406	1	0.0406
$-\omega_6$	221	200	40	40	1	$\delta_5 - \delta_6$	$\frac{K_{56}}{2H_6a}$	0.0310	1.0310	10	0.1031

(Mechanical System - Full Model continued)

OUT Var.	Pot No.	Ampl. No.	L_0	L_i	L_0/L_i	In Var.	CONSTANTS	C	$C \times \frac{L_0}{L_i}$	Ampl. Gain	Pot Set
δ_1	212	220	40	40	1	$-\omega_1$	$\frac{\omega_B}{a}$	9.4250	9.4250	10	0.9425
δ_2	213	221	40	40	1	$-\omega_2$	$\frac{\omega_B}{a}$	9.4250	9.4250	10	0.9425
δ_3	303	230	40	40	1	$-\omega_3$	$\frac{\omega_B}{a}$	9.4250	9.4250	10	0.9425
δ_4	802	231	40	40	1	$-\omega_4$	$\frac{\omega_B}{a}$	9.4250	9.4250	10	0.9425
δ_5	603	410	40	40	1	$-\omega_5$	$\frac{\omega_B}{a}$	9.4250	9.4250	10	0.9425
δ_6	601	610	40	40	1	$-\omega_6$	$\frac{\omega_B}{a}$	9.4250	9.4250	10	0.9425
$\Delta\omega_5$	232	613	200	40	5	1 pu	1.0	1.0	5.0	10	0.5000
-	231	-	200	40	5	$-\omega_5$	1.0	1.0	5.0	10	0.5000
δ_5 (degrees)	803	233	0.5	40	0.0125	$-\delta_5$ (rad.)	180/Π	57.2960	0.7162	1	0.7162

(Mechanical System - Full Model continued)

OUT Var.	Pot No.	Ampl. No.	L_0	L_i	L_0/L_i	In Var.	CONSTANTS	C	$C \times \frac{L_0}{L_i}$	Ampl. Gain	Pot Set
(A)	203	032	10	100	0.10	-100	1.0	1.0	0.10	1	0.1000
-	611	-	10	100	0.10	$\pm$100	0.10	0.10	0.01	1	0.0100
(B)	220	X	40	100	0.40	+100	$\frac{\omega_B}{a}$	9.4250	3.770	10	0.3770
(C)	700	X	40	100	0.40	+100	1.0	1.0	0.40	1	0.4000

(Mechanical System - Reduced Model for Modal Analysis)

OUT Var.	Pot No.	Ampl. No.	L_0	L_i	L_0/L_i	In Var.	CONSTANTS	C	$C \times \frac{L_0}{L_i}$	Ampl. Gain	Pot Set
$-\Delta\omega_{E2}$	212	210	500	10	50	T_m	$\frac{1.1865}{(3)2H_{E2}a}$	0.00018	0.0089	1	0.0089
-	813	-	500	10	50	$+T_e$	$\frac{1}{(3)2H_{E2}a}$	0.00015	0.0075	1	0.0075
-	222	-	500	80	6.25	$-\delta_{E2}$	$\frac{K_{E2}}{2H_{E2}a}$	1.0699	6.6868	10	0.6687
δ_{E2}	210	200	80	500	0.16	$-\Delta\omega_{E2}$	$\frac{\omega_B}{a}$	9.4250	1.5080	10	0.1508
$\Delta\omega_{E0}$	801	800	500	10	50	$-T_{a0}$	$\frac{1}{(3)2H_{E0}a}$	0.0014	0.0720	1	0.0720
$-\delta_{E0}$	802	801	80	500	0.16	$\Delta\omega_{E0}$	$\frac{\omega_B}{a}$	9.4250	1.5080	10	0.1508
$-\omega_u$	031	212	40	100	0.40	+100	1.0	1.0	0.40	1	0.4000
-	232	-	40	500	0.08	$\Delta\omega_{E0}$	1.0	1.0	0.08	1	0.0800
-	220	-	40	500	0.08	$-\Delta\omega_{E2}$	1.0	1.0	0.08	1	0.0800

(Mechanical System - Reduced Model for Modal Analysis continued)

OUT Var.	Pot No.	Ampl. No.	L_0	L_i	L_0/L_i	In Var.	CONSTANTS	C	$C \times \frac{L_0}{L_i}$	Ampl. Gain	Pot Set
δ_{gen} (degrees)	032	023	0.50	80	0.00625	δ_{E2}	$\frac{180}{\Pi}$	57.296	0.3581	1	0.3581
-	810	--	0.50	80	0.00625	$-\delta_{E0}$	$\frac{180}{\Pi}$	57.296	0.3581	1	0.3581

(Electrical System)

OUT Var.	Pot No.	Ampl. No.	L_0	L_i	L_0/L_i	In Var.	CONSTANTS	C	$C \times \frac{L_0}{L_i}$	Ampl. Gain	Pot Set
$-\lambda_d$	000	000	30	40	0.75	$-v_d$	$\frac{\omega_B}{a}$	9.4250	7.0688	10	0.7069
-	100	-	30	12	2.50	$-\lambda_q\omega$	$\frac{\omega_B}{a}$	9.4250	23.562	100	0.2356
$-\lambda_D$	001	001	30	30	1	λ_{AD}	$\frac{\omega_B r_D}{\ell_D a}$	7.00	7.00	10	0.7000
-	101	-	30	30	1	$-\lambda_D$	$\frac{\omega_B r_D}{\ell_D a}$	7.00	7.00	10	0.7000
λ_{AD}	002	002	30	10	3	$-\lambda_F$	$\frac{L_{MD}}{\ell_F}$	0.0782	0.2346	1	0.2346
-	102	-	30	30	1	$-\lambda_D$	$\frac{L_{MD}}{\ell_D}$	0.8727	0.8727	1	0.8727
-	202	-	30	30	1	$-\lambda_d$	$\frac{L_{MD}}{\ell_d}$	0.0369	0.0369	1	0.0369
$-\lambda_F$	201	201	10	30	1/3	λ_{AD}	$\frac{\omega_B r_F}{\ell_F a}$	0.2137	0.0712	1	0.0712

(Electrical System continued)

OUT Var.	Pot No.	Ampl. No.	L_0	L_i	L_0/L_i	In Var.	CONSTANTS	C	$C \times \frac{L_0}{L_i}$	Ampl. Gain	Pot Set
-	301	-	10	10	1	$-\lambda_F$	$\frac{\omega_B r_F}{\ell_F a}$	0.2137	0.2137	1	0.2137
-	302	-	10	100	0.10	E_{FD}	$\frac{\sqrt{3}\omega_B r_F (2.4007)}{L_{AD} a}$	0.0332	0.0033	1	0.0033
λ_{AQ}	012	012	30	30	1	$-\lambda_{Q2}$	$\frac{L_{MQ}}{\ell_{Q2}}$	0.4800	0.4800	1	0.4800
-	412	-	30	30	1	$-\lambda_{Q1}$	$\frac{L_{MQ}}{\ell_{Q1}}$	0.1399	0.1399	1	0.1399
-	013	-	30	30	1	$-\lambda_q$	$\frac{L_{MQ}}{\ell_q}$	0.3508	0.3508	1	0.3508
$-\lambda_q$	010	010	30	40	0.75	$-v_q$	$\frac{\omega_B}{a}$	9.4250	7.0688	10	0.7069
-	110	-	30	12	2.50	$+\lambda_d \omega$	$\frac{\omega_B}{a}$	9.4250	23.562	100	0.2356
$-\lambda_{Q1}$	011	011	30	30	1	λ_{AQ}	$\frac{\omega_B r_{Q1}}{\ell_{Q1} a}$	0.4064	0.4064	1	0.4064

(Electrical System continued)

OUT Var.	Pot No.	Ampl. No.	L_0	L_i	L_0/L_i	In Var.	CONSTANTS	C	$C \times \frac{L_0}{L_i}$	Ampl. Gain	Pot Set
-	111	-	30	30	1	$-\lambda_{Q1}$	$\frac{\omega_B r_{Q1}}{\ell_{Q1}{}^a}$	0.4064	0.4064	1	0.4064
$-\lambda_{Q2}$	400	400	30	30	1	λ_{AQ}	$\frac{\omega_B r_{Q2}}{\ell_{Q2}{}^a}$	0.8158	0.8158	1	0.8158
-	401	-	30	30	1	$-\lambda_{Q2}$	$\frac{\omega_B r_{Q2}}{\ell_{Q2}{}^a}$	0.8158	0.8158	1	0.8158
$-i_{qt}$	413	401	20	20	1	$-i_{qt}$	$\frac{\omega_B R_e}{L_e{}^a}$	0.2693	0.2693	10	0.0270
-	500	-	20	40	0.50	v_q	$\frac{\omega_B}{L_e{}^a}$	13.464	6.732	10	0.6732
-	501	-	20	100	0.20	$-V_\infty \cos\delta$	$\frac{\sqrt{3}\omega_B}{L_e{}^a}$	23.32	4.6642	100	0.0466
-	502	-	20	8	2.50	ωi_{dt}	$\frac{\omega_B}{a}$	9.425	23.562	100	0.2356

(Electrical System continued)

OUT Var.	Pot No.	Ampl. No.	L_0	L_i	L_0/L_i	In Var.	CONSTANTS	C	$C \times \frac{L_0}{L_i}$	Ampl. Gain	Pot Set
-	503	-	20	40	0.50	$-v_{cq}$	$\frac{\omega_B}{L_e a}$	13.464	6.732	10	0.6732
$-i_{dt}$	402	411	20	40	0.50	v_d	$\frac{\omega_B}{L_e a}$	13.464	6.732	100	0.0673
-	403	-	20	100	0.20	$V_\infty \sin\delta$	$\frac{\sqrt{3}\omega_B}{L_e a}$	23.32	4.6642	10	0.4664
-	410	-	20	8	2.50	$-\omega i_{qt}$	$\frac{\omega_B}{a}$	9.425	23.562	100	0.2356
-	411	-	20	40	0.50	$-v_{cd}$	$\frac{\omega_B}{L_e a}$	13.464	6.732	100	0.0673
-	300	-	20	20	1	$-i_{dt}$	$\frac{\omega_B R_e}{L_e a}$	0.2693	0.2693	10	0.0270
i_d	003	003	20	30	2/3	λ_{AD}	$\frac{1}{\ell_d}$	7.6923	5.1282	10	0.5128
-	103	-	20	30	2/3	$-\lambda_d$	$\frac{1}{\ell_d}$	7.6923	5.1282	10	0.5128

(Electrical System continued)

OUT Var.	Pot No.	Ampl. No.	L_0	L_i	L_0/L_i	In Var.	CONSTANTS	C	$C \times \frac{L_0}{L_i}$	Ampl. Gain	Pot Set
i_q	602	602	20	30	2/3	λ_{AQ}	$\frac{1}{\ell_q}$	7.6923	5.1282	10	0.5128
-	610	-	20	30	2/3	$-\lambda_q$	$\frac{1}{\ell_q}$	7.6923	5.1282	10	0.5128
$-T_e$	020	202	10	6	5/3	$\lambda_d i_q$	1.0	1.0	1.6667	10	0.1667
-	[illegible]	-	10	6	5/3	$-\lambda_q i_d$	1.0	1.0	1.667	10	0.1667
$-v_{cd}$	023	211	40	20	2	i_{dt}	$\frac{\omega_B X_c}{a}$, X_c=0.371 pu	3.4967	6.9934	10	0.6993
-	030	-	40	16	2.50	$-\omega v_{cq}$	$\frac{\omega_B}{a}$	9.425	23.56	100	0.2356
$-v_{cq}$	033	601	40	20	2	i_{qt}	$\frac{\omega_B X_c}{a}$	3.4967	6.9934	10	0.6993
-	600	-	40	16	2.50	ωv_{cd}	$\frac{\omega_B}{a}$	9.425	23.56	100	0.2356
V_∞	811	810	100	100	1	+100	0.8865	0.8865	0.8865	1	0.8865

(Electrical System continued)

OUT Var.	Pot No.	Ampl. No.	L_0	L_i	L_0/L_i	In Var.	CONSTANTS	C	$C \times \frac{L_0}{L_i}$	Ampl. Gain	Pot Set
v_d	112	412 HG	40	20	X	$i_{dt} - i_d$	$\frac{L_i}{L_0 R}$, R = 100 pu	0.0050	X	X	0.0050
v_q	113	413 HG	40	20	X	$i_{qt} - i_q$	$\frac{L_i}{L_0 R}$	0.0050	X	X	0.0050

(Three-phase Fault[1])

OUT Var.	Pot No.	Ampl. No.	L_0	L_i	L_0/L_i	In Var.	CONSTANTS	C	$C \times \frac{L_0}{L_i}$	Ampl. Gain	Pot Set
$-i_{qt}$	231	401	20	20	1	$-i_{qt}$	$\frac{\omega_B R_e}{L_L a}$, $L_L = L + \frac{L_s L_f}{L_s + L_f}$	0.2845	0.2845	100	0.0029
-	232	-	20	40	0.50	v_q	$\frac{\omega_B}{L_L a}$	14.2264	7.1132	100	0.0711
-	611	-	20	100	0.20	$-V_\infty \cos\delta$	$\frac{\sqrt{3}K\omega_B}{L_L a}$, $K = \frac{L_f}{L_s + L_f}$	9.2403	1.8481	100	0.0185
-	200	-	20	40	0.50	$-v_{cq}$	$\frac{\omega_B}{L_L a}$	14.2264	7.1132	100	0.0711
$-i_{dt}$	022	411	20	40	0.50	v_d	$\frac{\omega_B}{L_L a}$	14.2264	7.1132	100	0.0711
-	813	-	20	100	0.20	$V_\infty \sin\delta$	$\frac{\sqrt{3}K\omega_B}{L_L a}$	9.2403	1.8481	100	0.0185

[1]These potentiometers are added to Amplifiers 401 and 411. They are switched only when the 3ϕ-phase fault is applied.

(Three-phase Fault continued)

OUT Var.	Pot No.	Ampl. No.	L_0	L_i	L_0/L_i	In Var.	CONSTANTS	C	$C \times \frac{L_0}{L_i}$	Ampl. Gain	Pot Set
-	702	-	20	40	0.50	$-v_{cd}$	$\frac{\omega_B}{L_L a}$	14.2264	7.1132	100	0.0711
-	703	-	20	20	1	$-i_{dt}$	$\frac{\omega_B R_e}{L_L a}$	0.2845	0.2845	100	0.0029

(Excitation System[1])

OUT Var.	Pot No.	Ampl. No.	L_0	L_i	L_0/L_i	In Var.	CONSTANTS	C	$C \times \frac{L_0}{L_i}$	Ampl. Gain	Pot Set
V_{REF}	022	033	50	100	0.5	-100	To be adjusted around unity	1.0	0.50	1	0.5000
V_R	223	020	1	50	0.02	$-V_e$	$\frac{K_A}{\tau_A a}$	20	0.40	1	0.4000
-	233	-	1	1	1	V_R	$\frac{1}{\tau_A a}$	0.50	0.50	1	0.5000
$-E_{FD}$	213	021	10	1	10	V_R	$\frac{1}{\tau_E a}$	0.50	5.0	10	0.5000
-	303	-	10	10	1	E_{FD}	$\frac{K_E + S'_E}{\tau_E a}$	0.0130	0.0130	1	0.0130
V_3	613	803	50	10	5	$-E_{FD}$	$\frac{K_F}{\tau_F}$	0.0559	0.2797	1	0.2797
-	612	-	50	100	0.50	V_3/S	$\frac{1}{\tau_F}$	1.3986	0.6993	1	0.6993
$-V_3/S$	221	030	100	50	2	V_3	$\frac{1}{a}$	0.025	0.050	1	0.0500

[1]IEEE Type-1 Exciter (fast type).

(Excitation System continued)

OUT Var.	Pot No.	Ampl. No.	L_0	L_i	L_0/L_i	In Var.	CONSTANTS	C	$C \times \frac{L_0}{L_i}$	Ampl. Gain	Pot Set
$-V_1$	800	600	50	40	1.25	V_t	$\frac{K_R}{\tau_R{}^a}\left(\frac{1}{\sqrt{3}}\right)$	1.4434	1.8042	10	0.1804
-	211	-	50	50	1	$-V_1$	$\frac{1}{\tau_R{}^a}$	2.50	2.50	10	0.2500
$-\lambda_F$	302	201	10	10	1	E_{FD}	$\frac{\sqrt{3}\omega_B r_F}{L_{AD}{}^a}$ (2.4007)	0.0332	0.0332	1	0.0332

(Stabilizing Control Circuit (SCC))

OUT Var.	Pot No.	Ampl. No.	L_0	L_i	L_0/L_i	In Var.	CONSTANTS	C	$C \times \frac{L_0}{L_i}$	Ampl. Gain	Pot Set
Ω_0	812	410	0.50	500	0.001	$-\Delta\omega_{E2}$	b	28275.0	28.275	30	0.9425
-	230	-	0.50	300	0.0017	Ω_0/s	c	125.0	0.2083	1	0.2083
$-\Omega_0/s$	231	611	300	0.50	600	Ω_0	$\frac{1}{a}$	0.025	15.0	100	0.1500
Ω	700	232	0.10	0.50	0.20	$-\Omega_0$	d	56.60	11.298	30	0.3766
-	701	-	0.10	300	0.00033	Ω_0/s	e	525.0	0.1750	1	0.1750
-	601	-	0.10	56.56	0.0018	Ω/s	f	15074.0	26.652	30	0.8884
$-\Omega/s$	703	231	56.56	0.10	565.6	Ω	$\frac{1}{a}$	0.025	14.14	100	0.1414
Ω_T	803	221	0.50	0.10	5.0	$-\Omega$	g	5.6496	28.248	30	0.9416
-	603	-	0.50	56.56	0.0088	$-\Omega/s$	h	2.1153	0.0187	1	0.0187
-	702	-	0.50	377	0.0013	Ω_T/s	m	14213.0	18.85	30	0.6283
$-\Omega_T/s$	200	230	377	0.50	754	Ω_T	$\frac{1}{a}$	0.025	18.85	100	0.1885
$-V_e$	611	233	50	0.50	100	Ω_T	n	0.09316	9.3160	10	0.9316